WAVELET DOMAIN DIVERSITYMETHOD FOR TRANSMISSION OF IMAGES OVER WIRELESS SYTEMS USING HYBRID (OFDM –CDMA-SFH) CONCEPT AND ITS REAL TIME IMPLEMENTATION IN TMS320C6713 DSP DEVELOPMENT BOARD

by

MADHU RANGAPPAGOWDA

Presented to the Faculty of the Graduate School of

The University of Texas at Arlington in Partial Fulfillment

of the Requirements

for the Degree of

MASTER OF SCIENCE IN ELECTRICAL ENGINEERING

THE UNIVERSITY OF TEXAS AT ARLINGTON

DECEMBER 2005

ACKNOWLEDGEMENTS

I would like to thank my supervisor Prof. Dr JONATHAN BREDOW for the endless hours of help, suggestions, ideas and advice during the development of this thesis. I am greatly in indebted to him for his financial assistance (during my semesters at University of Texas at Arlington). I would like to thank him for believing in me and assigning several interesting topics during my graduate research work in RF DSP design research lab.

I would also like to thank Prof. HUA-MEI-CHEN for his advice, timely assistance and meetings to arrange the materials required for the thesis. His advice on the topic of wavelets and sub-band coding was very valuable.

My sincere thanks to Prof. ZHOU WANG for accepting to be a committee member and pointing out key facts and important questions that helped in improvising my work.

I would like to thank my parents, my friends and family members for being a constant source of inspiration and guidance to me during this thesis work.

Last but not the least I would like to thank my beloved fiancé Gowri Srinivas for keeping me in track during my distractions with constant love and affection

Once and all I would like to thank all those who have contributed to successful completion of this research endeavor.

NOVEMBER 10, 2005

ABSTRACT

WAVELET DOMAIN DIVERSITYMETHOD FOR TRANSMISSION OF IMAGES OVER WIRELESS SYTEMS USING NOVEL HYBRID (OFDM–CDMA-SFH) CONCEPT AND ITS REAL TIME IMPLEMENTATION IN TMS320C6713 DSP DEVELOPMENT BOARD

Publication No. _____

MADHU RANGAPPAGOWDA, MSEE

The University of Texas at Arlington, 2005

Supervising Professor: Dr. JONATHAN BREDOW

In this thesis a new OFDM based wavelet domain diversity combining method is proposed to combat errors during image transmission on wireless channels. A novel concept of utilizing OFDM sub-carriers to attain diversity is designed and analyzed.

For images represented in the wavelet domain, diversity is used to obtain multiple data streams using OFDM symbols corresponding to the transmitted image at the receiver. These individual image data streams are combined to form a composite image with higher perceptual quality. Both uncompressed and compressed images are considered. The SPIHT algorithm is used for image compression. Diversity combining methods for

both uncompressed and compressed images exploit the characteristics of the wavelet transform. For compressed images, COFDM is used providing unequal error protection in conjunction with diversity combining. A new method of HYBRID OFDM system (OFDM-CDMA-SFH) is thoroughly investigated and simulation results are used to show that a new level of Quality of Service can be provided for multimedia communication for the mobile network. Performance of this scheme over Rayleigh fading channels is evaluated in this paper. Real time implementation of OFDM system is done in TMS320C6713 DSP developmental board. MATLAB-RTDX protocols are used for data transfer between PC and the DSP board. A considerable improvement in the quality of the image with the diversity combining rule is shown in the results.

TABLE OF CONTENTS

LIST OF ILLUSTRATIONS

Figure Page

LIST OF TABLES

Table Page

CHAPTER 1

INTRODUCTION

1.1 Wireless communication and its challenges

Wireless communication has become increasingly important not only for professional applications but also for many fields in our daily routine using consumer electronics. Today's portable instruments are not only used for voice transmission but also for data transmission and multimedia files like images and video. More and more computers use wireless local area networks (WLANS), and audio and television broadcasting has become digital.

In his book Ramjee Prasad [1] said: "It is dangerous to put limits on wireless data rates, considering economic constraints". Data rates are really what broadband is about: broad band wireless communication will support applications up to 1 Gbps and will be proposed to operate in 60 GHz frequency. However, many people argue whether there is a need for such high capacity systems, bearing in mind all compression algorithms developed and types of applications that require at least tens of megabits per second. One can look at this issue from another perspective. There is a "personal mobility"that will impose new challenges as shown in fig 1.1 to the development of new personal mobile communication system. Today basically five wireless technologies have made an impact; namely, wireless global area networks (WGANs), wireless wide

area networks (WWANs), wireless local area networks (WLANs), wireless personal area networks (WPANs) and wireless broadband personal area networks (WB-PANs).

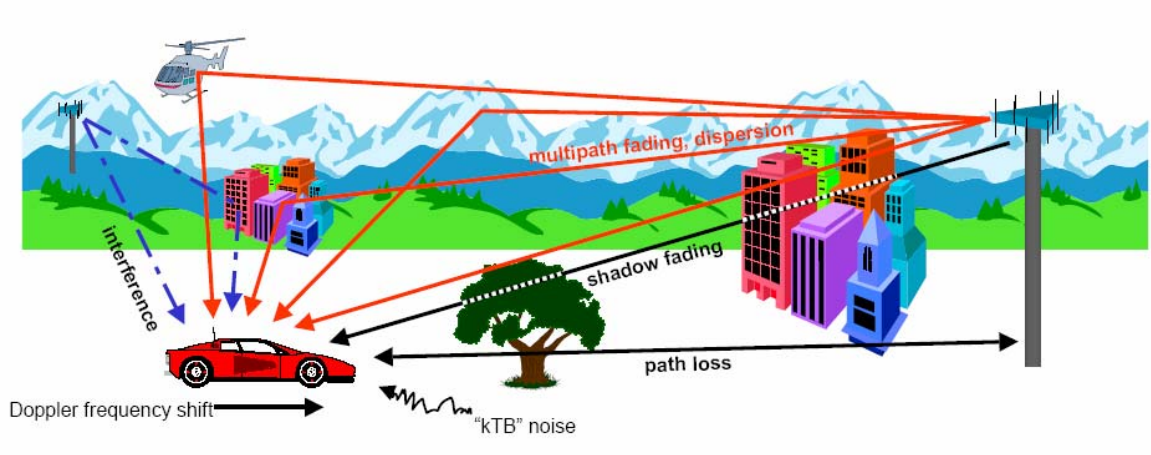

Fig 1.1 Showing the major challenges faced by mobile network.

Many of the above mentioned communication systems make use of one of the two sophisticated techniques that are known as *orthogonal frequency division multiplexing* (OFDM) and *code division multiple access* (CDMA).

Over the past few years, there has been increasing emphasis on extending the service available on wired public telecommunications networks to mobile/movable non wired telecommunications users. At present in addition to voice services, low-bit rate data services and also slow multimedia services are available. However, demands for wireless broadband multimedia communication systems (WBMCS) are anticipated within both public and private sectors.

To create broadband multimedia mobile communication systems, it is necessary to use high bit rate transmission of at least several megabits per second. However, if

digital data is transmitted at the rate of several megabits per second, the delay time of the delayed (multipath) waves is greater than 1 symbol time. Using adaptive equalization techniques at the receiver is one method for equalizing the signals. There are practical difficulties in performing this equalization at several megabits per second with compact and low cost hardware.

To overcome such multipath fading environment with low complexity and to achieve WBCMS, it is helpful to understand what OFDM offers us. OFDM is one parallel data transmission scheme which reduces the influence of the multipath, and makes complex equalizers unnecessary.

OFDM is a digital multi-carrier transmission technique that distributes the digitally encoded symbols over several sub-carrier frequencies in order to reduce the symbol clock rate to achieve robustness against long echoes in the multipath radio channel.

Another major contribution to multimedia systems is "Wavelets and Sub- band coding". This approach allows one to process the image into different resolution levels and analyze the picture to an extent which was not possible earlier. Its significant advantage over FFT has made wavelets popular tool for Image processing. For multimedia, it is helpful to understand how image transmission is done through wireless channels and how minute details affect the reconstruction of the image. Recent development in progressive coding of images has helped achieve greater image compression .But, this also has short comings: generally the first few bits contain

important information; if those information are lost then all received bits for the image are useless.

To combat the channel problem, diversity is frequently used. There are many kinds of diversity, which are explained in the chapter 7. One such diversity approach currently being investigated is wavelet domain diversity. Properties of wavelets are utilized to attain diversity in the transform domain rather than the image domain. This helps in correcting the errors rather than concealing the errors.

In this thesis considerable research is done utilizing the properties of OFDM and wavelet domain diversity methods. A new, novel OFDM- Wavelet domain diversity is proposed and analyzed for image transmission in wireless channels: with further research this can probably be expanded to video transmission.

To understand the flexibility of OFDM it is necessary to understand wireless channel fundamentals, noise effects, types of noise and mobile propagation models. These topics are dealt with detail in chapter 2. Overall system design is discussed in Chapter 3. Chapter 4 highlights the channel consideration done in the thesis, while Chapter 5 explains the basic OFDM signal characteristics designed in the thesis. Chapter 6 emphasizes on image compression components, wavelets and sub–band coding and various image coding techniques and very important SPIHT image coding. Chapter 7 explains the diversity combination techniques developed in the thesis and their benefits with both uncompressed images and compressed images. Chapter 8 shows the simulation methods and its results for the diversity combination techniques. Chapter 9 discusses the Hybrid OFDM system and the impact of the proposed OFDM diversity

algorithms on the system. Chapter 10 provides the insight about the DSP implementation and RTDX communication protocols. In chapter 11, discussions about future work and on-going research are done.

CHAPTER 2

BACKGROUND

2.1 Wireless channel fundamentals

Wireless transmission uses air or space for its transmission medium. The radio propagation is not as "smooth" as in wire transmission since the received signal is not only coming directly from the transmitter, but the combination of reflected, diffracted, and scattered copies of the transmitted signal. It is interesting and rewarding to examine the effects of propagation to a radio signal since consequences affect data rate, range, and reliability of the wireless system [5].

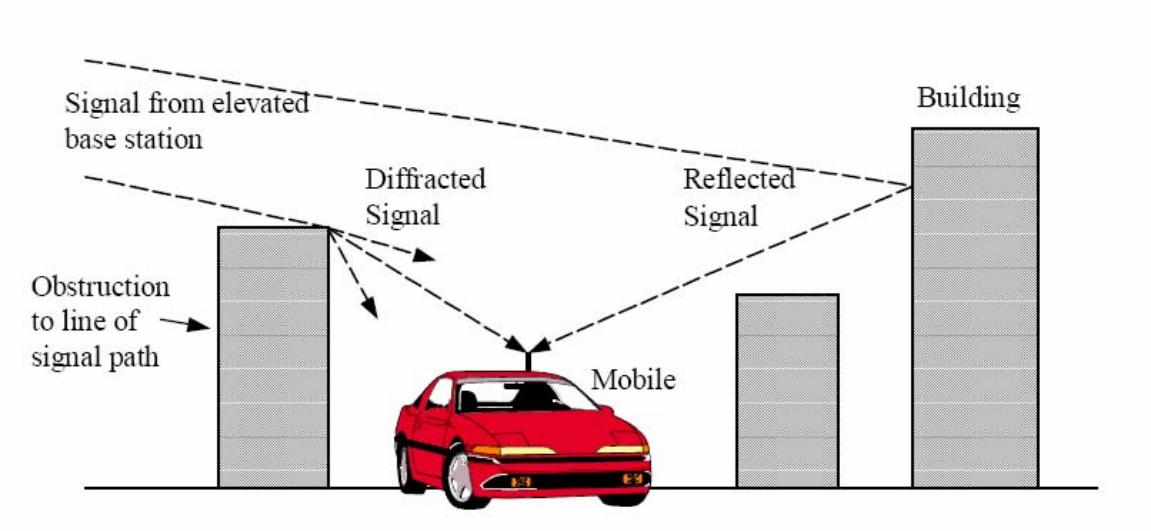

Figure 2.1 Various Channel Parameters affecting the signal.

Reflection occurs when the signal hits a surface where partial energy is reflected and the remaining is transmitted into the surface. The Reflection coefficient, the coefficient that determines the ratio of reflection and transmission, depends on the material properties.

Diffraction occurs when the signal is obstructed by a sharp object which derives secondary waves. Scattering occurs when the signal impinges upon rough surfaces, or small objects. The received scattered signal is sometimes stronger than the reflected and diffracted signals since scattering spreads out the energy in all directions, and consequently provides additional energy for the receiver which can receive more than one copies of the signal in multiple paths with different phases and powers. Figure 2.1 illustrates the propagation mechanisms. Channel models play an important role in the designs of wireless communication systems. There are key modeling parameters that help to characterize a wireless channel; i.e., path loss, delay spread, coherence band width, Doppler spread, and coherence time.

2. 1. 1 Path Loss

The average received power diminishes with distance. In free space when there is a direct path between transmitter and receiver and when there are no secondary waves from the medium objects, the received power is inversely proportional to square of the carrier frequency and square of the distance. If P_R and P_T are the received and transmitted powers respectively, the following relation describes free space propagation, [3]

$$P_R \quad \alpha \quad \frac{G * P_T}{f^2 * d^\alpha} \qquad \text{Eq (2.1)}$$

where f is the carrier frequency, d is the distance between transmitter and receiver, G is the product of power gains of the transmit and receive antennae, α=2 is the path loss

component and *path loss* is defined as P_T / P_R. One can infer from the Eq (2.1) that the higher the carrier frequency the shorter is the operating range.

When there is clutter in the medium, it is not easy to determine the received signal since now the direct path component is added with the multi-path components at the receiver. To estimate this, one accepter method is to use a model that is derived from physical principle and empirical results. A good model prediction agrees with the theoretical findings and test results, in some average sense.

2 .1 .2 Shadowing

Signal power attenuates unpredictably, i.e., randomly with distance when the medium includes obstructions. Eq 2.1 is not sufficient to describe the real environment since it gives the same path loss to different receivers having the equal distance apart from the transmitter, irrespective of channel conditions. If two locations have different surroundings then the average path loss in the signal should be different. This behavior is called *shadowing*. Measurements indicate that the path loss is approximated log-normally distributed for practical environments. A Modified version of Eq (2.1) for indoor path loss is includes log-normal shadowing and follows the formula,

$$PL(dB) = PL(d_o) + 10\alpha \log_{10}(d / d_o) + X_\sigma \qquad \text{Eq (2.2)}$$

where d_o is the reference distance and X_σ is a zero mean Gaussian random variable with a standard deviation σ. σ and α are determined from measure data.

One of the most interesting aspects in wireless communications is *fading* ,which is present when there are multipath components. Multipath components arrive at the receiver with different phases, leading to constructive and destructive interference effects. If there is movement in the system then there is also a time - rate - of change of phase difference between the received components which leads to small unpredictable shift in the frequency. These multiple received copies apply constructive or destructive interference to the signal and create a standing wave pattern that shows rapid signal strength changes, frequency shifts or echoes referred to as *Doppler spread*. Multipath propagation, movement and bandwidth are the factors that influence the fading. The Multipath delay nature of the channel is quantified by *delay spread* and *coherence bandwidth*. The time-varying nature of the channel caused by the movement is quantified by *Doppler spread* and *coherence time*.

2 .1 .3 Delay Spread:

The reflected signal arrives later than the direct path signal to the receiver. RMS delay spread (σ_T) is the metric to characterize this delay in terms of second order moment of the channel power profile. Typical values are on the order of microseconds in outdoor channels and on the order of nanoseconds in indoor radio channels. Depending on the symbol duration (T_S), (σ_T) plays an important role in describing how the signal is influenced by the channel.

2. 1. 4 Coherence Bandwidth

Coherence bandwidth (*Bc)* is used to quantify the channel frequency response and it is inversely proportional to RMS delay spread. Coherence bandwidth is used to

measure how flat the channel bandwidth is. Flatness is described as the cross correlation between the two frequency components. This is important since a signal having a larger bandwidth (*Bs*) than *Bc* is severely distorted. For a 0.9 correlation

$Bc \approx 1/50\sigma_T$. Eq (2.3)

2. 1. 5 Doppler Shift

When the one or both stations are moving, the received signal frequency is different than the original signal frequency. Doppler shift describes that change in the frequency. Suppose a mobile is moving at velocity *V,* the difference in path length of the received signals is $f_d = (1/2\pi) * \frac{\Delta\phi}{\Delta t} = \frac{v}{\lambda}\cos\theta$, where $d = v\Delta t$. The phase change is $\Delta\phi = 2\pi l/\lambda$ and Doppler shift is given by

$$f_d = (1/2\pi) * \frac{\Delta\phi}{\Delta t} = \frac{v}{\lambda}\cos\theta \quad \text{Eq (2.4)}$$

2. 1. 6 Flat Fading

Delay spread and coherence bandwidths are independent from Doppler spread and coherence time. Flat *fading* if when the channel bandwidth is greater than the signal bandwidth, i.e., (*Bc* > *Bs*). Spectral shape of the signal remains but the gain changes. Narrow-band signals fall in to this category since their bandwidth is small as compared to the channel bandwidth. Flat fading channels bring challenges such as variations in the gain and in the frequency spectrum. Variation in the gain may result in deep fades, thereby requiring significant increase in the power transmitted at some frequencies. For example destructive interference may cause deep nulls in the signal power spectrum

which is a particular problem for narrow band signals since any null in a may cause loss of the signal. There are various ways to reduce the fading distortion: diversity is one way which leverages multiple independent samples of the signals .For flat fading conditions the channel gains are independent and have lower probability to experience fades at the same time. Space diversity i.e., using multiple antennas is one of the most efficient diversity techniques compared to time or frequency diversity. Coding is a method of spreading the signal power over the bandwidth and lessening the power allocated to the null frequencies. As a result, there is a reduced loss of signal power. Frequency diversity improvement can be realized by chopping the bandwidth into smaller bandwidths as in *orthogonal frequency division multiplexing* (OFDM). In each sub-carrier a lower data rate signal is sent. Thus, if there is a loss in a sub carrier then it is recoverable since it corresponds to the small part of the code.

2. 1. 7 Frequency Selective Fading

If channel coherence bandwidth is smaller than the signal bandwidth then the channel creates frequency selective fading. Spectral response of a radio signal will show dips due to the multipath. Channel spectral behavior shapes the signal spectrum leading to overlapping of successive symbols in the time domain. The symbol duration increases and symbol shape is distorted as a result of apparent *inter-symbol interference* (ISI).

In OFDM, each sub carrier undergoes flat fading since its bandwidth is less than the coherence bandwidth. Therefore ISI is eliminated within an OFDM symbol but OFDM symbols may still overlap with each other. Therefore a portion of the OFDM symbol, larger than the coherence bandwidth, is appended to the symbol i.e., to

overcome i.e., the ISI between symbols. Equalization is simple in OFDM since each sub carrier only needs a one tap equalizer.

2.2 Multiple Access techniques

Multiple access schemes are used to allow many users simultaneously to use the same fixed bandwidth radio spectrum [5]. In any radio service, the bandwidth which is allocated to it is always limited. For mobile phone systems the total bandwidth is typically 50MHz, which is split in half to provide the forward and reverse links of the system. Sharing of the spectrum is required in order to increase the user capacity of any wireless network. FDMA, TDMA and CDMA are the three major methods of sharing the available bandwidth to multiple users in wireless system. There are many extensions, and hybrid techniques for these methods, such as OFDM, and hybrid TDMA and FDMA systems. However, an understanding of the three major methods is required for understanding of any extensions to these methods.

2. 2. 1 Frequency Division Multiple Access

In Frequency Division Multiple Access (FDMA), the available bandwidth is subdivided into a number of narrower band channels. Each user is allocated a unique frequency band in which to transmit and receive. During a call, no other user can use the same channel. Each user is allocated a forward link channel (from the base station to the mobile phone) and a reverse channel (back to the base station), each being a one way link. The transmitted signal on each of the channels is continuous due to the analog transmissions. The bandwidths of FDMA channels are generally low (30 kHz) as each

channel only supports one user. FDMA is used for primary division of large allocated frequency bands, to become most multi-channel systems.

2. 2. 2 Time Division Multiple Access

(TDMA) divides the available spectrum into multiple time slots, by giving each user a time slot in which they can transmit or receive. TDMA systems transmit data in a buffer and burst method, thus the transmission of each channel is non-continuous. The input data to be transmitted is buffered over the previous frame and burst transmitted at a higher rate during the time slot for the channel. TDMA is used only for transmitting digital data. TDMA can suffer from multipath effects as the transmission rate is generally very high. TDMA is most often used in conjunction with FDMA.

2. 2. 3 Code Division Multiple Access

Code Division Multiple Access (CDMA) is a spread spectrum technique. In CDMA, the narrow band message (typically digitized voice data) is multiplied by a wide bandwidth signal which is a pseudo random noise code (PN code). Many users in a CDMA system operate on the same frequency and transmit simultaneously. The transmitted signal is recovered by correlating the received signal with the PN code used by the transmitter.

Some of the properties that have made CDMA useful are:

• Signal hiding and non-interference with existing systems.

• Anti-jam and interference rejection

• Information security

• Accurate Ranging

• Multiple User Access

• Multipath tolerance

One of the most important concepts in CDMA is the idea of process gain. The process gain of a system indicates the gain or signal to noise improvement obtained during the de-spreading process. The process gain of a system is equal to the ratio of the spread spectrum bandwidth used, to the original data bit rate. Thus, the process gain can be written as:

$$Gp = \frac{BW_{RF}}{BW_{\inf o}} \qquad \text{Eq (2.5)}$$

where BW_{RF} is the transmitted bandwidth after the data is spread, and $BW_{\inf o}$ is the bandwidth of the information data being sent. Figure 2.2 shows the process of a CDMA transmission. The data to be transmitted (a) is spread before transmission by modulating the data using a PN code. This broadens the spectrum as shown in (b). In this example the process gain is 125 as the spread spectrum bandwidth is 125 times greater than the data bandwidth. Part (c) shows the received signal. This consists of the required signal, plus background noise,

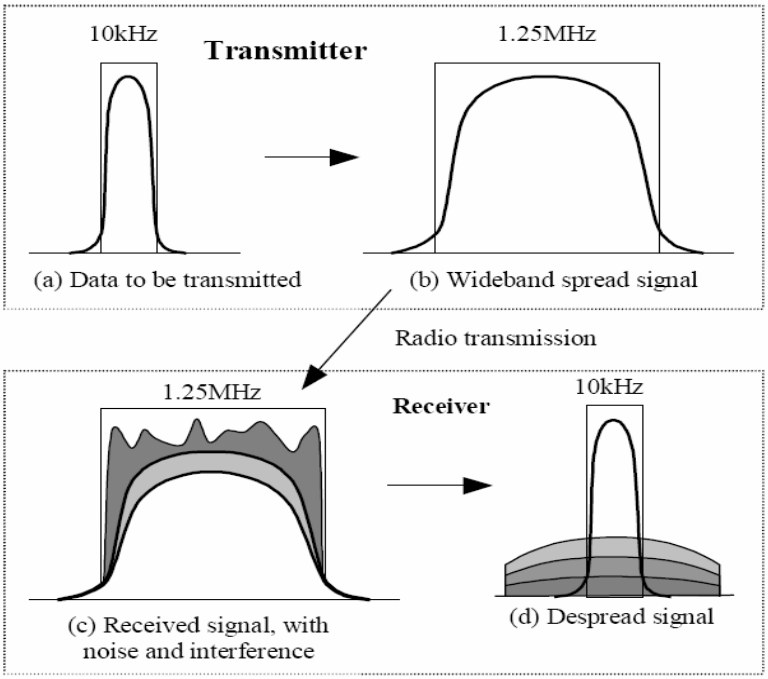

Figure 2.2 Basic CDMA transmission concept.

and any interference from other CDMA users or radio sources. The received signal is recovered by multiplying the signal by the original spreading code. This process causes the wanted received signal to be de-spread back to the original transmitted data.

The wanted signal in (d) is then filtered, removing the wide spread interference and noise signals.

2. 2. 4 CDMA Generation

Figure 2.3 illustrates CDMA generation: CDMA is achieved by modulating the data signal by a pseudo random noise sequence (PN code), which has a chip rate higher then the bit rate of the data. The PN code sequence is a sequence of ones and zeros (called chips), which alternate in a pseudo-random fashion. The data is modulated by

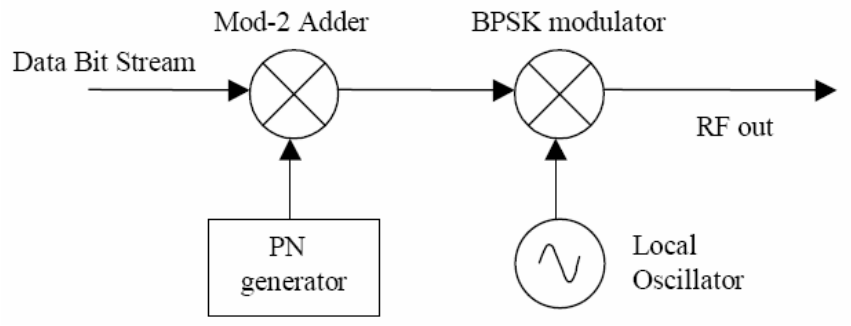

Figure 2.3 Basic CDMA transmitter.

modular-2 adding the data with the PN code sequence. This can also be done by multiplying the signals, provided the data and PN code is represented by 1 and -1 instead of 1 and 0. The PN code used to spread the data can be of two main types. A short PN code (typically 10-128 chips in length); can be used to modulate each data bit. The short PN code is then repeated for every data bit allowing for quick and simple synchronization of the receiver. Figure 2.4 shows the generation of a CDMA signal using a repeating 10-chip length short code. Alternatively a long PN code can be used. Long codes are generally thousands to millions of chips in length, thus are only repeated infrequently. Because of this they are useful for added security as they are more difficult to decode.

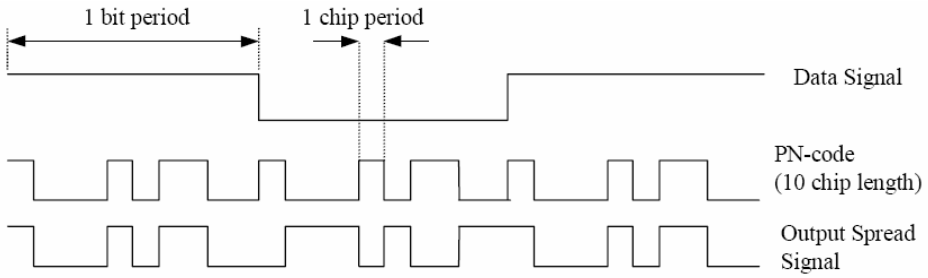

Figure 2.4 Generation of CDMA signal.

2. 2. 5 CDMA Forward Link Encoding

The forward link, from the base station to the mobile, of a CDMA system can use special orthogonal PN codes, called Walsh codes, for separating the multiple users on the same channel. These are based on a Walsh matrix, which is a square matrix with binary elements, and dimensions which are a power of two. It is generated from the basis that Walsh (1) = W1 = 0 and that:

$$W_{2n} = \begin{bmatrix} W_n & W_n \\ W_n & \overline{W_n} \end{bmatrix} \qquad \text{Eq (2.6)}$$

where, Wn is the Walsh matrix of dimension n. For example:

$$W_2 = \begin{bmatrix} 0 & 0 \\ 0 & 1 \end{bmatrix}$$

$$W_4 = \begin{bmatrix} 0 & 0 & 0 & 0 \\ 0 & 1 & 0 & 1 \\ 0 & 0 & 1 & 1 \\ 0 & 1 & 1 & 0 \end{bmatrix} \qquad \text{Eq (2.7)}$$

Walsh codes are orthogonal, which means that the dot product of any two rows is zero. This is due to the fact that for any two rows exactly half the number of bits match and half do not. Each row of a Walsh matrix can be used as the PN code of a user in a CDMA system. By doing this the signal from each user is orthogonal to the signal for

every other user, resulting in no interference between the signals. However, in order for Walsh codes to work the transmitted chips from all users must be synchronized. If the Walsh code used by one user is shifted in time by more then about 1/10 of chip period, with respect to all other Walsh codes, it looses its orthogonal nature. This results in inter-user interference.

2. 2. 6 CDMA Reverse Link Encoding

The reverse link is different from the forward link because the signals from each user do not originate from the same source, as in the forward link. The transmission from each user will arrive at a different time, due to propagation delay, and synchronization errors. Due to the unavoidable timing errors between the users, there is little point in using Walsh codes as they will no longer be orthogonal. For this reason simple pseudo random sequences which are uncorrelated, but not orthogonal are used for the PN codes of each user. The capacity is different for the forward and the reverse links because of this difference in modulation: the reverse link is not orthogonal, resulting in significant inter-user interference. For this reason the reverse channel sets the capacity of the system.

2.3 Orthogonal Signals and Vectors

The concept of orthogonal signals is essential for the understanding of OFDM (orthogonal frequency division multiplexing) and CDMA (code division multiple access) systems. In the normal sense, it seem unexpected that one can separately demodulate overlapping carriers (for OFDM) or detect a signal among other signals that share the same frequency band (for CDMA).

To understand orthogonality, it is very helpful to interpret signals as vectors. Like vectors, signals can be added, multiplied by a scalar, and they can be expanded into some basis system [2]. In fact, signals fit into a mathematical structure of a vector space. Although this concept may seem a bit abstract, vectors can be visualized by geometrical objects, and many conclusions can be drawn by simple geometrical arguments without lengthy formal derivations. So it is worthwhile to become familiar with this point of view.

2. 3. 1 The Fourier base signals

To visualize signals as vectors, consider the familiar example of a Fourier series. For reasons that will become obvious later, only the tie interval of one period of length T is considered. This means that some well behaved (e.g. integrable) real signal $x(t)$ may be non zero inside the time interval $0 <= t <= T$, but is set to $x(t)$=0 outside. Inside the interval, the signal can be written as a Fourier series.

$$x(t) = \frac{a_0}{2} + \sum_{k=1}^{\infty} a_k \cos(2\pi \frac{k}{T} t) - \sum_{k=1}^{\infty} b_k \sin(2\pi \frac{k}{T} t). \qquad \text{Eq (2.8)}$$

The Fourier coefficients a_k and b_k are given by-

$$a_k = \frac{2}{T}\int_0^T \cos(\frac{2\pi k}{T}t)x(t)dt \ , \ b_k = -\frac{2}{T}\int_0^T \sin(\frac{2\pi k}{T}t)x(t)dt \qquad \text{Eq (2.9)}$$

The coefficients are the amplitudes of the cosine and (negative) sine waves at the respective frequencies $f_k = k/T$. The cosine and (negative) sine waves are interpreted as the *basis* system for the (well-behaved) signals inside the time interval of length *T*. Every such signal can be expanded in to that basis system according to Eq (2.8) inside that interval. The underlying mathematical structure of the Fourier series is similar to the expansion of an N- dimensional vector $x \in R^N$ into a basis system $\{V_i\}_{i=1}^N$ according to

$$X = \sum_{i=1}^{N} \alpha_i V_i(t) \qquad \text{Eq (2.10)}$$

The basis system $\{V_i\}_{i=1}^N$ is called *orthonormal* if two different vectors are orthogonal (perpendicular) to each other and if they are normalized to length one, that is,

$$V_i \,.\, V_k = \partial_{ik} \qquad \text{Eq (2.11)}$$

where ∂_{ik} is the Kronecker Delta (∂_{ik}=1 for *i*=*k* and ∂_{ik}=0 otherwise) and the dot denotes the usual scalar product

$$X \,.\, Y = \sum_{i=1}^{N} x_i \, y_i = X^T Y \qquad \text{Eq (2.12)}$$

for real N-dimensional vectors. In that case, the coefficients α_i are given by

$$\alpha_i = V_i \,.\, \mathrm{X} \qquad \text{Eq (2.13)}$$

For an orthonormal basis system, the coefficients α_i can thus be interpreted as the projections of the vector X on to the base vectors, as depicted in figure 2.5 for N=2 Thus, α_i can be interpreted as the *amplitude* of X in the direction of V_i.

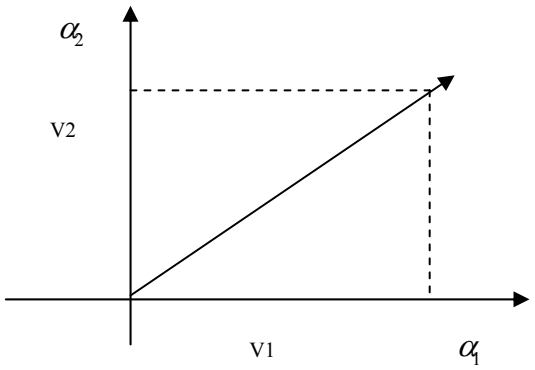

Figure 2.5 Signal Vector in two dimensions.

The Fourier expansion Eq (2.8) is of the same type as the expansion of Eq (2.8), except that the sum is infinite. For a better comparison, we may write

$$x(t) = \sum_{i=0}^{\infty} \alpha_i V_i(t) \qquad \text{Eq (2.14)}$$

with the normalized base signal vectors V_i defined by

$$V_0(t) = \sqrt{\frac{1}{T}}\Pi(\frac{t}{T} - \frac{1}{2}) \qquad \text{Eq (2.15)}$$

And

$$V_{2k}(t) = \sqrt{\frac{2}{T}}\cos(\frac{2\pi k}{T}t)\Pi(\frac{t}{T} - \frac{1}{2}) \qquad \text{Eq (2.16)}$$

for even $i > 0$ and

$$V_{2k+1}(t) = -\sqrt{\frac{2}{T}}\sin(\frac{2\pi k}{T}t)\Pi(\frac{t}{T}-\frac{1}{2}) \qquad \text{Eq (2.17)}$$

for odd *i* with coefficients given by

$$\alpha_i = \int_{-\infty}^{\infty} V_i(t)x(t)dt \qquad \text{Eq (2.18)}$$

that is,

$$\alpha_{2k} = \sqrt{T/2a_k} \qquad \text{Eq (2.19)}$$

and

$$\alpha_{2k+1} = \sqrt{T/2b_k} \qquad \text{Eq (2.20)}$$

Here Π(x) is the rectangular function, which takes the value one between x=-1/2 and x=1/2 and zero outside. Thus, Π(x-1/2) is the rectangle between x=0 and x=1. The basis of signals V_i fulfills the *orthonormality* condition.

$$\int_{-\infty}^{\infty} V_i(t)V_k(t)dt = \delta_{ik} \qquad \text{Eq (2.21)}$$

The Fourier basis systems forms one set of orthogonal signals, where the basis signals for different frequencies are orthogonal and for the same frequency $f_k = k/T$, the sine and cosine waves are orthogonal.

Note that the orthonormal condition and the formula for α_i are very similar to the case of finite-dimensional vectors. One just has to replace sums by integrals. A similar geometrical interpretation is also possible; one has to regard signals as vectors, that is, identify $V_i(t)$ with V_i and *x (t)* with X. The interpretation of α_i as a projection

on V_i is obvious. For only two dimensions, $x(t) = \alpha_1 V_1(t) + \alpha_2 V_2(t)$, and the signals can be adequately described by figure 2.5. In this special case, where $V_1(t)$ is a cosine signal and $V_2(t)$ is a (negative) sine signal, the figure 2.5 depicts nothing else but the familiar phasor diagram. However, this is just a special case of a very general concept that applies to many other scenarios in communications.

2.4 Evolution of OFDM

The use of Frequency Division Multiplexing (FDM) goes back over a century, where more than one low rate signal, such as telegraph, was carried over a relatively wide bandwidth channel using a separate carrier frequency for each signal [3]. To facilitate separation of signals at the receiver, the carrier frequencies were spaced sufficiently far apart between the signals so that they could be separated with readily realizable filters. The resulting spectral efficiency was therefore quite low.

Instead of carrying separate messages, the different frequency carriers can carry different bits of a single high rate message. The source may be in such a parallel format, or a serial source can be presented to a serial-to-parallel converter whose output is fed to the multiple carriers. Spectrum of such parallel system is shown in figure 2.6

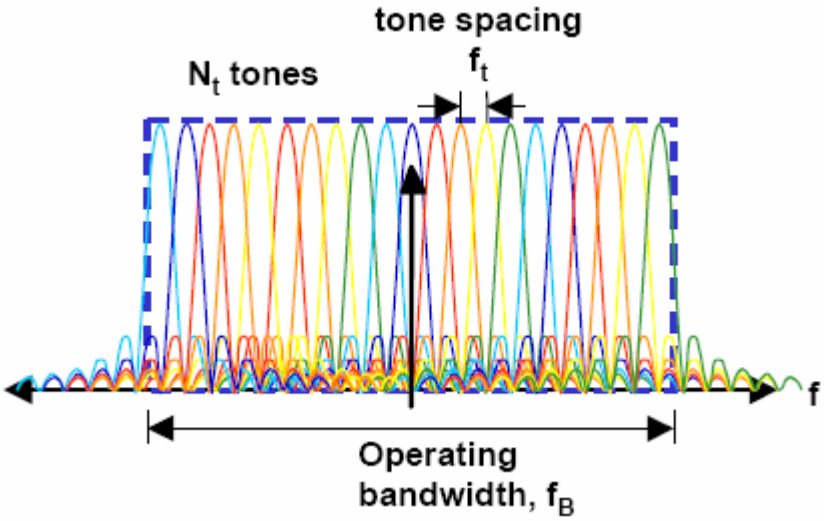

Figure 2.6 Spectrum Overlap in OFDM.

Such a parallel transmission scheme can be compared with a single high rate serial scheme using the same channel. The parallel system, if built straightforwardly as several transmitters and receivers, will certainly be more costly to implement. Each of

the parallel sub-channels can carry a low signaling rate, proportional to its bandwidth. The sum of these signaling rates is less than can be carried by a single serial channel of that combined bandwidth because of the unused guard space between the parallel sub-carriers. On the other hand, the single channel will be far more susceptible to inter-symbol interference. This is because of the short duration of its signal elements and the higher distortion produced by its wider frequency band, as compared with the long duration signal elements and narrow bandwidth in sub-channels in the parallel system.

Before the development of equalization, the parallel technique was the preferred means of achieving high rates over a dispersive channel. In spite of its high cost and relative bandwidth inefficiency, an added benefit of the parallel technique is reduced susceptibility to most forms of impulse noise.

An earlier version of OFDM is shown in figure 2.7 where separate I and Q modulators are used for every sub-carrier: the signals from the sub-carriers are then added together to form one single band. Block diagram of a very basic DMT (*Discrete Multi-tone*)(OFDM) system is shown in figure 2.8 [3] . The issue is how to transmit the sequence of complex numbers from the output of the inverse FFT over the channel. The process is straightforward if the signal is to be further modulated by a modulator with *I* and Q inputs. This is discussed in greater depth in section 3.3.

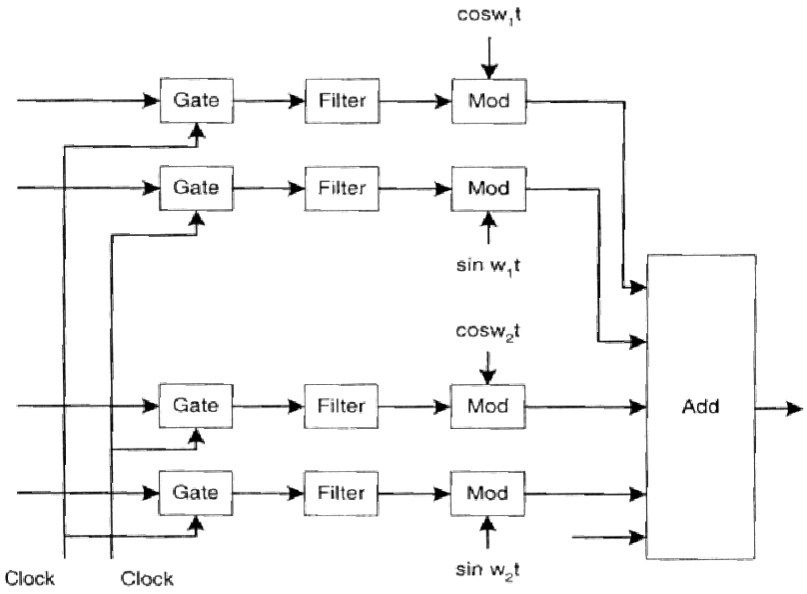

Figure 2.7 An early version of OFDM.

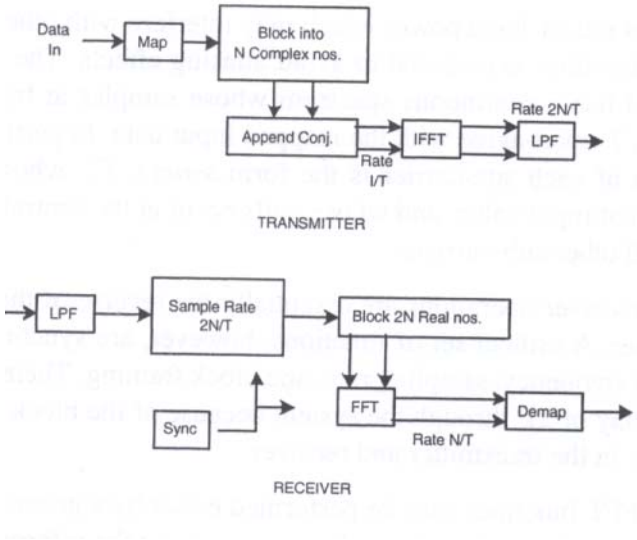

Figure 2.8 Very basic OFDM system.

The issue brought up in above section leads to the identification of major contribution to the OFDM complexity problem, i.e. Fast Fourier Transform (FFT) to the modulation and demodulation processes. Fortunately, this occurred at the same time digital signal processing techniques were being introduced in to the design of modems. The technique involved assembling the input information in to blocks of N complex numbers, on for each sub-channel. An inverse FFT is performed on each block, and the resultant transmitted serially. At the receiver, the information is recovered by performing an FFT on the received block of signal samples. This form of OFDM is often referred to as *Discrete Multi-tone* (DMT) [3]. The spectrum of the signal on the line is identical to that of N separate QAM signals, at N frequencies separated by the signaling rate. Each such QAM signal carries one of the original input complex numbers. The spectrum of each QAM signal is of the form $\sin(kf)/f$, with nulls at the center of the other sub-carriers,

As told earlier, if the output of IFFT is modulated again by separate I and Q modulator the approach is straight forward. Due to the present day development in simulation tools and software's, it makes it very easy to operate on real signal .If we consider real signal, it is necessary to transmit real quantities. This can be accomplished by first appending the complex conjugate to the original input block. A 2N-point inverse FFT now yields 2N real numbers to be transmitted per block which is equivalent to N complex numbers. This concept is very crucial for this thesis, which is why this is explained in detail in section (3.3).

The most significant advantage of this DMT approach (figure 2.8) [3] is the efficiency of the FFT algorithm. An N-point FFT requires only on the order of $N \log N$ multiplications, rather than N^2 as in a straightforward computation. The efficiency is particularly good when N is a power of 2, although that is not generally necessary. Because of the use of FFT, a DMT system typically requires fewer computations per unit time than an equivalent single channel system with equalizations. An overall cost comparison between the two systems is not as clear, but the costs should be approximately equal in most cases. It should be noted that the band limited system of figure can also be implemented with FFT techniques, although the complexity and delay will be greater than DMT. Over the last 20 years, or so, OFDM techniques and, in particular, the DMT implementation, has been used in a wide variety of applications. Several OFDM voice-band modems have been introduced, but did not succeed commercially because they were not adopted by standards bodies. DMT has been adopted as the standard for the Asymmetric Digital Subscriber Line (ADSL), which provides digital communication at several Mbps from a telephone company central office to a subscriber, and a lower rate in reverse direction, over a normal twisted pair to wires in the loop plant. OFDM has been particularly successful in numerous wireless applications, where its superior performance in multi-path environments is desirable. Wireless receivers detect signals distorted by time and frequency selective fading. OFDM in conjunction with proper coding and interleaving is a powerful technique for combating the wireless channel impairments that a typical OFDM wireless system might face, as is shown in figure 2.9

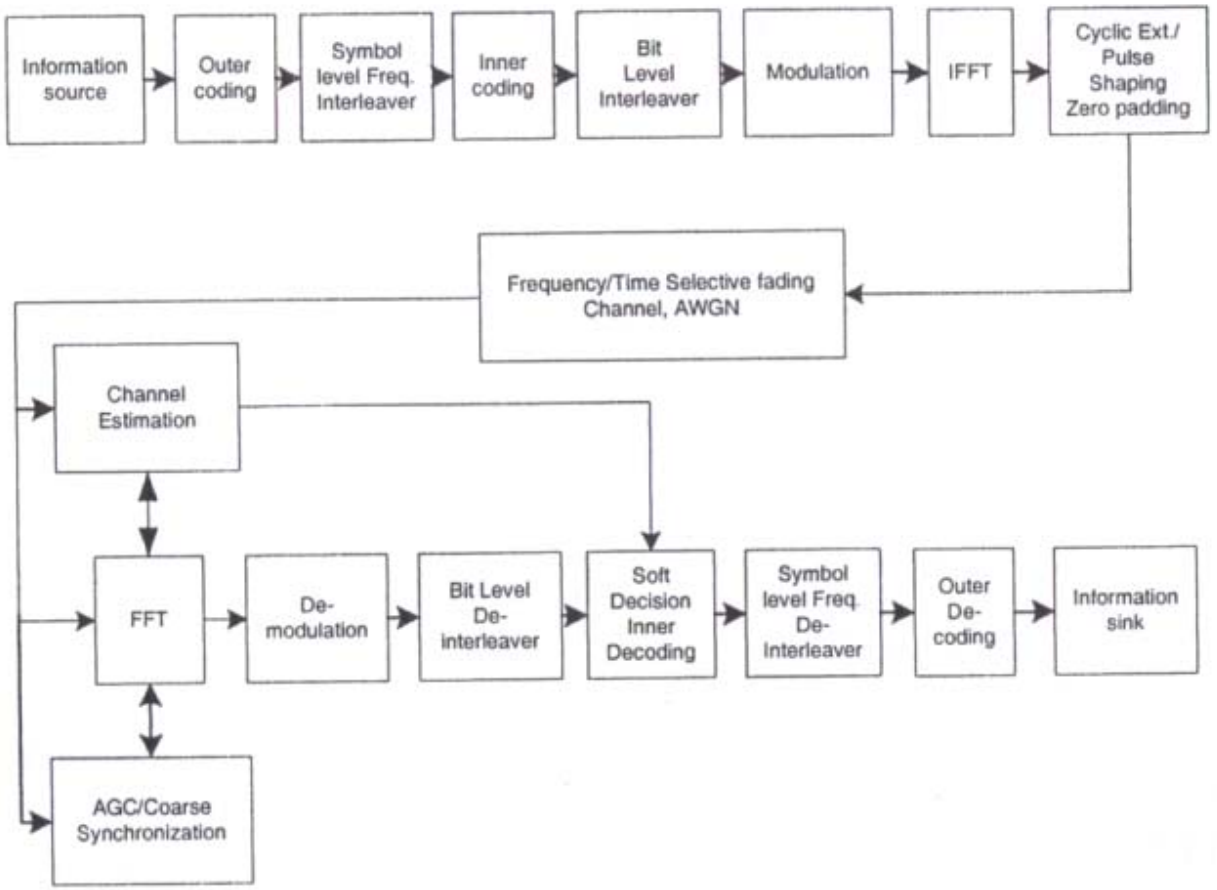

Figure 2.9 A typical OFDM wireless system.

2.5 Multi- carrier system fundamentals

In this section we will discuss the ability of OFDM to avoid inter symbol interference and the concept of transmitting real quantities, instead of I and Q components separately [2]

Let $[D_0, D_1, ...D_{N-1}]$ denote data symbols which is where $D = S_i(t)$ for $i \in \{1, ...M\}$.Digital signal processing techniques, rather than frequency synthesizers, can be deployed to generate orthogonal sub-carriers. The DFT as a linear transformation maps the complex data symbols $[D_0, D_1, ...D_{N-1}]$to OFDM symbols $[d_0, d_1, ...d_{N-1}]$ such that

$$d_k = \sum_{n=0}^{N-1} D_n e^{j2\pi n \frac{k}{N}} \qquad \text{Eq (2.22)}$$

The Linear mapping can be represented in matrix form as:

$$\bar{d} = \bar{W}\bar{D}, \qquad \text{Eq (2.23)}$$

where

$$\bar{W} = \begin{bmatrix} 1 & \cdots & 1 & 1 \\ 1 & W & \cdots & W^{N-1} \\ 1 & W^2 & \cdots & W^{2(N-1)} \\ \vdots & & & \vdots \\ 1 & W^{N-1} & & W^{N(N-1)} \end{bmatrix} \qquad \text{Eq (2.24)}$$

and

$$W = e^{j\frac{2\pi}{N}} \qquad \text{Eq (2.25)}$$

$\overline{W}$, is a symmetric and orthogonal matrix. After FFT, a cyclic pre/postfix of lengths *k1* and *k2* will be added to each block (OFDM symbol) followed by a pulse shaping block. Proper pulse shaping has an important effect in improving the performance of OFDM systems in the presence of some channel impairments. The output of this block is fed into a D/A at the rate of *f* and low-pass filtered. A basic representation of the equivalent complex baseband transmitted signal is

$$x(t) = \sum_{n=0}^{N-1} \{D_n e^{j2\pi \frac{n}{N} f_s t}\} \qquad \text{Eq (2.26)}$$

for

$$-\frac{k_1}{f_s} < t < \frac{N + k_2}{f_s} \qquad \text{Eq (2.27)}$$

A more accurate representation of OFDM signal including windowing effect is,

$$x(t) = \sum_{l=-\infty}^{\infty} \sum_{k=-k_1}^{N+k_2} \sum_{n=0}^{N-1} \{D_{nl} e^{j2\pi \frac{n}{N} k}\} w(t - \frac{k}{f_s} - lT) \qquad \text{Eq (2.28)}$$

D_{nl} represents the *nth* data symbol transmitted during the *lth* OFDM block, $T = (N+k1+k2) / fs$, is the OFDM block duration, and *w(t)* is the window or pulse shaping function.

The extension of the OFDM block is equivalent to adding a cyclic pre/postfix in the discrete domain. The received signal for a time-varying random channel is

$$r(t) = \int_0^{\infty} x(t-\tau)h(t,\tau)d\tau + n(t). \qquad \text{Eq (2.29)}$$

The received signal is sampled at $t = \frac{k}{f_s}$ for $k = \{-k1, \ldots N+k2-1\}$. With no inter-block interference, and assuming that the windowing function satisfies $w(n-1) = \delta_{nl}$, the output of the FFT block at the receiver is

$$\tilde{D}_m = \frac{1}{N}\sum_{k=0}^{N-1} r_k e^{-j2\pi m\frac{k}{2N}}, \qquad \text{Eq (2.30)}$$

where,

$$r_k = \sum_{n=0}^{N-1} H_n D_n e^{j2\pi\frac{n}{2N}k} + n(k). \qquad \text{Eq (2.31)}$$

A complex number *H,* is the frequency response of the time-invariant channel *h(t — r)* at frequency *n/T.* So,

$$\tilde{D}_m = \begin{cases} H_n D_n + N(n), & n = m \\ N(n), & n \neq m \end{cases} \qquad \text{Eq (2.32)}$$

n(t) is white Gaussian noise with a diagonal covariance matrix of $E(n(k)n(1)) = \delta I$

Therefore, the noise components for different sub- carriers are not correlated,

$$E(\bar{n}(k)\bar{n}^*(l)) = W\delta I W^T = \delta I. \qquad \text{Eq (2.33)}$$

where *ñ(k)* is the vector of noise samples **{** *n(k),. . ,n(k — N)*}.

2.6 Complex number TX systems and its simplification to real sequence transmission

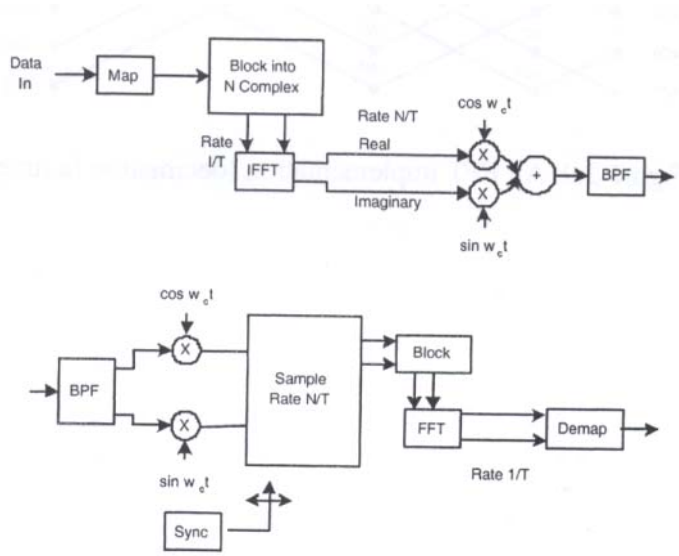

Figure 2.10 System with complex transmission.

Above figure 2.10, represents the transmitter and receiver for transmitting complex numbers. The complex number $a + ib$ is divided into in-phase and quadrature components and multiplied separately with a separate carrier and combined in the end to form a band pass signal. Opposite procedures are followed while receiving the information. To reduce the complexity of I and Q transmitter and receiver block we can transmit the real sequence. The following section illustrates the feasibility of such transmission system.

Figure 2.11 below represents the IFFT block based 2N real sequence number transmission system.

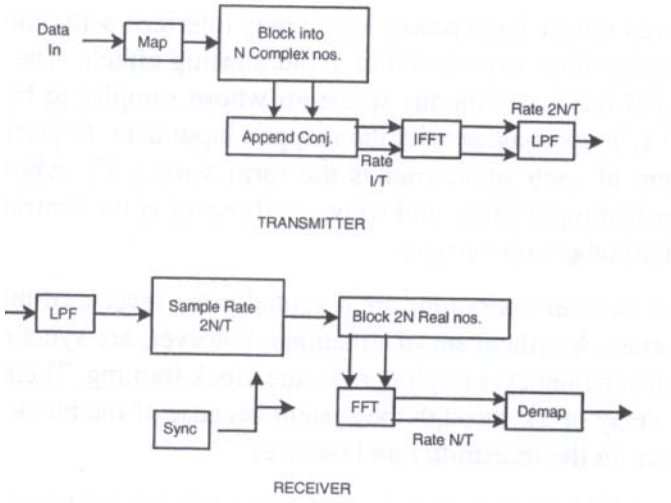

Figure 2.11 System with real transmission.

The key components of an OFDM system are the Inverse DFT in the transmitter and DFT in the receiver.

The augmented sequence is formed from the original sequence as

$$D'_n = \begin{cases} D_n, & n = 1, \cdots, N-1 \\ D^*_{2N-n}, & n = N+1, \cdots, 2N-1 \end{cases} \qquad \text{Eq (2.34)}$$

In order to maintain conjugate symmetry, it is essential that D'_0 and D'_N be real. If the original D_0 is zero, as is common, then D'_0 and D'_N, are set to zero. Otherwise, D'_0 may be set to Re (D_0) and D'_N, to Im (D_0).

For the simple case of $D_0 = 0$, the output of the IFFT is:

$$
\begin{aligned}
d_m &= \sum_{n=0}^{2N-1} D'_n e^{\frac{j\pi mn}{N}} \\
&= 2Re \sum_{n=0}^{N-1} D_n e^{\frac{j\pi mn}{N}} \\
&= 2 \sum_{n=0}^{N-1} [A_n cos\frac{\pi mn}{N} - B_n sin\frac{\pi mn}{N}], \quad m = 0, \cdots, 2N-1,
\end{aligned}
$$

Eq (2.35)

where, $D_n = A_n + jB_n$. Of course a scaling by 2 is immaterial and can be dropped. This real orthogonal transmission is fully equal to complex one, and all subsequent analysis are applicable.

2.7 Cyclic Extension

The signal and channel, however, are linearly convolved. After adding prefix and postfix extensions to each block, the linear convolution is equivalent to a circular convolution as shown in Figure 2.12. Instead of adding a prefix and a postfix, some systems use only prefix, then by adjusting the window position at the receiver proper cyclic effect will be achieved. Using this technique, a signal, otherwise aliased appears infinitely periodic to the channel. Let's assume the channel response is spread over *M* samples, and the data block has *N* samples then:

Eq (2.36)

$$y(n) = \sum_{m=0}^{N-1} d(m)h(n-m) \quad X\, R_N(n), \quad n = 0,1,....., N+M-1$$

Where $R_N(n)$ is a rectangular window of length *N*. To describe the effect of distortion, we proceed with the Fourier Transform noting that convolution is linear

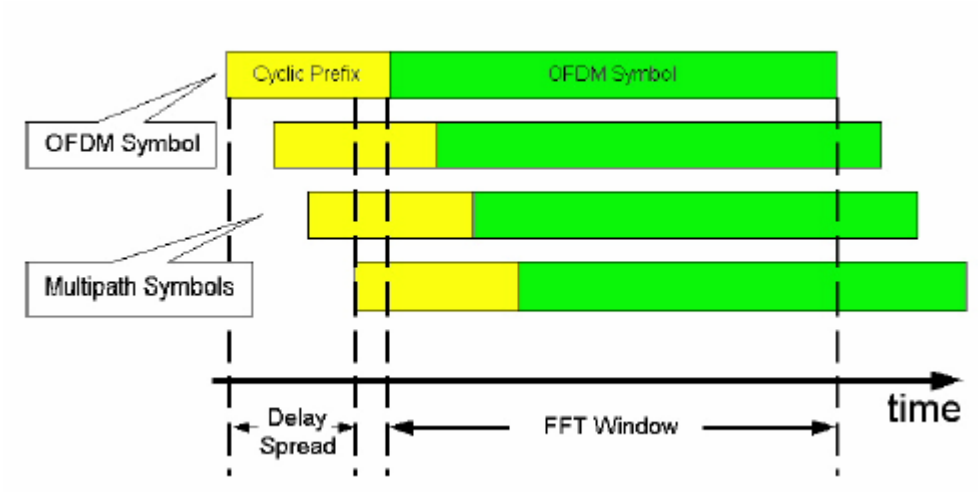

Figure 2.12 Prefix and post fix cyclic extension.

$$Y(k) = Y(e^{jw})\Big|_{\omega = k\omega_s} = \{D(e^{jw}) \times H(e^{jw})\} * \frac{sin\omega\frac{N}{2}}{sin\frac{\omega}{2}} e^{j\omega\frac{N-1}{2}}\Big|_{\omega = k\omega_s} \quad \text{Eq (2.37)}$$

After linear convolution of the signal and channel impulse response, the received sequence is of length $N + M - 1$. The sequence is truncated to N samples and transformed to the frequency domain, which is equivalent to convolution and truncation. However, in the case of cyclic pre/postfix extension, the linear convolution is the same as the circular convolution as long as channel spread is shorter than guard interval. After truncation, the DFT can be applied, resulting in a sequence of length N because the circular convolution of the two sequences has period of N.

Intuitively, an N-point DFT of a sequence corresponds to a Fourier series of the periodic extension of the sequence with a period of N. So, in the case of no cyclic extension we have

$$\sum_{i=-\infty}^{\infty} \sum_{m=0}^{N-1} d(m)h(n+iN-m), \qquad \text{Eq (2.38)}$$

Which is equivalent to repeating a block of length N + M — 1 with period N. This results in aliasing or inter-symbol interference between adjacent OFDM symbols. In other words, the samples close to the boundaries of each symbol experience considerable distortion, and with longer delay spread, more samples will be affected. Using the cyclic extension, the convolution changes to a circular operation, Circular convolution of two signals of length N is a sequence of length N so the inter-block interference issue is resolved.

CHAPTER 3

OVERALL SYSTEM DESIGN

3.1 Design of the OFDM Signal

The proposal of a realistic OFDM-based wavelet diversity communications system was one of the goals of this research project. Therefore, we elaborate here on some hardware- related design considerations. Elements of the transmission chain that have impact on the design of the transmitted OFDM signal include the following:

The time-dispersive nature of the mobile channel: the transmission scheme must be able to cope with this. The bandwidth limitation of the channel: The signal should occupy as little bandwidth as possible and introduce a minimum amount of interference to systems on adjacent channels [1][2].

The Transfer functions of the transmitter/receiver hardware. This TF reduces the useable bandwidth compared to the theoretical one given by the sampling theorem.
That is, some over sampling is required. Phase jitter and frequency offsets of the up- and down-converters, and Doppler spreading of the channel. As mentioned earlier, a GI (*guard interval*) is introduced to preserve the orthogonality of the SCs and the independence of subsequent OFDM symbols, when the OFDM signal is transmitted over a multipath radio channel. The GI, a cyclic prefix, is a copy of the last part of the OFDM symbol, which is transmitted before the so-called effective part of the symbol (see Figure 3.1). Its duration T_{guard} is simply selected to be larger than the maximum

excess delay of the (worst-case) radio channel. Therefore, the effective part of the received signal can be seen as the cyclic convolution of the transmitted OFDM symbol by the channel impulse response.

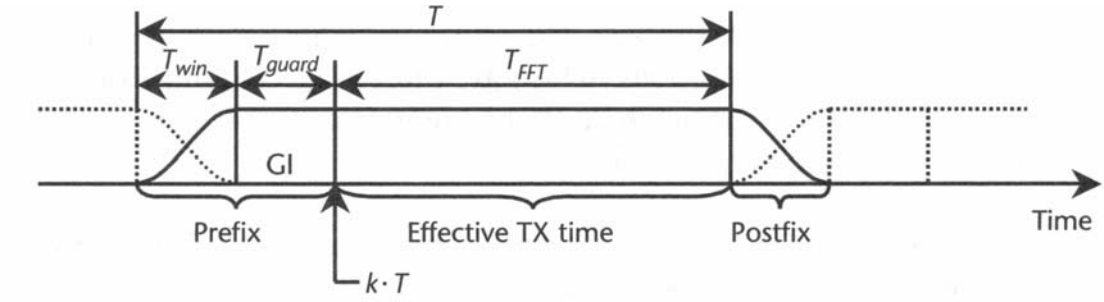

Figure 3.1 Time domain OFDM symbol.

3.1.1 Spectrum of the Transmitter Pulse Shape

Because of the low pass filters required for the analog-to-digital (ADC) and digital- to-analog (DAC) conversion of the transmitted and received (baseband) signals, not all N SCs can be used, if an N-point IFFT is applied for modulation. The SCs close to the Nyquist frequency $f_s / 2$ will be attenuated by these filters and, thus, cannot be used for data transmission (see Figure 3.2*)*. (f_s=1/Ts is the sampling frequency.) Also the dc SC might be heavily distorted by dc offsets of the ADCs and DACs, by carrier feed through, and so forth, and should thus be avoided for data.

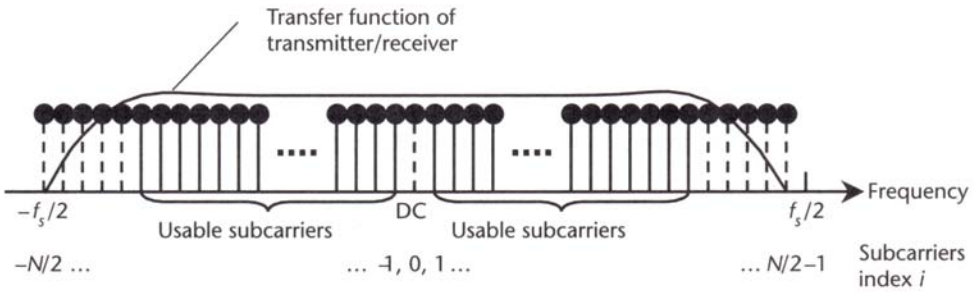

Figure 3.2 Transfer function of OFDM symbols.

3.2 OFDM system Model

The above-introduced features of the OFDM signal are defined mathematically in this section. This will lead to the conclusion that, using the OFDM principle, data symbols can be transmitted over multipath radio channels without influencing each other. Signal Model and Definitions **.**Mathematically, the OFDM signal is expressed as a sum of the prototype pulses shifted in the time and frequency directions and multiplied by the data symbols. In continuous-time notation, the k^{th} OFDM symbol is written

$$s_{RF,k}(t-kT)=\begin{cases}\mathrm{Re}\left\{w(t-kT)\sum_{i=-N/2}^{N/2-1}x_{i,k}e^{j2\pi\left(f_c+\frac{i}{T_{FFT}}\right)(t-kT)}\right\} \\ kT-T_{win}-T_{guard}\le t\le kT+T_{FFT}+T_{win} \quad otherwise \\ 0\end{cases} \qquad \text{Eq (3.1)}$$

Most of the mathematical symbols have been defined in the previous figures already. A complete list of symbols is given here:

T : Symbol length; time between two consecutive OFDM symbols;

T_{FFT} : FFT time; effective part of the OFDM symbol;

T_{guard} : GI; duration of the cyclic prefix;

T_{win} : Window interval; duration of windowed prefix/postfix for spectral shaping;

f_c : Center frequency of the occupied frequency spectrum;

$F = 1/T_{FFT}$: Frequency spacing between adjacent SCs;

N: FFT length; number of FFT points;

k : Index on transmitted symbol;

i: Index on SC; $i \in \{-N/2, -N/2+1, \ldots -1, 0, 1, \ldots N/2-1\}$

$x_{i,k}$: Signal constellation point; complex {data, pilot, null) symbol modulated on the i^{th} SC of the k^{th} OFDM symbol;

$w(t)$: The transmitter pulse shape defined as

$$w(t) = \begin{cases} \frac{1}{2}\left[1 - \cos\pi\left(t + T_{win} + T_{guard}\right)/T_{win}\right] & -T_{win} - T_{guard} \le t < -T_{guard} \\ 1 & -T_{guard} \le t \le T_{FFT} \\ \frac{1}{2}\left[1 - \cos\pi\left(t - T_{FFT}\right)/T_{win}\right] & T_{FFT} < t \le T_{FFT} + T_{win} \end{cases} \quad \text{Eq (3.2)}$$

Finally a continuous sequence of transmitted symbols is expressed as

$$s_{RF}(t) = \sum_{k=-\infty}^{\infty} S_{RF,k}(t - kT) \quad \text{Eq (3.3)}$$

From (3.1) to (3.3), the complex equivalent low-pass signal transmitted can be given. The complex envelope of the OFDM signal is written

$$s(t) = \sum_{k=-\infty}^{\infty} S_k(t - kT) \qquad \text{Eq (3.4)}$$

with

$$s_k(t - kT) = \begin{cases} w(t - kT) \sum_{i=-N/2}^{N/2-1} x_{i,k} e^{j2\pi\left(\frac{i}{T_{FFT}}\right)(t-kT)} \\ kT - T_{win} - T_{guard} \le t \le kT + T_{FFT} + T_{win} \; otherwise \\ 0 \end{cases} \qquad \text{Eq (3.5)}$$

Note the similarities of this expression with Fourier series.

$$v(t) = \sum_{n=-\infty}^{\infty} c(nf_0) e^{j2\pi nf_0 t} \qquad \text{Eq (3.6)}$$

where the complex-valued Fourier coefficients *c(nf0)* represent the complex-valued signal constellation points $x_{i,k}$, and the frequencies *nf0* correspond to the SC frequencies i/T_{FFT}.

In a digital system, this modulated waveform can be generated by an IDFT or by its computationally efficient implementation, the IFFT. The data constellations $x_{i,k}$ are the input to this IFFT; the TD OFDM symbol is its output.

3.3 OFDM demodulation

The demodulation of the OFDM signal should be performed by a bank of filters, which are "matched" to the effective part $[kT, kT + T_{FFT}]$ of the OFDM symbol. The reverse operation to (3.6), that is, the extraction of the Fourier coefficients $c(nf_0)(= x_{i,k})$ from the TD signal *v(t)(=r(t)),* exactly formulates such a bank of matched filters. It is written

$$c(nf_0) = \frac{1}{T_0} \int_{T_0} v(t) e^{-j2\pi n f_0 t} \, dt \qquad \text{Eq (3.7)}$$

where T_0 is the integration period equivalent to T_{FFT}. In a digital implementation, a DFT or (preferably) an FFT is used to realize these filters.

Assuming knowledge of the exact time instants kT at which the OFDM symbols start, we try to extract the transmitted signal constellations $x_{i,k}$ from the received signal *r(t).* The received signal constellations are denoted by $y_{i,k}$.

$$y_{i,k} = \frac{1}{T_{FFT}} \int_{t=kT}^{kT+T_{FFT}} r(t) e^{-j2\pi i(t-kT)/T_{FFT}} \, dt = \frac{1}{T_{FFT}} \int_{t=kT}^{kT+T_{FFT}} \left[\int_{\tau=0}^{\tau_{max}} h_k(\tau) s(t-\tau) d\tau + n(t) \right] e^{-j2\pi i(t-kT)/T_{FFT}} \, dt \qquad \text{Eq (3.8)}$$

Because of the integration ranges in (3.8) and $T_{\max} < T_{guard}$ there is no influence on the adjacent OFDM symbols transmitted, and *s(t)* can be replaced by $s_k(t)$ [see (3.5)]

$$y_{i,k} = \frac{1}{T_{FFT}} \int_{t=kT}^{kT+T_{FFT}} \left[\int_{\tau=0}^{\tau_{max}} h_k(\tau) \sum_{i'=-N/2}^{N/2-1} x_{i',k} e^{j2\pi \left(\frac{i'}{T_{FFT}} \right)(t-kT-\tau)} d\tau \right] e^{-j2\pi i(t-kT)/T_{FFT}} \, dt + \frac{1}{T_{FFT}} \int_{t=kT}^{kT+T_{FFT}} n(t) e^{-j2\pi i(t-kT)/T_{FFT}} \, dt \qquad \text{Eq (3.9)}$$

Note that $w(t-KT)=1$ in the range of integration. The window is thus omitted in this equation. The second integral in (3.9) leads to independent additive noise samples *n* Since the complex exponential terms represent orthogonal functions.

Substituting $u = t - KT$ for the ease of notation and changing the order of integration and summation yields

$$y_{i,k} = \sum_{i'=-N/2}^{N/2-1} x_{i',k} \frac{1}{T_{FFT}} \int_{u=0}^{T_{FFT}} \left[\int_{\tau=0}^{\tau_{max}} h_k(\tau) e^{-j2\pi i'(u-\tau)/T_{FFT}} d\tau \right] e^{-j2\pi iu/T_{FFT}} du + n_{i,k} = \sum_{i'=-N/2}^{N/2-1} x_{i',k} \frac{1}{T_{FFT}} \int_{u=0}^{T_{FFT}} \left[\int_{\tau=0}^{\tau_{max}} h_k(\tau) e^{-j2\pi i'\tau/T_{FFT}} d\tau \right] e^{-j2\pi (i-i')u/T_{FFT}} du + n_{i,k} \quad \text{Eq (3.10)}$$

The inner integral of the second expression represents the FT of $h_k(t)$ at the frequency instants i'/T_{FFT}. = $i'F$, which is the sampled channel TF at time *kT*. It is expressed by the channel coefficients

$$h_{i',k} = FT\{h_k(\tau)\} = \int_{\tau=0}^{\tau_{max}} h_k(\tau) e^{-j2\pi i'\tau/T_{FFT}} d\tau = H(i'F, kT) \quad \text{Eq (3.11)}$$

Using this notation, the output of the receiver filter bank simplifies to

$$y_{i,k} = \sum_{i'=-N/2}^{N/2-1} x_{i',k} h_{i',k} \frac{1}{T_{FFT}} \int_{u=0}^{T_{FFT}} e^{-j2\pi (i-i')u/T_{FFT}} du + n_{i,k} \quad \text{Eq (3.12)}$$

The integral in this equation has the value 1, only if $i = i'$. For $i \neq i'$, with *i* and *i'* being integer values, the integral is zero. Thus, we finally obtain.

$$y_{i,k} = x_{i,k} h_{i,k} + n_{i,k} \quad \text{Eq (3.13)}$$

From this form **it** is seen that a perfectly synchronized OFDM system can be viewed as a set of parallel Gaussian channels. The multipath channel introduces an attenuation/amplification and phase rotation according to the (complex-valued) channel coefficients $\{h_{i,k}\}$.

Channel estimation is required in order to retrieve the data contained in these signal constellations because the receiver must have a phase (and amplitude) reference to detect the transmitted symbol correctly. Differential detection can be used alternatively, in which case the decision is made by comparing the phases (and amplitudes) of symbols transmitted over adjacent SCs or subsequent OFDM symbols.

CHAPTER 4

CHANNEL CONSIDERATIONS

4.1 Performance of OFDM in RAYLEIGH fading channel

In general, OFDM is a parallel transmission technique in which N complex symbols modulate N orthogonal waveforms $\psi_i(t)$ which maintain their orthogonality at the output of the channel. This requires that the correlation function of the channel output process, in response to different waveforms, has orthogonal Eigen functions [3].

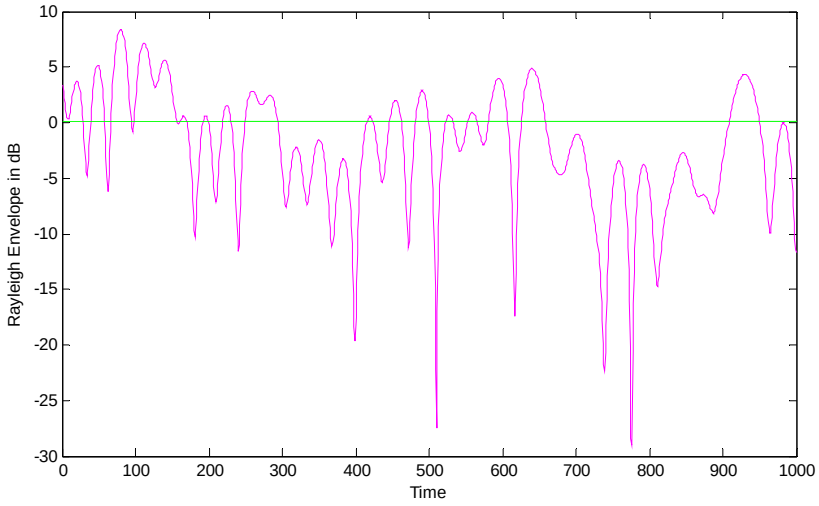

Figure 4.1 Rayleigh channel envelope.

Let $h(t,\tau)$ be the Rayleigh distributed, time-varying complex impulse response of the channel, while $R(t,\tau)$ denotes the complex correlation of the output in response to a basic pulse shape $f(t)$:

$$R(t,\tau) = E\{y(t)y(t+\tau)^*\}. \qquad \text{Eq (4.1)}$$

Using Karhunen-Loeve expansion, the output of the channel y(t) can be represented as

$$y(t) = \sum_i D_i y_i \varphi_i(t), \qquad \text{Eq (4.2)}$$

where the $\varphi_i(t)$ s are eigen functions of the correlation function $R(t,\tau)$ and

$$y_i = \int y(t)\varphi_i(t)dt, \qquad \text{Eq (4.3)}$$

The corresponding eigen values of the correlation function are λ_i , where

$$\int R(t,\tau)\varphi_i(\tau)d\tau = \lambda_i \varphi_i(t). \qquad \text{Eq (4.4)}$$

For a Gaussian random process *y(t),* the coefficients in Equation 4.2 are Gaussian random variables and their powers are the corresponding eigen values. If the input consists of orthogonal modulating functions which are harmonics of the form

$$\psi_k(t) = u(t)e^{j2\pi f_k t}, \qquad \text{Eq (4.5)}$$

where, $u(t)$ is the basic waveform such as time-limited gating function. The eigen functions of the received signal correlation function $R(t,\tau)$ are,

$$\varphi_i(t)e^{j2\pi f_i t}, \qquad \text{Eq (4.6)}$$

where , again $\varphi_i(t)$ are the eigen functions' output correlation functions in response to basic waveform $u(t)$ .Therefore, the orthogonality condition is,

$$\int \varphi_i(t)\varphi_k^*(t)e^{j2\pi(f_i - f_k)}dt = 0 \qquad \text{Eq (4.7)}$$

which can be achieved by increasing $\delta f = f_{i+1} - f_i$. Analytically this means that l_2 sub-spaces spanned by different eigen functions are mutually orthogonal. In other words, the

frequency response of the channel for different frequency bins is independent. For a pure tone signal of frequency f_k, the output of random channel is:

$$\begin{aligned} y_k(t) &= \int h(t,\tau)x(t-\tau)d\tau = \int h(t,\tau)e^{j2\pi f_k(t-\tau)}d\tau \\ &= e^{j2\pi f_k t}\int h(t,\tau)e^{-j2\pi f_k \tau}d\tau \end{aligned} \quad \text{Eq (4.8)}$$

The transfer function of a time-varying channel is defined as

$$H(f,t) = \int e^{-j2\pi f\tau}h(t,\tau)d\tau, \quad \text{Eq (4.9)}$$

so the output of channel can be represented as

$$y_k(t) = H(f_k,t)e^{j2\pi f_k t}, \quad \text{Eq (4.10)}$$

and the orthogonality requirement of the output processes holds. If the filter gains $H(f_k,t)$ are orthogonal, and the tap filters are non- correlated and Gaussian, then they will be independent too. As an example, consider orthogonal functions of the form

$$\varphi_{ik}(t) = u(t-iT)e^{2j\pi f_k(t-jT)}. \quad \text{Eq (4.11)}$$

This set of orthogonal functions is used to modulate data symbols and transmit them in a single OFDM symbol timing interval such that the orthogonality in the frequency domain is preserved. By choosing the above set of orthogonal functions, the eigen functions used in Karhunen-Loeve expansion will be related as shown in Equation 4.2. The optimum receiver maximizes a posteriori probability (conditional probability of the received signal given a particular sequence is transmitted). Usually, channel characteristics do not change during one or a few symbols. Therefore, the channel output can be represented as

$$y(t) = \sum_k H(f_k, t) e^{j2\pi f_k t}. \qquad \text{Eq (4.12)}$$

The received signal $r(t) = y(t) + n(t)$ with *n(t)* representing additive white Gaussian noise can be expanded as

$$r(t) = \sum_i r_i \varphi_i(t), \qquad \text{Eq (4.13)}$$

where

$$\begin{aligned} r_i &= y_i + n_i \\ n_i &= \int n(t)\varphi_i(t)dt \\ y_i &= \int y(t)\varphi_i(t)dt \end{aligned} \qquad \text{Eq (4.14)}$$

Notice that the noise projection should be interpreted as a stochastic integral, because a Riemann integral is not defined for white noise. r_i s are independent zero mean Gaussian random variables and their powers are

$$E|r_i|^2 = E|H_i|^2 + \bar{n_i^2}, \qquad \text{Eq (4.15)}$$

assuming that, data symbols are of equal and unit power. So, the problem at hand reduces to the detection of a Gaussian random process corrupted by Gaussian noise.

4.2 OFDM with pilot symbols for channel estimation

Coherent demodulation requires the knowledge of the channel, that is, of the coefficients c_{kl}, in the discrete-time model for OFDM transmission in a fading channel. The two-dimensional structure of the OFDM signal makes a two-dimensional pilot grid especially attractive for channel measurement and estimation. An example of such a grid is depicted in Figure 4.2. These pilots are usually called *scattered pilots* [2].

At certain positions in time and frequency, the modulation symbols S_{kl} will be replaced by known pilot symbols. At these positions, the channel can be measured. Figure 4.2 shows a rectangular grid with pilot symbols at every third frequency and every fourth time slot .The pilot density is thus 1/12, that is, 1/12 of the whole capacity is used for channel estimation. This lowers not only the data rate, but also the available energy E_b per bit. Both must be taken into account in the evaluation of the spectral and the power efficiency of such a system. To illustrate this by a numerical example, we consider the grid of Figure 4.2 for an OFDM system with carrier spacing Δ_f = 1 / T = 1 kHz and symbol duration T_s = 1250 μs .At every third frequency, the channel will be measured once in the time $4T_s$ = 5 ms, that is, the unknown signal (the time-variant channel) is sampled at the sampling frequency of 200 Hz. For a noise-free channel, we can conclude from the sampling theorem that the signal can be recovered from the samples if the maximum Doppler frequency $v_{\max}$ fulfills the condition $v_{\max}$ <100 Hz. More generally, for a pilot spacing of $4T_s$, the condition $v_{\max}\ T_s$ <1/8 must be fulfilled.

In frequency direction, the sample spacing is 3 kHz. From the (frequency domain) sampling theorem, we conclude that the delay power spectrum must be inside an interval of the length of 333 us. Since the guard interval already has the length 250 μs, this condition is automatically fulfilled if we can assume that all the echoes lie within the guard interval. We can now start the interpolation (according to the sampling theorem) either in time or in frequency direction and then calculate the interpolated values for the other direction. Simpler interpolations are possible and may be used in practice for a very coherent channel, for example, linear interpolation or piecewise constant approximation. However, for a really time-variant and frequency-selective channel, these methods are not adequate. For a noisy channel, even the interpolation given by the sampling theorem is not the best choice because the noise is not taken into account. The optimum linear estimator will be derived in the next subsection. In some systems, the pilot symbols are boosted, that is, they are transmitted with a higher energy than the modulation symbols. In that case, a rectangular grid as shown in

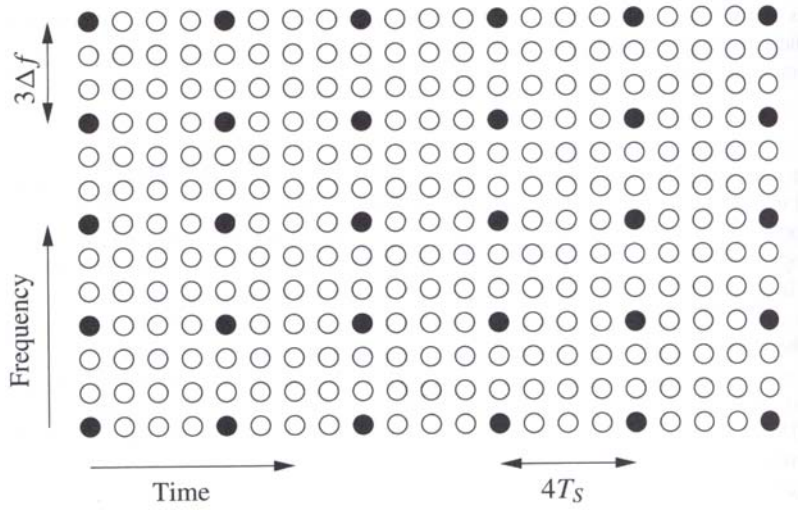

Figure 4.2 Rectangular or Block based Pilot estimation.

4.3 Interleaving and Channel Diversity for OFDM Systems

Requirements of the mobile radio channel As already discussed in Chapter 3 and beginning of chapter 5, channel coding is one important method to introduce diversity into the mobile radio transmission. To achieve the full diversity gain of the code, the transmitted bits must be affected by independent fading[2]. Independent or uncorrelated fading amplitudes can only be realized by a physical separation of the parts of the signal corresponding to the different bits. Bits that are closely related by the code should not

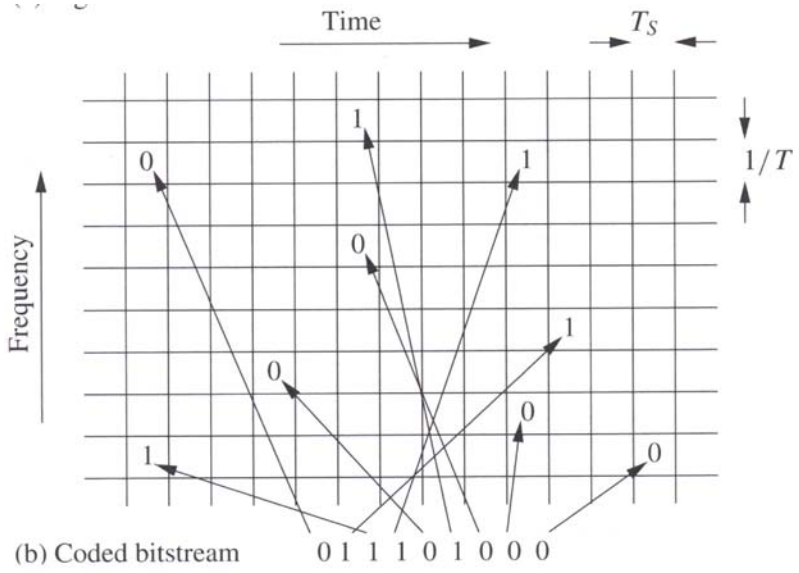

Figure 4.3 Interleaving the coded bits.

be transmitted at closely related locations of the channel. For a block code (RS code), bits are closely related by the code if they are part of the same code word. For a convolutional code, they are closely related unless there are many constraint lengths between them. For a moving receiver (or transmitter), the separation of closely related bits can be realized in the physical dimension of time.

This separation is called *time interleaving*. Obviously, one must wait some time until all closely related bits are received and can be decoded. Thus, time interleaving introduces a *decoding delay*.

For multi-carrier transmission, there is an obvious additional way to realize a physical separation in frequency direction. This is called *frequency interleaving*. Thus, as depicted in Figure 4.3, multi-carrier transmission provides us with two degrees of freedom to separate the information in the physical transmission channel: time and frequency. The physical reasons that cause de-correlation in time and in frequency direction are independent, so that multi-carrier transmission with time and frequency interleaving is a very powerful technique for mobile radio transmission systems.

The de-correlation in time has its origin in the time variance of the channel due to the Doppler spread that is caused by multipath reception for a moving vehicle. It can equivalently be interpreted as caused by the motion of a vehicle through a spatial interference pattern. The spatial correlation length is $x_{corr} = \lambda$, where $\lambda = c / f_0$ is the wavelength, c is the velocity of light and f_0 is the radio frequency. The corresponding correlation time is $t_{corr} = x_{corr} / v = v^{-1}{}_{\max}$ where v is the vehicle speed and

$$\nu_{\max} = \frac{v}{c} f_0 \qquad \text{Eq (4.16)}$$

is the maximum Doppler frequency. The correlation time is then given by

$$t_{\text{corr}} = \frac{c}{f_0 v} \approx \frac{1080 \text{ MHz km/h}}{f_0} \frac{}{v} \text{ seconds.} \qquad \text{Eq (4.17)}$$

The time separation of closely related bits should be significantly larger that this correlation time.

4.4 Channel Coding

Coded Orthogonal Frequency Division Multiplexing (COFDM) is the same as *OFDM, e*xcept that forward error correction is applied to the signal before transmission. This is to overcome errors in the transmission due to lost carriers from frequency selective fading, channel noise and other propagation effects. For this discussion the terms OFDM and COFDM are used interchangeably, as the main focus of this thesis is on OFDM, but it is assumed that any practical system will use forward error correction, thus would be COFDM.[4][5][6]

4. 4. 1 Reed-Solomon Codes

Reed-Solomon codes are block-based error correcting codes with a wide range of applications in digital communications and storage [2] Reed-Solomon codes are based on the *byte arithmetic rather* than on bit arithmetic. Thus, RS codes correct byte errors instead of bit errors. As a consequence, RS codes are favorable for channels with bursts of bit errors as long as these bursts do not affect too many subsequent bytes.

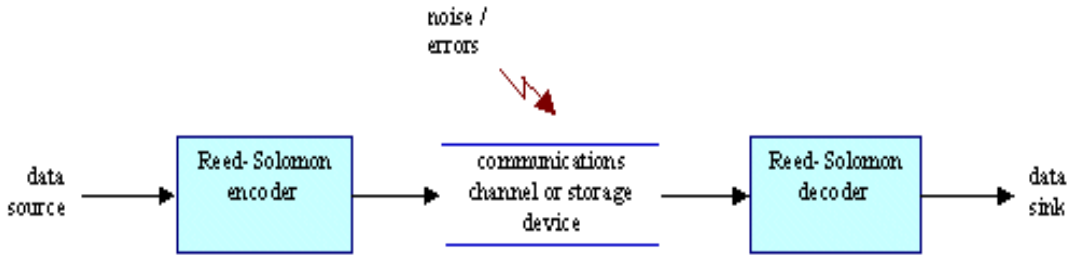

Figure 4.4 Reed Solomon Coding Illustration.

This can be avoided by a proper interleaving scheme. A typical system is shown in figure 4.4. The Reed-Solomon encoder takes a block of digital data and adds extra "redundant" bits. Errors occur during transmission or storage for a number of reasons (for example noise or interference, scratches on a CD, etc). The Reed-Solomon decoder processes each block and attempts to correct errors and recover the original data. The number and type of errors that can be corrected depends on the characteristics of the Reed-Solomon code.

4. 4. 1. 1 Properties of Reed-Solomon codes

Reed Solomon codes are a subset of BCH codes and are linear block codes. A RS code is specified as RS (*n,k*) with *s*-bit symbols. This means that the encoder takes *k* data symbols of *s* bits each and adds parity symbols to make an *n* symbol codeword. There are *n-k* parity symbols of s bits each. A Reed-Solomon decoder can correct up to *t* symbols that contain errors in a codeword, where $2t = n-k$.

The following diagram shows a typical Reed-Solomon codeword (this is known as a Systematic code because the data is left unchanged and the parity symbols are appended):

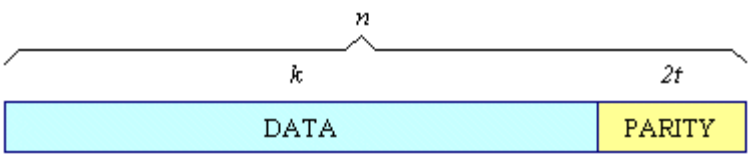

Figure 4.5 Reed Solomon code word.

Example: Reed-Solomon code is RS (255,223) with 8-bit symbols. Each codeword contains 255 code word bytes, of which 223 bytes are data and 32 bytes are parity. For this code: $n = 255$, $k = 223$, $s = 8$

$2t = 32$, $t = 16$,

The decoder can correct any 16 symbol errors in the code word: i.e. errors in up to 16 bytes anywhere in the codeword can be automatically corrected. Given a symbol size s, the maximum codeword length (n) for a Reed-Solomon code is $\boldsymbol{n = 2^s - 1}$ for example, the maximum length of a code with 8-bit symbols (s=8) is 255 bytes.

The amount of processing "power" required to encode and decode Reed-Solomon codes is related to the number of parity symbols per codeword. A large value of t means that a large number of errors can be corrected but requires more computational power than a small value of t.

Symbol Errors: One symbol error occurs when 1 bit in a symbol is wrong or when all the bits in a symbol are wrong.

Example: RS (255,223) can correct 16 symbol errors. In the worst case, 16 bit errors may occur, each in a separate symbol (byte) so that the decoder corrects 16 bit errors. In the best case, 16 complete byte errors occur so that the decoder corrects 16 x 8 bit errors. Reed-Solomon codes are particularly well suited to correcting burst errors (where a series of bits in the codeword are received in error).

4. 4. 1. 2 Decoding

Reed-Solomon algebraic decoding procedures can correct errors and erasures. An erasure occurs when the position of an erred symbol is known. A decoder can correct up to *t* errors or up to *2t* erasures. Erasure information can often be supplied by the demodulator in a digital communication system, i.e. the demodulator "flags" received symbols that are likely to contain errors.

4. 4. 1 .3 Finite (Galois) Field Arithmetic

Reed-Solomon codes are based on a specialist area of mathematics known as Galois fields or finite fields. A finite field has the property that arithmetic operations (+,-, x, / etc.) on field elements always have a result in the field. A Reed-Solomon encoder or decoder needs to carry out these arithmetic operations. These operations require special hardware or software functions to implement.

4. 4. 1. 4 Generator Polynomial

A Reed-Solomon codeword is generated using a special polynomial. All valid code-words are exactly divisible by the generator polynomial. The general form of the generator polynomial is:

$$g(x) = (x - \alpha^{i})(x - \alpha^{i+1})\dots(x - \alpha^{i+2t})$$

and the codeword is constructed using: *c(x) = g(x).i(x)*

Where g(x) is the generator polynomial, i(x) is the information block, c(x) is a valid code-word and α is referred to as a primitive element of the field.

Example: Generator for RS (255,249)

$$g(x) = (x - \alpha^0)(x - \alpha^1)(x - \alpha^2)(x - \alpha^3)(x - \alpha^4)(x - \alpha^5)$$
$$g(x) = x^6 + g_5x^5 + g_4x^4 + g_3x^3 + g_2x^2 + g_1x^1 + g_0$$

4. 4. 1. 5 Finding the Symbol Error Locations

This involves solving simultaneous equations with *t* unknowns. Several fast algorithms are available to do this. These algorithms take advantage of the special matrix structure of Reed-Solomon codes and greatly reduce the computational effort required. In general two steps are involved:

4. 4. 1. 6 Find an error locator polynomial

This can be done using the Berlekamp-Massey algorithm or Euclid's algorithm. Euclid's algorithm tends to be more widely used in practice because it is easier to implement: however, the Berlekamp-Massey algorithm tends to lead to more efficient hardware and software implementations.

CHAPTER 5

BASIC SIGNAL CHARACTERSTICS

5.1 Objective and design

These parameters are designed for this research work, theoretical analysis considered here are explained in detail in previous chapters. The notations used here will be used for further theoretical analysis and to solve simulation and numerical problems.

Given: Since we are operating at the range of 20 GHz we assume enough bandwidth is available. [1]

Here are the few parameters derived and assumed for further research

1. Typical practical high speed multimedia system require 100- 155Mbps, therefore, goal is to achieve minimum of 100Mbps.
2. As already noticed, that we are operating at millimeter wavelength, hence bandwidth limitation is not a critical criterion. So, a bandwidth of 150 MHz is made available to this research.
3. For typical mobile network a guard time of 300ns is taken into consideration

Therefore system parameters can be designed by starting with guard time,

$T_{guard} = 0.3\ \mu s$

$T_s = 12 * T_{guard} = 3.6\ \mu s$.

Therefore total time $T = T_{guard} + T_s$ i.e 0.3 μs +3.6 μs =3.9 μs

The minimum bit rate of our system has been considered as 155Mbps. Now we calculate the number of Sub-carriers that are required to attain this bit rate.

Therefore the symbol rate is 1/T = 256.410Ksymbols/sec

$N_{\min imum\_sub-carriers}$ =Total bit rate / (2 x symbol rate) =155Mbps/(2 x 256.410Ksym/sec)

$N_{\min imum\_sub-carriers}$ = 302

Total sub-carriers with coding and pilot symbols is almost twice the $N_{\min imum\_sub-carriers}$, hence 302 x 2 approximately 512. $N_{sub-carriers}$ = 512

Here we use sub-carriers are less than half of IIFT size because we use 2N real number transmission instead of N complex numbers . Hence we need 1024 point IFFT and FFT to implement this system. We have arbitrarily chosen the factor or 12 to calculate the symbol interval T_s . Choosing a higher factor will give us the better OFDM performance, consequently a greater number of sub-carriers for pilot signals, making a better system. We see from the below table that pilot share rate is 12.5%. I.e. 100-12.5% =87.5% of the transmission rate is the data signals and 12.5% for the pilot signals.

Using 256QAM and coding rate of 0.5 we can achieve the rate of 4bits per symbol.

Recheck the design:

Total Bandwidth is equal to = $N_{sub-carriers}$ x carrier spacing

512 x $(1/T_s)$ = 512 x 256e+005 = 133.678 MHz

Therefore bandwidth occupied by the total carriers is less than the available bandwidth.

5.2 OFDM system parameters summary

Parameter	Value (L=8, 12.5%)
Modulation type	256QAM
Pilot Spacing	8
$N_{sub-carriers}$ total	1024
$N_{sub-carriers}$ pilot	128
$N_{\min imum\_sub-carriers}$	520
$N_{\inf o\_sub-carriers}$	896
Num of bits/OFDM symbol	8192
Num of data bits/OFDM sym	7168
Num of pilots /OFDM sym	128
Step Interval $T = T_{guard} + T_s$	10.4 μs
Symbol Interval T_s	9.6 μs
Guard interval T_{guard}	0.8 μs
Symbol rate (1/T)	96.154Ksymbols/sec
Carrier frequency spacing ($\Delta f = 1/T_s$)	104.17KHz
Total Bandwidth	106.67MHz

5.3 Channel Simulation

To evaluate the performance of a digital communication system in a mobile radio channel by means of computer simulations, we need a simulation method that can be implemented in a computer program and that reflects the relevant statistical properties of the channels discussed above. In this section, we introduce a practical simulation method that is quite simple to implement and has been adopted by many authors because of its computational efficiency. [2][4][5][6]

In this thesis the computer simulation is done using the below equation

$$H_N(f,t) = \frac{1}{\sqrt{N}} \sum_{k=1}^{N} e^{j\theta_k} e^{j2\pi\nu_k t} e^{-j2\pi f\tau_k}, \qquad \text{Eq (5.1)}$$

The main idea of this simulation model is to reverse the line of thought that leads to the statistical Gaussian WSSUS model to reflect the physical reality. The central limit theorem gives the justification to apply the mathematical model of a Gaussian process for a physical signal that is the superposition of many unknown, that is, (pseudo-) random components. On the other hand, owing to the central limit theorem, a superposition of sufficiently many independent random signal components should be a good approximation for a Gaussian process and should thus be a good model for computer simulations. The remaining task is to find out what statistical properties of the components are needed to achieve the appropriate statistical properties of the composed process. For a zero mean GWSSUS channel, we make use of the above Eq (5.1) for the process of the simulation model.

where θ_k, v_k, τ_k are random variables that are statistically independent and identically distributed for different values of k. To be more specific, the random phase θ_k is assumed to be independent of v_k and τ_k and it is uniformly distributed over the unit circle. Eq (5.1) has been introduced to normalize the average power to one. Note that we did not introduce different amplitudes for the different fading paths. It turns out that this is not necessary. Because of the central limit theorem, in the limit $N \to \infty$, Eq (5.1) approaches a Gaussian process. The following theorem states that Eq (5.1) is WSSIJS for any finite value of N.

Probablity density function is show below in Figure 5.1

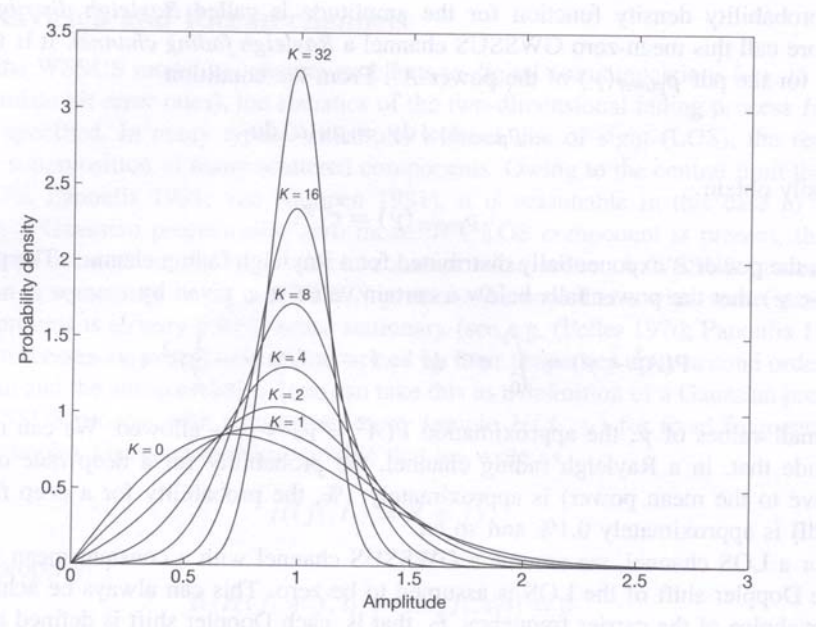

Figure 5.1 The RICIAN PDF, for K =0 (RAYLEIGH).

CHAPTER 6

IMAGE COMPRESSION COMPONENTS

6.1 Wavelet Theory

In this chapter the wavelets are introduced. The application of wavelets in image Coding is explained and this is used to derive design parameters for a coding scheme.

The field of wavelet theory is vast and only the general idea of wavelets will be discussed here. For a more thorough discussion the reader is referred to [10]. The wavelets are a family of functions generated from a single function by translation and dilation. The general form of these wavelets is described by

$$\psi^{a,b}(t) = |a|^{-1/2}\psi\left(\frac{t-b}{a}\right) \qquad \text{Eq (6.1)}$$

ψ is called the mother wavelet and it is used to generate all other members of the family. A common choice for *a* and *b* is

$$a = 2^m, b = n2^m, n, m \in Z$$

This reduces equation Eq (6.1) to

$$\psi_{m,n}(t) = 2^{-m/2}\psi\left(2^{-m}t - n\right) \qquad \text{Eq (6.2)}$$

These wavelets are used in the wavelet transform. The purpose of the wavelet transform is to represent a signal, ***x(t),*** as a superposition of wavelets. For special choices of ψ the signal can be represented as [1]

$$x(t) = \sum_{m,n} c_{m,n}\psi_{m,n}(t)$$
$$c_{m,n} = 2^{-m/2}\int x(t)\psi_{m,n}(t)dt \qquad \text{Eq (6.3)}$$

The purpose of obtaining this description is that it provides a representation of the signal ***x(t)*** in terms of both space and frequency localization (explained below). In comparison, the Fourier transform is excellent at providing a description of the frequency content of a signal. But if the signal is non-stationary the frequency characteristics vary in space, that is in different regions the signal **x**(t) may exhibit very different frequency characteristics, the Fourier transform does not take this into account. The wavelet transform on the other hand produces a representation that provides information on both the frequency characteristics and where these characteristics are localized in space. The coefficients $c_{m,n}$ characterizes the projection of x onto the base formed by $\psi_{m,n}$ For different $m\psi_{m,n}$ represents different frequency characteristics, n is the translation of the dilated mother wavelet, therefore $c_{m,n}$ represent the combined space-frequency characteristics of the signal. The $c_{m,n}$, are called wavelet coefficients.

6.2 Wavelet and Sub-Band coding

Sub-band coding is a coding strategy that tries to isolate different characteristics of a signal in a way that collects the signal energy into few components. This is referred

to as energy compaction. Energy compaction is desirable because it is easier to efficiently code these components than the signal itself [10].

The sub-band coding scheme tries to achieve energy compaction by filtering a signal with filters of different characteristics. By choosing two filters that are orthogonal to each other and decimating the output of these filters a new two component representation is achieved (see Figure 6.1). In this new representation, hopefully, most of the signal energy will be located in either ***a*** or ***d***.

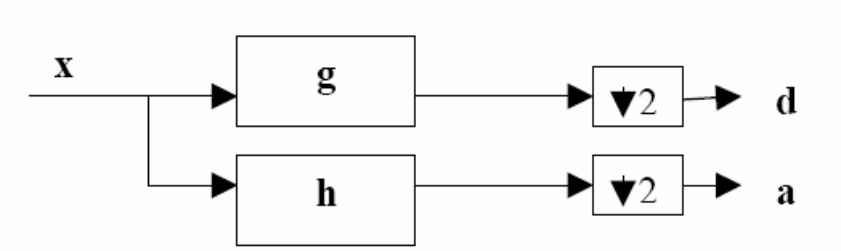

Figure 6.1 Splitting of signal x into two parts.

The filters ***h*** and ***g*** are usually low-pass and high-pass filters. The two components ***a*** and ***d*** will then be a low-pass and a high-pass version of the signal ***x***. Images have a typical low-pass character, that's why we would expect ***a*** to contain most of the energy if ***x*** was an image. Besides trying to achieve energy compaction the filters ***h*** and ***g*** should be chosen so that perfect reconstruction of ***x*** from ***a*** and ***d*** is possible. How to choose ***h*** and ***g*** will be described later.

In Figure 6.1 a two-component representation of ***x*** is achieved. It might be desirable to divide the signal into more components. This can of course be done by using several filters with different characteristics. A more common choice however is to cascade the

structure in Figure 6.1. In the hierarchical structure the output from the low-pass filter is treated as the input to a new filter pair as depicted in Figure 6.2.

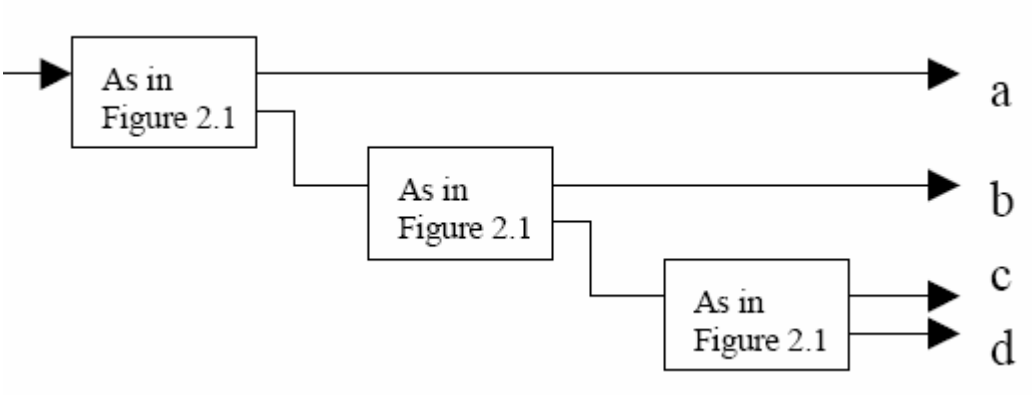

Figure 6.2 The hierarchical filter structure.

6.3 Smooth Wavelets

The main application of wavelet theory to image coding is in the design of filters for sub-band coding (see Section 6.2). This comes from the possibility to realize the projection in Eq (6.3) as a filter operation where the filters depend on the wavelets. The characteristics of the filters derived from the wavelets will be the same as the characteristics for the wavelets used. The properties of a sub-band coding scheme can then be discussed in terms of wavelet theory.

Images often display smoothness and it would therefore be desirable that the wavelets used in image coding are smooth; this should accomplish the desired energy compaction (high correlation between the image and the wavelets/filters). The wavelets should also be compactly supported. This is necessary to have perfect reconstruction. If the wavelets have infinite support the filters derived from these wavelets will have infinitely long impulse responses, leading to infinitely long transformed signals. Filters with a finite impulse response are called FIR-filters. Smooth wavelets with compact

support, leading to FIR-filters, can be obtained by solving a special dilation equation [10]. The solution to the dilation equation is the scaling function $\phi(t)$. From this scaling function smooth wavelets can be generated. There is a tight coupling between the wavelets and the scaling function. By introducing translated and dilated versions of $\phi(t)$ in the same manner as with the mother wavelet in Eq (6.2), we get.

$$\phi_{m,n}(t) = 2^{-m/2}\phi\left(2^{-m/2}t - n\right) \qquad \text{Eq (6.4),}$$

For a fixed *m* the $\phi_{m,n}$ constitute a basis for a vector space, V_m. V_m and W_m, the vector space spanned by $\psi_{m,n}$ for a fixed ***m***, are related to each other as [10]

$$V_{m-1} = V_m \oplus W_m \qquad \text{Eq (6.5)}$$

This means that W_m is the orthogonal complement to V_m in V_{m-1}. Projecting a signal ***x*** onto V_m produces an approximation of ***x*** in terms of $\phi_{m,n}$ and the relation Eq(6.5) tells us that the information lost when going from a finer approximation at resolution ***m-1*** to coarser at resolution ***m*** is exactly the projection of the resolution ***m-1*** approximation onto W_m. The W_m projection is referred to as detail information. If the signal is in sampled form (as images are) the ***m-1*** resolution approximation can be chosen as the data itself, Eq (6.5) then describe how to divide the data into approximation and detail parts which can be used to reconstruct the signal perfectly. We can achieve a representation of ***x*** in more than two components by recursively using Eq (6.5) on V_m:

$$V_m = V_{m+1} \oplus W_{m+1} \Rightarrow V_{m-1} = V_{m+1} \oplus W_{m+1} \oplus W_m \qquad \text{Eq (6.6)}$$

This means that ***x*** can be represented as an ***m+1*** resolution approximation and two detail signals. The process in (6.6) can be continued representing ***x*** as coarser and coarser approximations and more and more detail signals.

6.4 Decomposition with filters

The process of decomposing a signal into approximation and detail parts, corresponding to projecting ***x*** onto V_m and W_m in Eq (6.5), can be realized as a filter bank followed by sub-sampling ([10], [11]) (see Figure 6.1). In Figure 6.1 ***a*** and ***d*** are the resulting approximation and detail coefficients (signals) for one level of decomposition. The impulse responses ***h*** and ***g*** are derived from the scaling function and the mother wavelet ([10], [11]). Since the scaling function is used to create a basis for the approximation space we would expect ***h*** to be a low-pass filter. Since ***g*** is derived from the wavelets producing detail information, we would expect **g** to be a high-pass filter.

This gives a new interpretation of the wavelet decomposition as splitting the signal **x** into frequency bands. From Eq (6.6) it is known that a representation of **x** with more than two components is possible. Eq (6.6) also tells us how these components can be constructed. It suggests a hierarchical structure of the filter bank where the output from the low-pass filter *h* in Figure 6.1 constitutes the input to a new pair of low-pass high-pass filters. Graphically this is depicted in Figure 6.2

$d^1 - d^3$ are the detail signals at level 1-3 and a^3 is the approximation signal at level 3. The detail signals and the approximation signal are also referred to as sub-bands since they represent different frequency bands (see Section 2.2 Figure 6.2).

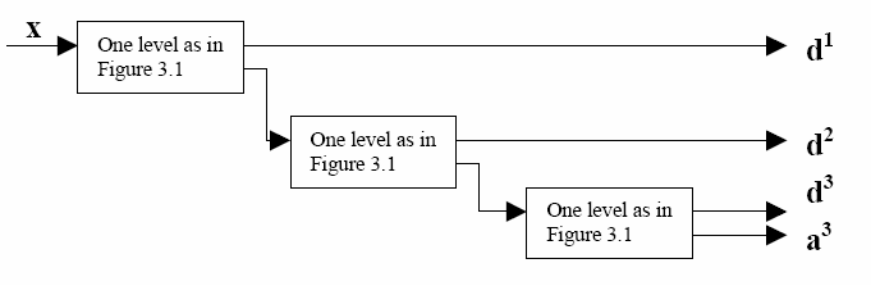

Figure 6.2 Multi-level decomposition of signal x.

6.5 Reconstruction with filters

From Eq (6.5) it is known that the process of decomposing the signal ***x*** can be reversed, that is given the approximation and detail information it is possible to reconstruct ***x***. This process can be realized as up-sampling followed by filtering the resulting signals and adding the result of the filters (see Figure 6.3).

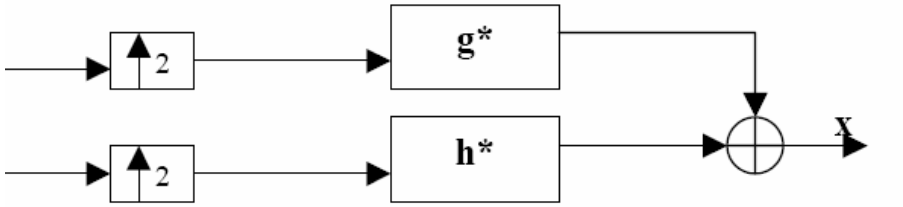

Figure 6.3 One level of reconstruction realized as an up sampling followed by a filter bank.

The impulse responses **h*** and **g*** can be derived from **h** and **g** [4]. If more than two bands are used in the decomposition we need to cascade the structure in Figure 6.3. An opposite structure from that in Figure 6.2 is used. Below the structure for reconstructing ***x*** from $d^1 - d^3$ and a^3 is shown.

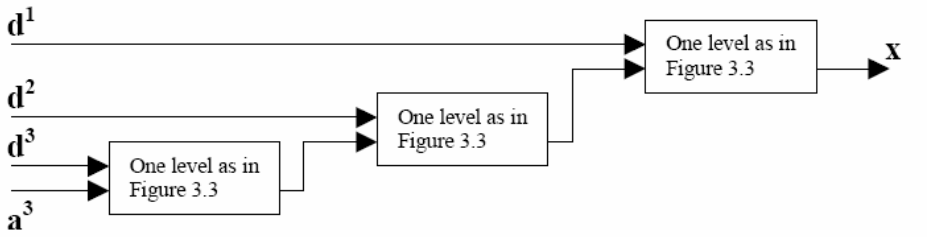

Figure 6.4 Multi-level reconstruction of ***x.***

The structure of the filter bank in Figure 6.2 is referred to as octave-band wavelet decomposition. In this thesis this structure will also be referred to as the Discrete Wavelet Transform (DWT). The above figure shows how to accomplish wavelet decomposition as a cascading of filters. So by choosing filters derived from wavelet bases a sub-band scheme with perfect reconstruction and high energy compaction potential can be accomplished. In Section 6.5 more desirable properties of the wavelets/filters will be derived.

To be able to use sub-band coding for images the scheme above has to be adapted to two-dimensional signals. The extension of the sub-band coding scheme to higher dimension is straight-forward. Apply the filters repeatedly to successive dimensions [10]. For an N x N image we first compute N one-dimensional transforms corresponding to transforming each row of the image as an individual one-dimensional signal. This results in 2 N x M sub-images, one corresponding to the low-pass filtered rows and one corresponding to the high-pass filtered rows. Each of these sub-images are then filtered along the columns splitting the data into 4 M x M sub-images (low-pass

row low-pass column, low-pass row high-pass column, high-pass row low-pass column, high-pass row high-pass column). This completes one stage of the decomposition of an image. The process is depicted in Figure 6.4. In the case of volumetric data in an image stack one stage of decomposition results in eight sub-volumes. This corresponds to transforming each slice in the stack as above and then applying a one dimensional transform along the slices

6.6 Characteristics of the filters

6.6.1 Filters and wavelets

In the previous section it was explained that the use of wavelet theory in image coding is in the area of filter design for a sub-band coding scheme. In this section some desirable properties of the filters to be used for image coding will be discussed. Filter characteristics will also in some cases be translated into properties of the wavelet bases used.

In the previous section it was explained that filters derived from smooth wavelets were desirable. This should lead to good correspondence with the low-pass character of images (high energy compaction), the main goal of sub-band coding. More desired characteristics of the filters can be found by looking at the resulting transform. A desirable property of the transform is that it is orthonormal. If the transform is orthonormal the reconstruction filters **h*** and **g*** in Figure 6.3 can be chosen as **h*=h** and **g*=g**, where **h** and **g** are as in Figure 6.1. An orthonormal transform (corresponding to an orthonormal wavelet basis) preserves the signal energy in the transform domain. This is especially important when a lossy coding scheme is applied to the transformed

structure. The orthonormality guarantees that the distortion in the transform domain is the same as in the reconstructed domain [10]. That is if we quantize transform components (sub-bands), and by that introduce distortion the distortion will be the same after inverse transformation of the quantized components. This is a form of Parseval's identity and it gives control of the distortion in the reconstruction by controlling the distortion in the transform domain. Besides smoothness and orthonormality it is desirable that the filters derived from the wavelets should be short for fast computation and have linear phase. The phase linearity makes the cascading of filters in a sub-band coding scheme possible without phase compensation. The linear phase also implies symmetry of the wavelet and also symmetry of the filters derived [12]. This symmetry is most desirable for filters used in image coding, which will be discussed below.

According to [12] keeping orthonormality linear phase and smoothness is not possible. By relaxing the orthonormality requirement and using bi-orthogonal wavelet bases, filters with linear phase and smoothness can be designed. Though we have removed the orthogonality we can still achieve perfect reconstruction by choosing **h*** and **g*** differently than in the orthonormal case. By using bi-orthogonal bases in the filter design the resulting transform is not orthonormal; this takes away the nice feature of being able to control the distortion in the reconstruction by controlling the distortion in the transform domain. The bi-orthogonal base can however be chosen close to orthonormal in which case distortion in the transform domain almost corresponds to distortion in the reconstruction. The relaxation of the orthogonality property is done so that smooth filters with linear phase can be constructed. The linear phase property, or

rather the symmetry of the filters, enables the construction of a non-expansive symmetric extension transform [13].

6.7 SPIHT

In this section methods for quantizing and coding wavelet coefficients are discussed. Special attention is directed towards a zero-tree coding method. This method is explained in some detail to put forward some interesting properties of the method. In the previous chapter the link between wavelet theory and sub-band coding was established. Wavelet theory is used to design filters in a sub-band coding scheme. The sub-band coding scheme should achieve energy compaction of the signal. The motivation for this was that it should be easier to quantize and code the signal if it was split into parts [10].

A more efficient quantization scheme could be constructed if the intra band dependencies were considered [10]. One way to utilize the inter band dependencies is to use contexts when coding. With contexts the quantization and coding of a coefficient is made dependant on other, previously, coded coefficients. The use of contexts often leads to complex schemes with a lot of specially tuned entropy coders ([14]). A quantization and coding algorithm that utilizes the intra band dependencies but does not use complex contexts is SPIHT, or *Set Partitioning In Hierarchical Trees SPIHT* was introduced in [15]. It is a refinement of the algorithm presented by Shapiro in [16]. SPIHT assumes that the decomposition structure is the octave-band structure and then uses the fact that sub-bands at different levels but of the same orientation display similar characteristics. As is seen in Figure 6.5 the band LL HL has similarities with the band

HL (both have high-pass filtered rows). To utilize the above observation SPIHT defines spatial parent-children relationships in the decomposition structure. The squares in Figure 6.5 represent the same spatial location of the original image and the same orientation, but at different scales. The different scales of the sub-bands imply that a region in the sub-band LL HL is spatially co-located (represent the same region in the original image) with a region 4 times larger (in the two dimensional case) in the band HL. SPIHT describes this collocation with one to four parent-children relationships,

$$\begin{aligned} parent &= (x, y) \\ children &= \left[(2x,2y),(2x+1,2y),(2x,2y+1),(2x+1,2y+1)\right] \end{aligned} \qquad \text{Eq(6.7)}$$

where the parent is in a sub-band of the same orientation as the children but at a smaller scale. If the data is ordered as previously described (Figure 7.6) and every level of decomposition produces sub-bands of exactly half the size of the previous sub-bands (see discussion on non-expansive transforms), then the parent-children relationships in two dimensions become

Using these relationships SPIHT makes the hypothesis that if a parent coefficient is below a certain threshold then it is likely that all its descendants is below the threshold to. If this prediction is successful then SPIHT can represent the parent and all its descendants with a single symbol called a zero-tree, introduced in [10]. To predict energy of coefficients in lower level sub-bands (children) using coefficients in higher level sub-bands (parents) makes sense since there should be more energy per coefficient in these small bands, than in the bigger ones. To see how SPIHT uses zerotrees the

workings of SPIHT are briefly explained below. For more information the reader is referred to [9].

Working of SPIHT consists of two passes, the ordering pass and the refinement pass. In the ordering pass SPIHT attempts to order the coefficients according to their magnitude. In the refinement pass the quantization of coefficients is refined. The ordering and refining is made relative to a threshold. The threshold is appropriately initialized and then continuously made smaller with each round of the algorithm. SPIHT maintains three lists of coordinates of coefficients in the decomposition. These are the List of Insignificant Pixels (LIP), the List of Significant Pixels (LSP) and the List of Insignificant Sets (LIS). To decide if a coefficient is significant or not SPIHT uses the following definition. A coefficient is deemed significant at a certain threshold if its magnitude is larger then or equal to the threshold. Using the notion of significance the LIP, LIS and LSP can be explained.

- The LIP contains coordinates of coefficients that are insignificant at the Current threshold,
- The LSP contains the coordinates of coefficients that are significant at the Same threshold
- The LIS contains coordinates of the roots of the spatial parent-children trees defined in Eq (6.7).

Below is a schematic of how SPIHT works.

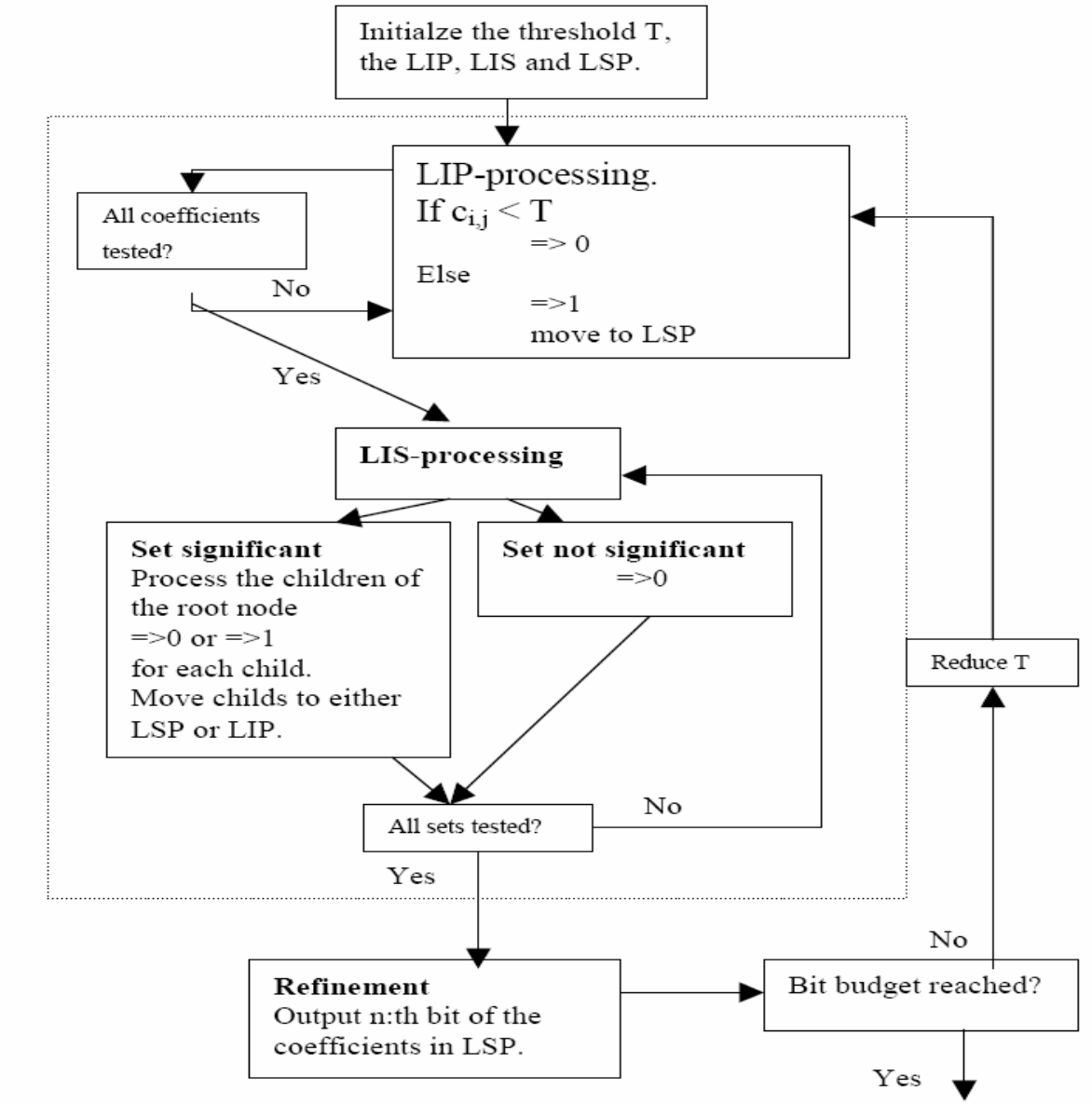

Fig 6.6 Schematic 1- Illustrating the SPIHT algorithm.

In the ordering pass of SPIHT (marked by the dotted line in the schematic above) the LIP is first searched for coefficients that are significant at the current threshold, if one is found 1 is output then the sign of the coefficient is marked by outputting either 1 or 0 (positive or negative). Now the significant coefficient is moved to the LSP. If a coefficient in LIP is insignificant a 0 is outputted.

Next in the ordering pass the sets in LIS are processed. For every set in the LIS it is decided whether the set is significant or insignificant. A set is deemed significant if at least one coefficient in the set is significant. If the set is significant the immediate children of the root are sorted into LIP and LSP depending on their significance and 0s and 1s are output as when processing LIP. After sorting the children a new set (spatial coefficient tree) for each child is formed in the LIS. If the set is deemed insignificant, that is this set was a zero-tree, a 0 is outputted and no more processing is needed. The above is a simplification of the LIS processing but the important thing to remember is that entire sets of insignificant coefficients, zero-trees, are represented with a single 0. The idea behind defining spatial parent-children relationships as in (4.1) is to increase the possibility of finding these zero-trees.

3. The SPIHT algorithm continues with the refinement pass. In the refinement pass the “next bit” in the binary representation of the coefficients in LSP is outputted. The “next bit” is related to the current threshold. The processing of LSP ends one round of the SPIHT algorithm, before the next round starts the current threshold is halved. The above is just the outline of the SPIHT algorithm. It was presented firstly for explaining the use of zero-trees in SPIHT and putting forward that the efficiency of SPIHT is

heavily dependant on finding zero-trees in the LIS, secondly to show that SPIHT is an embedded bit-stream coder [15]. SPIHT's embedding property means that when generating a code with R_n bits (SPIHT is stopped when it has output R_n bits) all SPIHT-codes with rate R_i , $R_i < R_n$ has also been generated as the prefix of the rate R_n code [9]. The implications of this are discussed below.

6. 7. 1 Wavelet bases

In [9], where SPIHT is introduced, it is assumed that the decomposition proceeding SPIHT is octave-band decomposition with filters corresponding to orthonormal wavelets. The orthonormality is used to motivate sending information in bit-planes (leading to the embedding property) starting with most significant bits. Sending the most significant bits first reduces the MSE in the transform domain the most per bit.

In [15], then, the orthonormality is used to conclude that this also leads to the largest reduction in MSE in the reconstruction. If bi-orthogonal bases are used no optimality can be derived in this way. It seems however that SPIHT works well with filters derived from bi-orthogonal wavelets in the decomposition. SPIHT was originally designed for image coding, but it can easily be extended to more dimensions. The only part of SPIHT that is dependant on dimensions is the parent-children relationship. To extend SPIHT to higher dimensionality all that has to be done is extend the parent-children relationship.

6. 7. 2 Applications of Embedding

The embedding property of SPIHT is very useful, especially when there is multiple users with different QOS needs .Also its application in image stack, An image stack is usually very large and it could take a long time to decode the entire stack to its coded rate. With the embedded bit-stream that SPIHT produces there is the possibility to view intermediate results. When a certain number of bits have been received (of course this number is arbitrary) the image stack can be reconstructed and a low rate version of the stack can be viewed. If the quality of the stack is not good enough, the decoding can continue progressively producing higher quality reconstructions. The intermediate results also make it possible to end the decoding at an early stage if it is discovered that the data being decoded is not the data wanted. The use of such a scheme is highly desirable when data is sent over a network. It should be mentioned that the progressive properties of SPIHT comes hand in hand with the property of graceful degradation at low bit rates in the sub-band coding scheme [10]. This graceful degradation makes intermediate low bit rate results meaningful not just noise-like.

6. 7. 3 Implementation of SPIHT

So far we have discussed some issues concerning the implementation of the transform in the coding scheme. The pseudo-code below is simplified to highlight some important points. For a better presentation of SPIHT see [15].

1)Initialization: output n=$\lfloor \log 2(\max_{(i,j)} \{|c_{i,j}|\}) \rfloor$
LSP={}
LIS={(x,y)|(x,y) has descendants and is in the lowest level sub-band}
LIP={(x,y)|(x,y) is in the lowest level sub-band}
2)Sorting Pass:

LIP-processing
for each (x,y) in LIP do:
if (x,y) is significant
output 1 and the sign of the coefficient then move (x,y) to LSP.
else
Output 0.
end for each

LIS-processing
For each (x,y,T) in LIS
Decide whether (x,y,T) is significant
If (x,y,T) was significant
process the children of (x,y) differently depending on the value of T.
else
ouput 0
end for each

3)Refinement Pass:
output the n:th bit of the coefficients in LSP added prior to this round.

4) Quantization-step update:
decrement n by 1.

CHAPTER 7

DIVERSITY COMBINATION METHODS

7.1 Diversity

Wireless communications systems are susceptible to fading phenomenon that causes bursty channel errors [2]. This fading phenomenon presents different problems for image transmission when compared to image transmission in a wired environment. An image may arrive at the receiver with errors that severely degrade image quality. On wireless channels bandwidth constraints are also an important consideration, so compressed images will be considered for wavelet domain diversity methods. For an error resilient representation, wavelet based decomposition will be implemented for transmitting the image in its uncompressed state.

Diversity is a communication method used to improve wireless transmission that utilizes independent (or highly uncorrelated) communication signal paths to combat channel noise. The independent signal paths provide the receiver with multiple signals for appropriate diversity processing of the received signals. The types of diversity typically used for wireless communications include spatial, frequency and time diversity methods. Space or antenna diversity works by having spatially separated antennas at the receiver to obtain the independent or uncorrelated signals. Frequency diversity involves transmission of data on multiple carrier frequencies to get uncorrelated fading channels, but a disadvantage of this method is the need for extra bandwidth. Time diversity retransmits information at time intervals that allow for

independent fading conditions. In all of the above diversity methods, multiple independent (or highly uncorrelated) signals are available at the receiver that needs to be combined to generate the received information. Selection diversity is one simple example of diversity combining that takes the signal from the diversity branch with the highest SNR. Other common methods for diversity combining are equal gain combining and maximal ratio combining. All of these methods carry out diversity combining in the data domain, in that they attempt to obtain the best estimate of the received digital data. For image transmission, a diversity technique has been employed in conjunction with ARQ [17]. This approach involves switched antenna diversity that operates in the data domain.

Unlike the data domain diversity combining methods mentioned above, the diversity combining method proposed earlier [18] operates in the image domain by using the properties of the original image or its wavelet transform.

In this thesis OFDM system is designed in such a way that SC s are used to obtain diversity and same diversity algorithms proposed in [18] is used with slight modifications for the compressed images. Our novel approach of using OFDM sub-carriers to attain diversity wireless image transmission is more effective in combating the fading and other channel impairments due to its immunity *to inter channel interference* and *inter symbol interference*.

Not only does this method help in improving the received image quality but it also gives us flexibility in high data rate transmission with multiple user access.

This diversity combining method was inspired by the image fusion work of [18]. Where, for image transmission over wireless channels, two or more diversity channels are utilized to obtain multiple bit streams at the receiver, with each bit stream independently representing the image data. Then those bit streams are combined in the image domain to improve the perceptual quality of the received image.

Due to single carrier transmission and deep fading effects, the data rates are limited. This thesis work on its entirely is inspired from the work of [18] .Their work is the main base for this thesis. Even though comparative analysis is not recommended here with the system of [18], this work gives enough results and evidence to conclude that high data rate with good image quality is possible in the present day mobile network.

Also the hybrid system takes advantage of progressive image coding techniques, where low distortion images are more meaningful because different users may want the same image with different compression rates as well as with different distortion level.

7.2 Diversity Combination for Uncompressed Images

Our diversity combining method for uncompressed images involves computing the two-dimensional wavelet decomposition of the source image and quantizing the resulting wavelet coefficients. The coefficients are then transmitted as a bit stream over a wireless communications system employing diversity without any error control. Diversity is used to obtain multiple copies of the decomposed image data at the receiver. At the receiver, the individual decomposed images are combined to form composite wavelet decomposition and then the final received image is reconstructed. This diversity combining method is depicted in Figure 7.1 The error resilience of diversity combining method is explained using two methods. In each method the data bits are 40 bit interleaved and they are formed a data symbol of 8 bits each.

7.2.1 Method 1

Block diagram depicts the processing of the data symbols. In method 1 data symbols are coded with Reed Solomon block code (*n, k*) capable of correcting 2t errors. Then code words are fed into OFDM section of the transmitter. The first block in the OFDM section of the transmitter is the QAM block. Where it's mapped to 256 QAM constellations symbols

For the purpose of simulation a 256 by 256, 8 bit per pixel "lena image" is used and following steps explains the procedure used to for transmission and reception

Step 1: The Image used for experiment is decomposed up to 2 levels using Discrete Wavelet transform. The topic about wavelet theory and its multi resolution analysis is

thoroughly discussed in Chapter 3. In this method same wavelet i.e. “bior 4.4” is used for dilations.

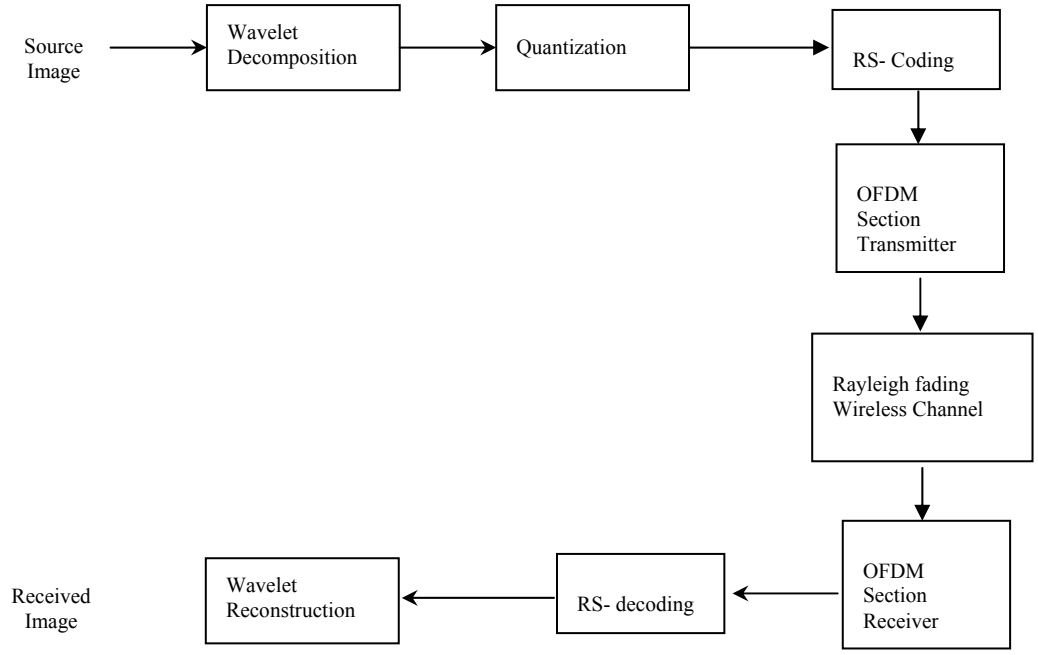

Figure 7.1 Test set up for diversity combination for un compressed images.

Step 2: The coefficients are fed through 10 bit quantizer block to keep the complete coefficients value without truncating any of its floating point components. The quantizer is designed with 10 bit data part for fixed point and 5 bits for the floating point representation. This is the inbuilt function in the MATLAB which can be configured as per the user requirement.

Step 3: The quantized data is deep interleaved with 40 bits and then 8 bits symbols are formed. Therefore total number of bits that has to be transmitted is equal to 256*256=65536 * 10=655360 bits. 10 in the equation is 10 bit/ pixel quantization.

The total data of 655360 bits is again grouped into 8 bit symbol. i.e. 655360/8= 81920 data symbols.

Step 4: 81920 data symbols are divided into 32 blocks of each 40 x 64 data symbol. Each block is protected with RS (78, 64), capable of correcting up to 16 bits or error or 16 bytes of error, given there is only one bit in each of 16 bytes. Thorough discussion of Reed Solomon codes are done in chapter,,,,,,

Step 5: These blocks of data is fed to OFDM transmission block described earlier and is let to undergo mobile radio propagation effects simulated by Rayleigh fading environment

Step 6: The receiver does the exact opposite of transmitter but no diversity. After recovering the bits from the OFDM symbols, QAM demodulation is done followed by error correction if it's necessary. Then inverse wavelet transform is taken and the image is reconstructed.

Step 7: Performance is measured using peak signal to noise ratio for various bit error rates using the formulae shown below

$$\text{PSNR} = 10\log_{10}\frac{255^2}{\frac{1}{N}\sum_i\sum_j (p(i,j) - \hat{p}(i,j))^2}$$

Where $p(i,j)$ and $\hat{p}(i,j)$ are the pixel values of the original image and are the pixel values of the received image.

PSNR results are tabulated with images in table and figure respectively

7.2.2 Method 2

In this section, we use images transformed in the wavelet domain with uniform scalar quantization of the coefficients. The results obtained will help demonstrate the usefulness of image domain diversity combining for image transmission over wireless channels. For images without compression, the wavelet representations are obtained from the bit streams received on the individual OFDM sub-carrier channels. The block diagram is shown the figure 7.2

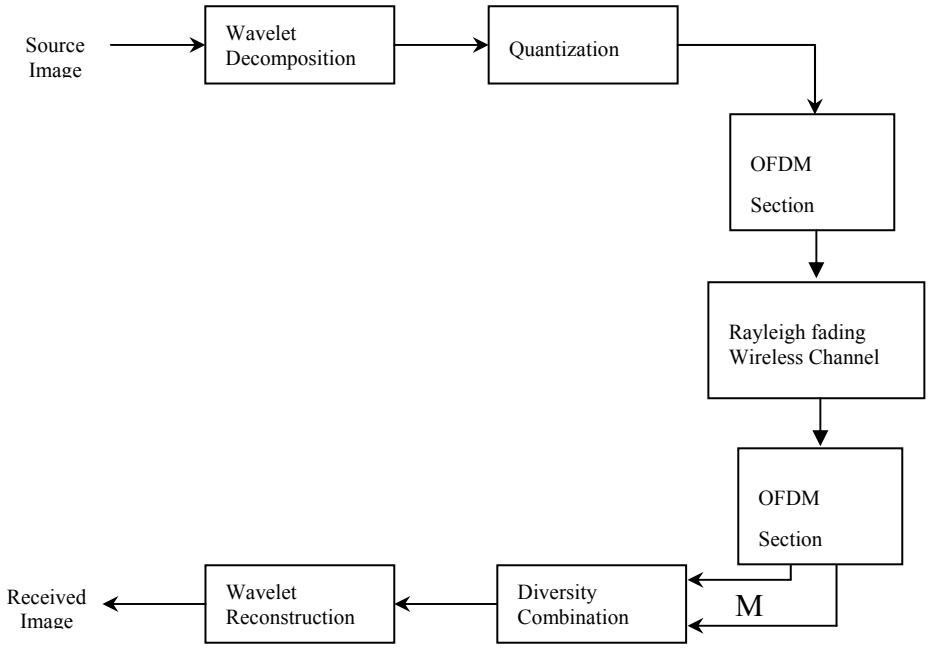

Figure 7.2 Block diagram for diversity combination Method 2.

Following steps will explain the diversity combination done using OFDM Sub-carriers

Step1: Steps 1 – 3 are repeated as done in method1

Step2: 81920 symbols are divided into 32 blocks where each block is of 40x64 bytes size. Reed Solomon coding is skipped in this method and the data is fed to QAM modulation part of OFDM section.

Diversity combination for uncompressed images is done mainly to emphasize on the error resilience of the combination algorithms the methods used to do that.

Step4: In this step the data is arranged in a different manner. Output of QAM modulator is reshaped such that all 81920 QAM symbols are presented in a serial stream of data. This is only due to software constraint in the MATLAB. If this system were to be implemented in that hardware, this step can be skipped and matrix block of data can be directly sent to the memory of the DSP processor. Barrel shifter can be used to shift the register data from memory to accumulator forming a virtual matrix manipulator.

Step 5: In this step the arrangement of data is shown in the figure8.3

Symbol stream of 225 symbols are arranged in the block *block_data1* and the same data is duplicated into another block data called *block_data2*.

Note: block_data1 and block_data2 carry same data. In other words redundant information

block_data1= | 225 QAM SYMBOLS |

block_data2= | 225 QAM SYMBOLS
Duplicate |

As we have already discussed the formation of OFDM symbols and its carrier spacing procedure and its rules. We will abide by those rules and regulations in this section.

The coherence bandwidth spacing necessary for frequency diversity is also revisited here and reader is advised to review that part in wireless fundamental section as well as in system parameter section where detail calculation is done regarding the coherence bandwidth *Bc.* [1] [2]

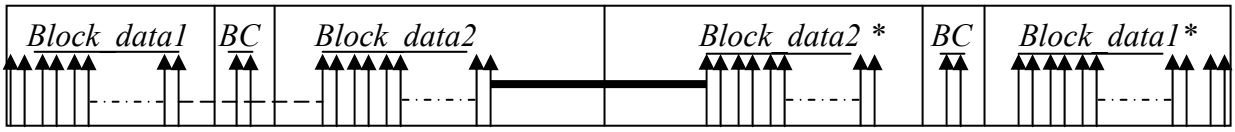

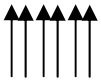 → Sub-carriers with carrier spacing of 1 IFFT bin

 → Zero Padded bins

Bc → Coherence Bandwidth multiplied by 10

- → Reverse Conjugate of the blocks necessary to construct real IFFT sequence output.

Figure 7.3 Arrangement of data on Sub-carriers in OFDM symbol.

Specific numbers for Sub-carriers and spacing including zero padding are discussed in chapter 6.

Total Sub carriers $N_{sub-carriers}$ are divided into 3 parts i.e.

$N_{sub-carriers\_block1}$

$N_{sub-carriers\_block2}$

$N_{sub-carriers\_coherence}$

Block_data1 is placed in sub_carriers_block1 and Block_data2is placed in sub_carriers_block2. Sub_carriers_coherence is used as the separation necessary for frequency diversity.

Step 6: After arrangement of the data as shown in the figure, the OFDM symbol is generated from the IFFT block, giving us orthogonal sub-carriers.

Step 7: Appropriate channel simulation is done, same as in method 1 and OFDM symbols are recovered from the receiver.

Step 7: In this section data symbols are recovered from sub-carriers and separated out from the conjugate data. Then QAM demodulation is done and data symbols are recovered and again grouped as per the sub-carriers associated during transmission.

There fore we have successfully received the two sets of data i.e. *Block_data1 and Block_data2*.

Due to the orthogonality of the sub-carriers and spacing between two carrier blocks, the noise effect on the blocks is not the same. Since the channels are highly uncorrelated the burst errors are spread out though the block. This is the exact

phenomena which help us to recreate a block of data capable of generating image of good quality using two blocks of data.

Step 9: This is repeated till the complete set of data blocks are sent. i.e 81920/225 with some extra zero padding and pilot symbols.

Step 10: Between step 8 and step 9, Diversity combinations are done on received blocks of data. These algorithms are described in section below.

7.3 Diversity Combination Algorithms

In general, the low-resolution sub-band is more important perceptually and a large error in pixel intensity can seriously affect image quality. An error in the high frequency sub-band is not as important to the overall image quality. Because the characteristics of the sub-bands are different, the diversity-combining rule for the low-resolution sub-band differs from the combination rule for the high frequency sub-bands. After obtaining the composite decomposed image from fusing the individual transformed images, the inverse wavelet transform is performed to obtain the final image.

The idea behind diversity combination is to significantly reduce visible errors in the received image without necessarily using techniques such as ARQ or error correction coding [18]. The low frequency sub-band and high frequency sub-bands have different sensitivities to bursty channel errors. Therefore, the rules for the two types of sub-bands are different. For both of the different sub-band types there are two combination modes: selection and coefficient combining. In the selection mode, one

coefficient is selected from the two decomposed images and placed in the composite. In the coefficient-combining mode, groups of coefficients from neighborhoods of both decomposed images are examined and a value is placed in the composite decomposed image based on measures from both coefficient neighborhoods. The combination method is similar to using both image averaging and spatial filtering to remove channel noise.

7.3.1 Low Resolution Sub- band diversity algorithm

Since the low-resolution sub-band is more perceptually important to the image, more care must be taken when dealing with detected channel errors in the low-resolution sub-band [18]. First, the coefficients from the two diversity bit streams are compared as they arrive at the receiver. If the received wavelet coefficient values are the same, we assume that the value is correct and select the coefficient from either channel to place in the combined transform. If the coefficient values are different, the receiver waits until an m by n neighborhood of coefficients surrounding the coefficient of interest is available from both channels. Small neighborhoods (i.e. 3 by 3) of an image are generally smooth. Therefore, the intensity values usually do not vary significantly within these neighborhoods. When the two received coefficients at location (i, j) are different, the m by n neighborhoods of coefficients around them are grouped into a set of $2mn$ values. Then the median value is chosen as the coefficient to place in the combined low-resolution sub-image at location (i, j). In general, this median-based method tends to be more robust to large channel errors than averaging the coefficients in order to obtain a combined coefficient value. Therefore, for each (i, j),

the coefficient placed in the combined low resolution sub-band image is defined as follows (assuming *m* and *n* are odd):

$$c_{Lc}(i,j) = \begin{cases} c_{L1}(i,j) & \text{if } c_{L1}(i,j) = c_{L2}(i,j) \\ med[\{c_{L1}(k,l)\},\{c_{L2}(k,l)\}] & \text{if } c_{L1}(i,j) \neq c_{L2}(i,j) \end{cases} \quad \text{Eq (7.2)}$$

for

$$(k,l) \in \left(\left\{ i - \frac{m-1}{2}, \cdots, i + \frac{m-1}{2} \right\}, \left\{ j - \frac{n-1}{2}, \cdots, j + \frac{n-1}{2} \right\} \right)$$

Where $C_{Lc}(i,j)$ the composite is transform matrix and $C_{L1}(i,j) \,\&\, C_{L2}(i,j)$ are reconstructed from *Block_data1 and Block_data2 symbol blocks.*

7.3.2 High Resolution Sub-band diversity algorithm

An error in the high frequency sub bands does not affect the quality of the final reconstructed image as much as in the low frequency sub bands. Also, most of the coefficients have magnitudes close to zero. Therefore, the errors in the detail sub bands are processed differently when the received wavelet coefficients are not the same. Again, if the received wavelet coefficient values are the same, we assume that the value is correct and place this value in the combined transform [18]. However, if the received coefficients are different, the coefficient with the minimum absolute value is chosen and

placed in the final combined transform. The idea behind this selection method is that a coefficient that implies a strong edge where one does not exist will visually degrade the image more than a coefficient that implies no edge where one really exists. Since most of the coefficients in the high frequency sub bands are near zero, there is a better chance that the coefficient with the minimum absolute value will be correct. Even if we set the coefficients to zero in the high frequency sub-bands, the quality of the final image will still be acceptable. The combined coefficient values for each location (i ,j) in the high frequency sub-bands are given as follows:

$$c_{Hc}(i,j) = \begin{cases} c_{H1}(i,j) & \text{if } c_{H1}(i,j) = c_{H2}(i,j) \\ c_{H1}(i,j) & \text{if } |c_{H1}(i,j)| < |c_{H2}(i,j)| \\ c_{H2}(i,j) & \text{if } |c_{H2}(i,j)| < |c_{H1}(i,j)| \end{cases} \qquad \text{Eq (7.3)}$$

Where $C_{Hc}(i,j)$ the composite is transform matrix and $C_{H1}(i,j)$ and $C_{H2}(i,j)$ are detail sub-band coefficients from *Block_data1 and Block_data2 symbol blocks.*

we expect the errors on the individual channels to be independent or at least highly uncorrelated. The independent nature of the diversity channels allows for a combining method in the image domain that yields excellent quality images in the presence of wireless channel errors.

The results are tabulated and compared in the next section, showing a considerable amount of improvement in the PSNR dB in method2 vs method1.

7.4 Diversity Combination for compressed Images

Our diversity combining method for compressed images is implemented using the SPIHT image compression algorithm without arithmetic coding. The compressed image data is first protected with interleaving and error control coding and then transmitted over a wireless communications system using OFDM sub-carriers and its diversity. Multiple bit streams representing the image data are obtained at the receiver. Then these multiple bit streams are decoded using appropriate channel decoding algorithms followed by image decompression based on the SPIHT method up to the point where the wavelet representations of the multiple images are obtained. Before computing the inverse wavelet transform, the individual wavelet representations are combined using rules based on wavelet transform characteristics. After diversity combining, a composite wavelet representation is obtained and the received image is reconstructed by performing the inverse wavelet transform on this composite representation. A block diagram of this diversity combining process is shown below

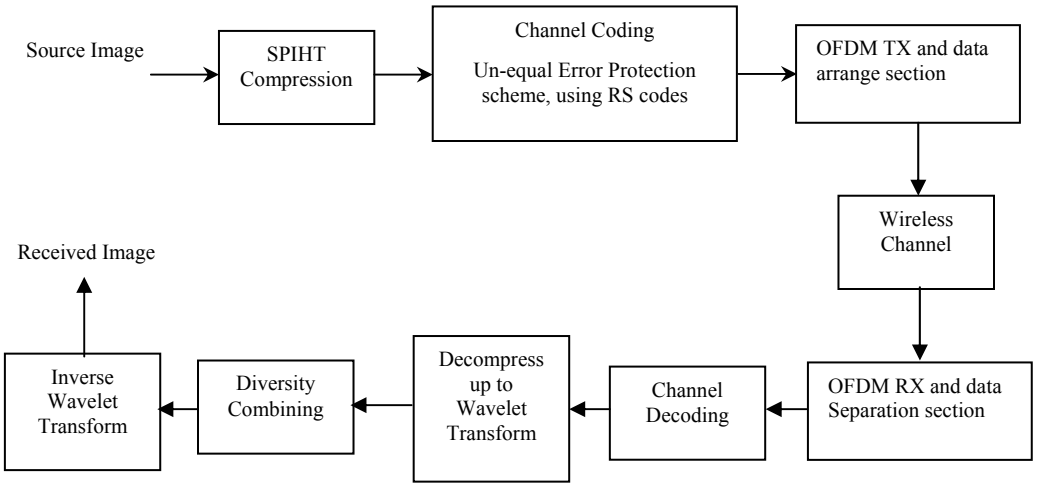

Figure 7.4 Block diagram for Diversity combination of compressed images.

The output bit stream of the SPIHT image compression algorithm consists of three types of data: 1) the header information, 2) the sorting information, and 3) the refinement information. Because the SPIHT algorithm uses variable length coding, one error can result in loss of synchronization and an unrecoverable image. The header information is a small portion of the data but most of the bits need to be received correctly so that the image can be recovered. Also, the sorting information bits must be received correctly (with the exception of the sign bits) in order to avoid a loss of synchronization and the resulting inability to reconstruct the image. The refinement bits do not contribute to any coefficient location information, so an error in these bits will not affect the ability to reconstruct the image. If a refinement bit is in error it may cause a perceptual error in the received image. However, these errors can be corrected or concealed in the final received image.

Another characteristic of the SPIHT bit stream is that the bits at the beginning are more important than the bits at the end. The majority of the bits at the beginning of the SPIHT bit stream tend to determine the coefficient placement and value of the most significant bit. These bits should be highly protected in order to insure that the received image can begin to be reconstructed. Toward the end of the SPIHT stream, there are still some bits that determine coefficient placement, but these bits contribute less to the perceptual quality of the image. Therefore, the bits at the beginning will be protected with a more powerful error correction code than the bits at the end of the bit stream. We employ interleaving and multiple channel codes for error protection of different

portions of the SPIHT stream. Similar ideas for error protection have been used in [19], [20].

The rules of the diversity combination for the compressed images are explained with the help of simulation example. For the purpose of simulation a 512 x 512, 8 bit" lena image" is used. The file is used in ".raw" format. The simulation is done for compression rates of 0.25bits per pixel and 0.5 bits per pixel.

Step by step procedure of diversity combination of compressed images is explained below.

Step1: The embedded bit stream is deep interleaved with 200 bits per block in row wise and then the unequal error protection is done using RS codes *(n k)* on column wise. Then 8 bit symbols are combined and transmitted row wise as show in the figure below.

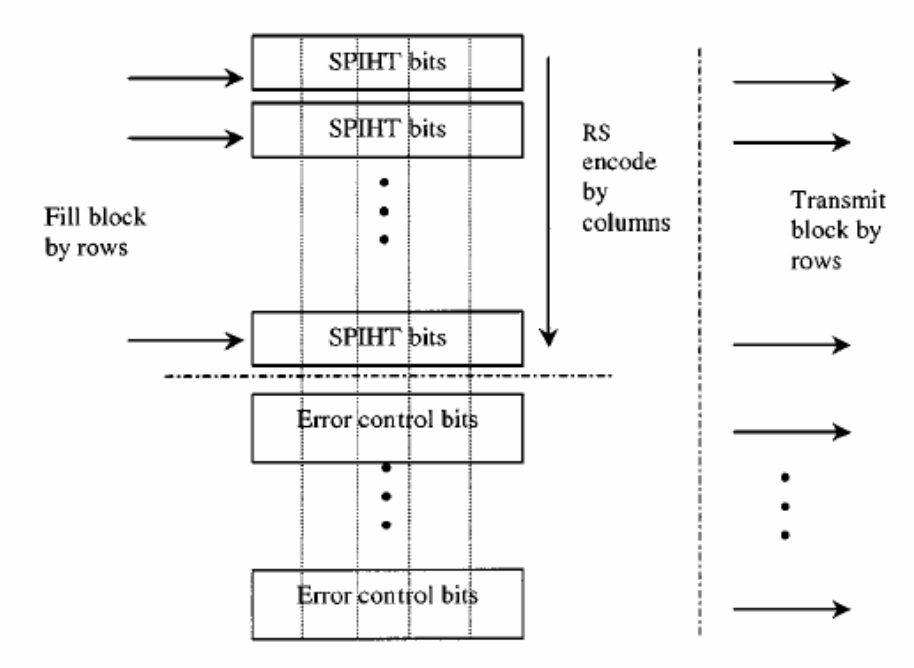

Figure 7.5 Figure showing the coding and interleaving procedure.

Step2 : Whole embedded stream is divided into three blocks *namely "low-resolution", "high-resolution-important" and "high resolution-not-so-important"*

As explained above as well as in chapter ……, first few bits of SPIHT stream are very important. But there is no measure for the number of bits that we can say precisely to divide into blocks. An arbitrary block of length 8000 bits are loaded into block" *low-resolution",* since this block is very important for proper reconstruction of the image, this block is protected using powerful error protection code RS(66,50). This code is capable of correcting 8 symbols worst case and 8*8bit = 64 symbols best case.

The next 12000 bits are grouped into the block *"high-resolution-important"*. Even though high resolution are not that important in other wavelet compression methods, in this method due to the properties of embedded zero tree coding techniques, some of immediate high-resolution bits carry important root information. Hence this block is protected using RS (56, 50);

The rest of the bits are grouped as *"high resolution-not-so-important"* and are block protected using RS (54, 50).

Step3: All the blocks described above are transmitted using the coding and interleaving scheme explained in the figure ….. These symbols are transmitted to the input of OFDM section to the QAM modulator.

Step4: Output of the QAM modulator is arranged in the OFDM symbol as shown and explained in the figure…. Then OFDM symbol is transmitted through Rayleigh fading channel and additive white Gaussian noise channel.

Step5: This is repeated till the entire blocks of data is transmitted and recovered at the receiver

The blocks are transmitted by rows, with all of the data bits in the block sent before the error control bits. Therefore, if the two blocks received from the individual diversity channels have the same bits we can assume no errors occurred on either channel. In this case, no channel decoding is necessary and the error control bits can be discarded. This is similar to the diversity combining rule employed in the image domain and here we use it in the data domain also.

After the data streams are decoded and the associated individual wavelet transforms are obtained, the transforms are combined. Like the rules for the uncompressed images, the combination rules are dependent on which sub-band is being processed. The actual combination rules for the SPIHT bit streams are slightly different from those rules in equations (7.2) and (7.3). An error in one of the sorting bits will contribute to random errors in the image, unlike the uncompressed images where the errors were generally isolated to certain areas in the images. The diversity combination rule for the low-resolution sub-band keeps the coefficient value at position (i, j) if the values are the same in both transforms. If the coefficient values are not equal, one of two types of error occurred at that location. Either 1) There was an error in the sorting pass of the SPIHT algorithm where one coefficient was assigned the wrong number of bits or 2) there was an error in the refinement pass where bits other than the most significant bit were in error. A threshold value, α_1, is set to determine which type of error occurred. If the coefficient values are not the same and the difference is greater

than the threshold, it is assumed the first type of error occurred, so one of the values is chosen based on the values of neighboring coefficients. But if the difference is less than α_1, it is assumed the second type of error occurred

7.4.1 Diversity algorithms

Two types of algorithms were designed and discussed in the previous work of [18]. In this thesis the second method [18] is used with new concept in the block based approach. If the wavelet transforms are combined after they have been completely reconstructed, the final image will have errors if both received transforms contain errors. Averaging can help to conceal errors but it does not correct them. To overcome this problem, the diversity-combining method uses block-based combining in the wavelet domain. The bit streams received from the uncorrelated OFDM sub-carrier blocks are grouped into *L* blocks of 4096 bits each.

Essentially if we can consider *Block_data1 (l) and Block_data2 (l)* where *l* is the incoming block .For each new block, the coefficients of the composite wavelet transform are updated based on the received bits. If the coefficients reconstructed from one block are judged more likely, then all of the coefficients from the more likely block are placed in the composite wavelet transform. If all of the chosen coefficient blocks are error free, then the reconstructed image will be error free.

This block-based diversity rule only selects blocks of bits *Block_data_final (l)* $\rightarrow b_f(l)$ from *Block_data1 (l)* $\rightarrow b_1(l)$ *and Block_data2 (l)* $\rightarrow b_2(l)$ based on the threshold $\omega_1(l)$ and $\omega_2(l)$ as explained below. The decision measures and selection rules for this weighted measure are given as

$$b_f(l) = \begin{cases} b_1(l) & \text{if } w_1(l) \le w_2(l) \\ b_2(l) & \text{if } w_1(l) > w_2(l) \end{cases} \quad \text{for } l = 1, 2, \cdots \qquad \text{Eq (7.4)}$$

where $b_1(l)$ *and* $b_2(l)$ are the data bits from blocks *Block_data1 and Block_data2* collected from the OFDM symbols and $\omega_1(l)$, $\omega_2(l)$ are expanded below.

Eq (7.5)

$$\begin{aligned} w_k(l) &= h_L^k(l) + h_H^k(l) \\ h_L^k(l) &= \sum_{\substack{(i,j)\in \text{low res.} \\ \text{subband}}} \left[d_k(i,j) + (c_{Lk}(i,j) - \mu_{Lk})^2\right] \\ h_H^k(l) &= \sum_{\substack{(i,j)\in \text{detail} \\ \text{subbands}}} \left[t_k(i,j) + c_{Hk}(i,j)\right] \\ \mu_{Lk} &= \frac{\sum_{\substack{(i,j)\in \text{low res.} \\ \text{subband}}} c_{Lk}(i,j)}{\begin{array}{c}\text{no. of coefficients} \\ \text{in low res. subband}\end{array}} \\ d_k(i,j) &= |c_{Lk}(i,j) - c_{Lk}(i,j+1)| \end{aligned}$$

and

Eq (7.6)

$$\begin{aligned} & t_k(i,j) \\ &= \left| c_{Hk}(i,j) - \left(\sum_{m=0}^{1} \sum_{n=0}^{1} c_{Hk}(2i+m, 2j+n) \Big/ 4 \right) \right| \end{aligned}$$

for *k=1,2* and *l refers to the lth blocks of bits.*

One important method here is, after the first block is identified the next incoming block is grouped with previously decided block, forming a concatenation of block with twice the block size. Then the diversity algorithms and are run again with the new block and the old block together. By doing this we can keep on collecting the important coefficients: thanks to the properties of embedded zero tree wavelets.

CHAPTER 8

SIMULATION AND RESULTS

8.1 Results of OFDM- Based Diversity algorithms

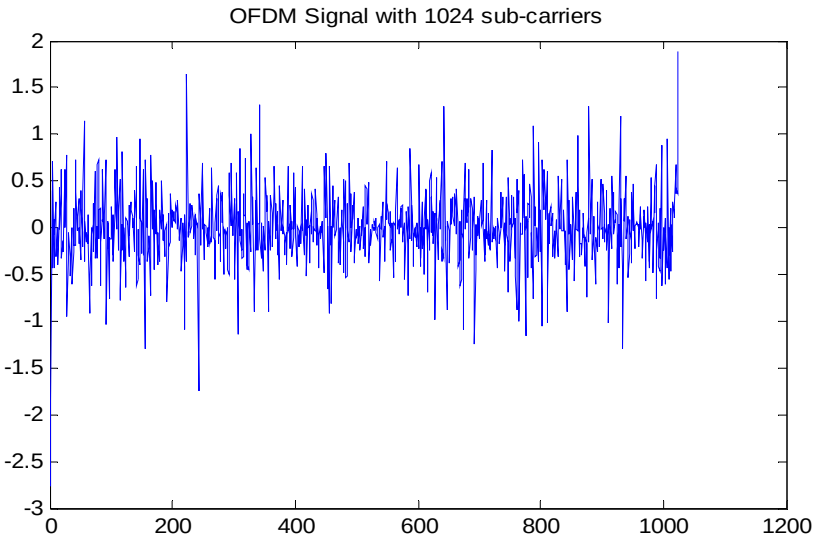

Figure 8.1 OFDM symbol with 1024 sub-carriers.

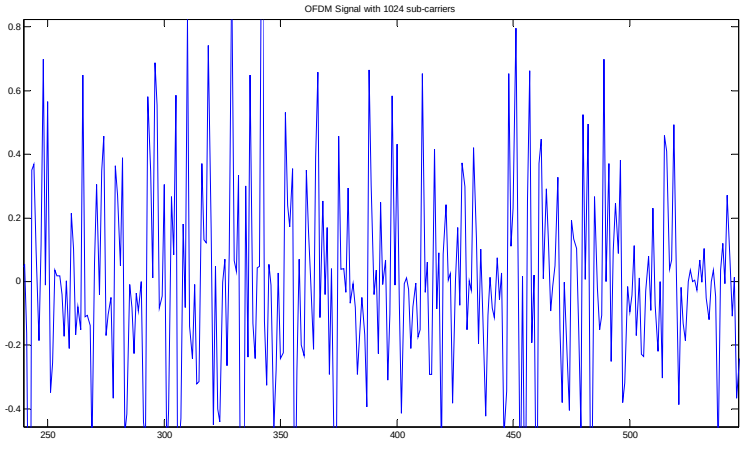

Figure 8.2 Zoom in version of OFDM symbols: To see the sub-carriers.

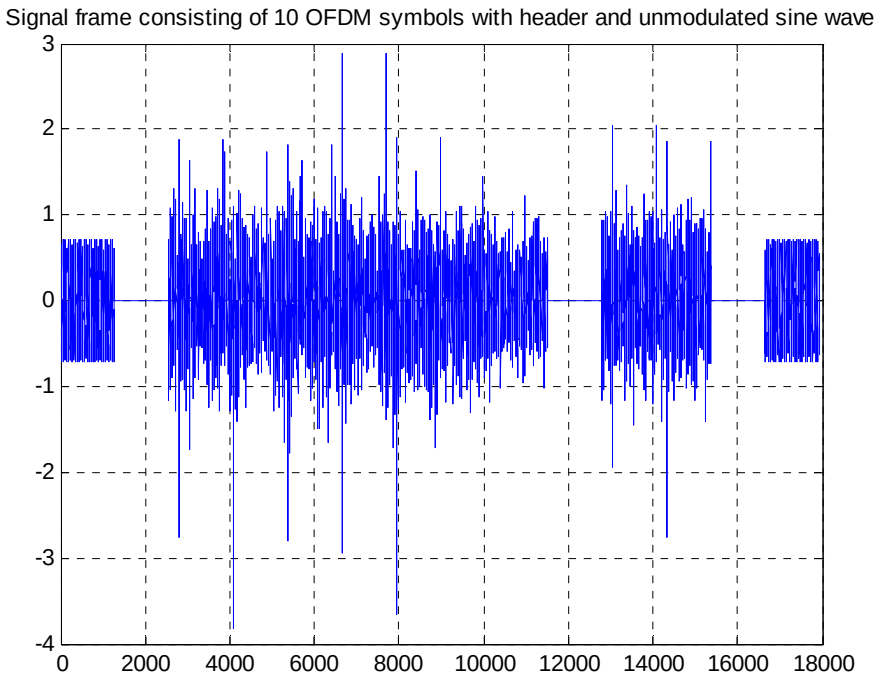

Figure 8.3 Frame based OFDM transmission scheme.

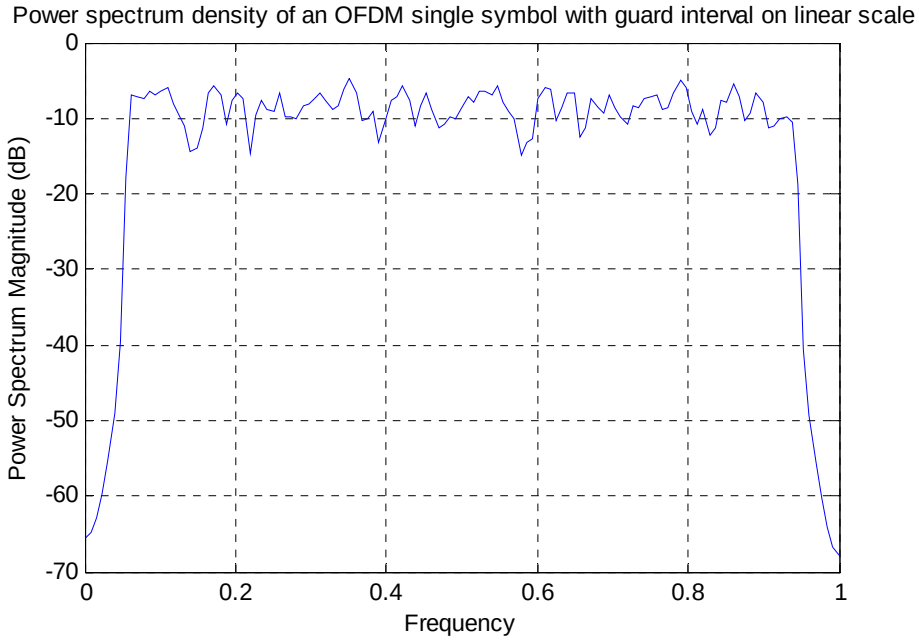

Figure 8.4 Power spectrum density of Diversity combination OFDM signal.

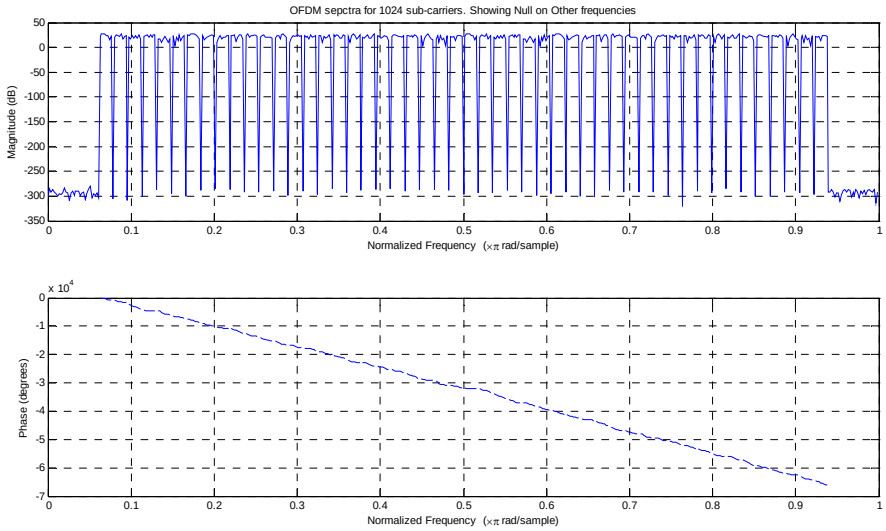

Figure 8.5 OFDM spectrum showing sub-carriers.

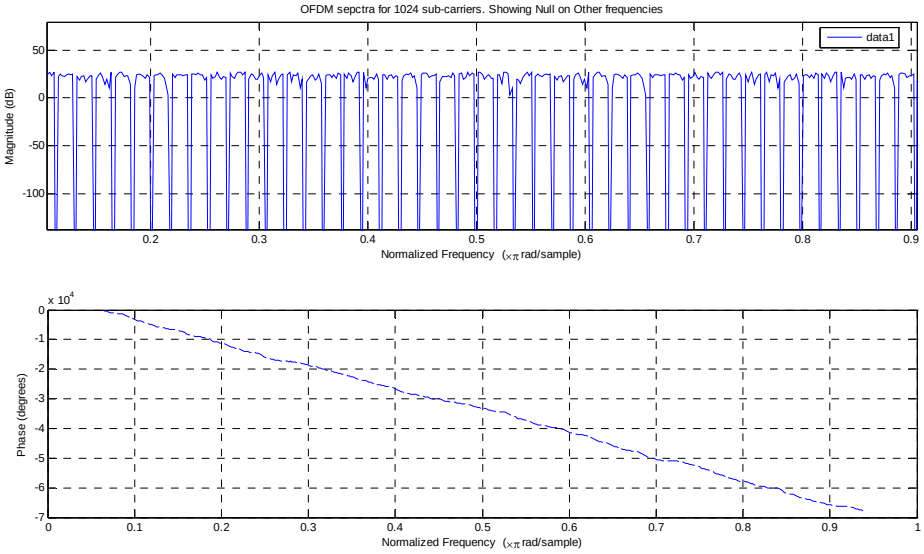

Figure 8.6 Zoom in version on sub-carriers.

image reconstructed without diversity for BER = 0.005

(a)

image reconstructed with diversity for BER 0.005

(b)

image reconstructed without diversity for BER = 0.010

(c)

image reconstructed with diversity for BER 0.010

(d)

Figure 8.7 Image (a) and (c) are without diversity, image (b) and (d) are with diversity and with OFDM for BER 0.005 and 0.010 respectively.

image reconstructed without diversity for BER = 0.020

(a)

image reconstructed with diversity for BER 0.020

(b)

image reconstructed without diversity for BER = 0.025

(c)

image reconstructed with diversity for BER 0.025

(d)

Figure 8.8 Image (a) and (c) are without diversity, image (b) and (d) are with diversity and with OFDM for BER 0.020 and 0.025 respectively.

8.2 Results for compressed images

Velocity 62miles/hr
SNR 15db noise level,
Compression rate 0.25 bits per pixel.

Table 8.1: SNR in dB illustrating the case of diversity algorithms for 0.25 bits/pixel rate

Transmission Method / BER	RS with INT w/o diversity	RS with INT with diversity	RS with INT With OFDM w/o diversity	RS with INT With OFDM with diversity	Hybrid system with diversity
BER=0.005	24.728	28.553	33.142	34.326	31.892
BER=0.010	23.831	25.434	32.148	33.628	30.75
BER=0.015	22.005	24.54	31.64	32.83	29.54
BER=0.020	21.86	24.028	29.526	30.09	30.002
BER=0.025	21.269	23.248	29.49	30.001	29.82

Table 8.2: SNR in dB illustrating the case of diversity algorithms for 0.5 bits/pixel rate

Transmission Method / BER	RS with INT w/o diversity	RS with INT with diversity	RS with INT With OFDM w/o diversity	RS with INT With OFDM with diversity	Hybrid system with diversity
BER=0.005	25.108	26.92	34.92	36.592	33.004
BER=0.010	23.182	24.785	33.96	35.627	32.992
BER=0.015	23.296	24.979	31.92	34.75	32.99
BER=0.020	23.242	24.128	30.94	33.527	32.75
BER=0.025	20.29	22.428	30.12	33.248	32.11

8.7 Results of Uncompressed Images

Refer figures in the next page.

image without diveristy, BER 0.005

image with diveristy, BER 0.005

image without diveristy, BER 0.015

image with diveristy, BER 0.015

image without diveristy, BER 0.025

image with diveristy, BER 0.025

Figure 8.9 in the previous page, images on the left hand side is without diversity and on the right side is with diversity for BER of 0.005, 0.015 and 0.025 respectively.

Table 8.3 PSNR table showing the results of diversity combining algorithm for uncompressed images

Transmission Method / BER	RS with INT w/o diversity	RS with INT With OFDM with diversity
BER=0.005	30.728	35.326
BER=0.010	28.831	33.628
BER=0.015	27.005	32.83
BER=0.020	25.86	31.09
BER=0.025	19.269	30.001

CHAPTER 9

HYBRID OFDM SYSTEMS

One of the candidates for a large data-rate modulation scheme is OFDM. In such systems very high data rates are converted to very low parallel-data rates using a series-to-parallel (SIP) converter. This ensures flat fading for all of the SCs; that is, a wideband signal becomes a packet of narrowband signals. This will automatically combat multipath effects, removing the need for equalizers and RAKE receivers. Hybrid approach (OFDM-CDMA-SFH) for short. It has essentially been developed for the 60-GHz frequency, but is equally applicable at any other frequency provided the necessary bandwidth is available [1].

9.1 OFDM-CDMA-SFH (Hybrid)

[1], In this case, suppose we have an eight-bit CDMA signal ("word"). We feed this word to a S/P converter. After this step comes a crucial difference. We do not carry out any Walsh spreading, but we straightaway carry out an 8-point IFFT (OFDM modulation). This means that one OFDM symbol equals the entire 8-bit CDMA word that we need to transmit. Hence, our information rate is eight times faster than in the previous two procedures. At the receiver, we carry out an FFT, but with another crucial difference: There is no need in our case to use RAKE combiners because we are not

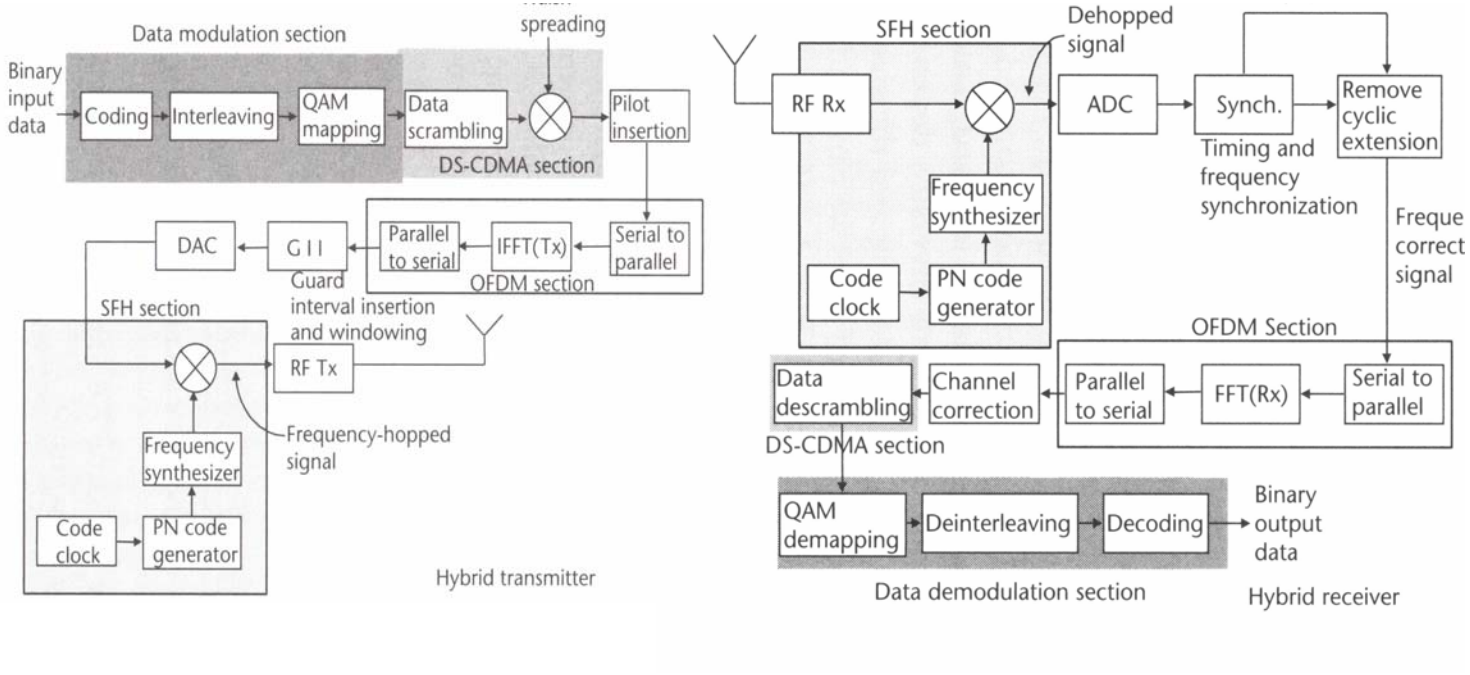

Figure 9.1 Hybrid OFDM system.

carrying Out Walsh spreading in the FD in the interests of frequency diversity. This is different from the OFDM-CDMA approach discussed earlier, wherein RAKE combiners are used after OFDM demodulation in order to take advantage of the entire frequency spread of that particular bit. In reality, if we use an N-point OFDM system, we will need to use an N-finger RAKE combiner. This is extremely costly and, hence, a compromise is achieved by using fewer of fingers, for example, a 7-finger combiner. This means that we do not take advantage of the entire frequency spread anyway. In a way, this is a waste of resources. Therefore, after FFT we carry out a P/S conversion and then de-spread the CDMA signal. For user separation, we can use Walsh spreading in the transmitter, but this is done before the SIP converter in the transmitter, that is, in the TD. In the receiver we de-spread the Walsh signal after the P/S converter. This will ensure user separation. Other spin-offs from this technique are discussed in this chapter. Finally, in the frequency-time diagram, we have shown slow FH of the entire symbol. The hopping techniques are discussed further in this chapter.

After convolution coding and repetition, symbols are sent to a 20-ms block inter-leaver, which is a 24 x 16 array. In the forward channel, direct sequence is used for data scrambling. The long PN sequence is uniquely assigned to each user and is a function of the mobile station's electronic serial number (ESN) and its mobile station identification number (MIN). The PN sequence is generated at a rate of 1.228 8 Mbps and is decimated to 19.2 Kbps. The data scrambling is then performed by modulo-2 addition of the inter-leaver output with the decimator output symbol. This is then multiplexed with four bits for power control and given an orthogonal covering using

Walsh code. The Walsh code constitutes the inner coding. This is necessary because the PN sequence is in practice not enough to ensure channel isolation. The final output of the forward channel is bits emerging at 1.2288 Mbps. Normally, in DS-CDMA systems this are then transmitted. In our case, these bits are directly fed to the OFDM unit, which treats this as a binary data stream. *Reader can refer to chapter 2 section 2.2.4*

Having interfaced CDMA unit with OFDM, we shall now examine how to achieve slow FH for this system. The hopping is carried out in the RF up-converter, and de-hopping is conducted in the RF down-converter.

9.2 SFH Interface

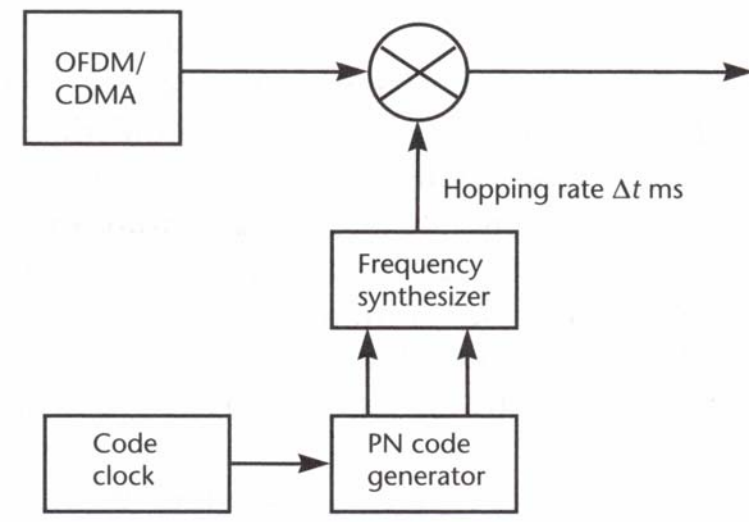

Figure 9.2 RF up-converter.

Slow FH is initiated in the RF up-converter. The principle is shown in Figure 9.2. The output from the D/A converter is fed to a mixer as shown in Figure 9.1. Hopping rate is

Δt ms, where Δt is the length of the transmission block as discussed below. This means that every At ms, we switch to a new frequency. If we assume a bandwidth of 100 MHz, we switch to another center frequency that is 100 MHz away. The hop set can be any number and is limited only by the extent of the available bandwidth. The RF down converter is shown in Figure 9.3

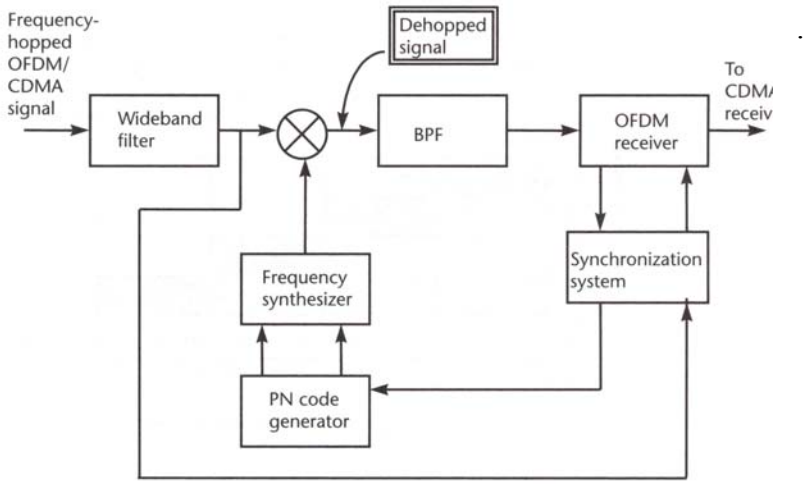

Figure 9.3 RF-down converter.

If the frequency pattern in the receiver synthesizer is synchronized with the frequency pattern of the received signal, then the mixer output is a de-hopped signal at a fixed-difference frequency. Before demodulation, the de-hopped signal is applied to a conventional RF receiver, that is, an RF amplifier, mixer, and so forth. In FR, whenever an undesired signal occupies a particular hopping channel, the noise and interference in that channel are translated in frequency so that they enter the demodulator. Thus, it is possible to have collisions in an FR system where an undesired user transmits in the

same channel at the same time as the desired user. Normally, the type of modulation used in FH is non-coherent FSK as is usually done in DS-CDMA-SFH systems and the possible OFDM channel, for example, 100 MHz (Δf = 100 MHz). Within this bandwidth there are SCs. The sum of the SC bandwidths equals 100 MHz. The maximum band spread is an integer multiple of 100 MHz, say, 4 x 100 = 400 MHz. This means that we can carry out four hops per user. The maximum transmission delay is the time allowed for the radio link (e.g., 20 ms). Δt is the length depending upon the number of symbols being transmitted in one hop. We require very large bandwidths that are integer multiples of the basic signal bandwidth. This kind of bandwidth availability is presently difficult to ensure, unless we operate at 60 GHz.

Therefore, each CDMA user will be subjected to n frequency hops for frequency diversity and interference diversity (which lowers the required SNR and increases capacity). The frequency hop rate of an FHSS system is determined by the frequency agility of the receiver synthesizers, the type of information being transmitted, the amount of redundancy used to code against collisions, and the distance to the nearest potential interfering user. The near-far problem is, however, not totally avoided in FH systems because there will be some interference caused by stronger signals bleeding into weaker signals due to realistic filtering of adjacent channels. To combat occasional hits, error-correcting coding is required on all transmissions. By applying strong Reed-Solomon or other burst error-correcting codes, performance can be increased dramatically, even with occasional collisions.

9.3 System Parameters

Bandwidth and other consideration: In this section, we are assuming Rayleigh fading conditions and AWGN. We are also assuming perfect OFDM synchronization with no carrier offset. Multimedia requirements of high bit rates, typically 155 Mbps, require high bandwidths of around 100 MHz or higher. The CDMA system in Figure 7.2 pertains to a voice channel with a band-spread factor of 128 for a data rate that is most 9,600 bps. This is due to adverse transmission conditions and to there being a lot of users at that frequency (around 850 MHz). In our case, however, we intend to operate at around 60 GHz, where larger bandwidths are available. This entails Rician fading conditions and LOS transmissions, conditions which are not so severe. Therefore, a band-spread factor of 128 is unnecessary. More likely, a band-spread factor of 10 or less will prove sufficient. This, however, has to be verified by extensive simulations. If we assume a band-spread factor of 10, then we acquire a bandwidth of atmost1 GHz for 100-Mbps data rate.

We can expect a steep rise in the number of users when high data rates become realizable, especially with regard to video telephones. The CDMA aspect (code diversity) really gives rise to lot of users because FH has been introduced to obtain frequency diversity to reduce the near-far problem. This limits the number of users in order to avoid collisions. The CDMA aspect makes up for this limitation by introducing a larger number of users due to code diversity. Interleaving and error-correction coding may be dispensed with if the need so arises, that is, if the channel is not severe. In case the channel does not pose problems in the foreseeable future, we can

increase the spread factor of the CDMA transmission (increase the bandwidth) or introduce FEC and interleaving. The OFDM aspect is required because it eliminates the need for RAKE receivers (as compared to pure DS-CDMA systems because there are no multipath delay effects) and allows us to use coherent modulation even when frequency hopping (because we will now hop on an OFDM symbol basis), unlike in most SFH systems wherein maintaining phase continuity during hopping is difficult. It also helps reduce the burden of synchronization related to CDMA systems .In this connection MC-CDMA also uses OFDM techniques, but with RAKE receivers (in the FD, due to Walsh spreading). In our style of signal processing we do not use RAKE receivers. This crucial change in the style of MC-CDMA design results in a massive saving of hardware. We will accept the risks that some SCs will be in deep fade and correct for this eventually using FEC coding (COFDM) or interleaving. This is different from the OFDM-CDMA approach discussed earlier, wherein RAKE combiners are used after OFDM demodulation in order to take advantage of the entire frequency spread of that particular bit. In reality, if we use N-point OFDM system, we will need to use an N-finger RAKE combiner. This is extremely costly; hence, a compromise is achieved using fewer fingers (e.g., a 7-finger combiner). This means that we do not take advantage of entire frequency spread anyway. In a way, this is a waste of resources. Taking such matters into consideration, the hybrid system does not spread each bit in the FD and does not, therefore, use RAKE combiners. Therefore, we call this approach the hybrid OFDM/CDMA/SFH approach and not MC-CDMA.

Coding: In CDMA transmitter (as in the IS-95 system), there are two levels of coding: convolution coding (for error correction) or concatenated coding and Walsh encoding (this is a spreading code, not an error-correction code). The latter is an orthogonal coverage because PN sequences by themselves are insufficient to ensure channel isolation. The Walsh coding ensures orthogonality between users. The convolutional coding ensures robustness of data.

Modulation: Unlike in pure DS-CDMA system, in our case, the CDMA sequence after Walsh coding does not get converted to RF, but instead is fed as input to the OFDM transmitter. In the OFDM transmitter it gets modulated as an OFDM signal, then via a P/S converter gets converted to RF.

CDMA receiver: Similarly, the OFDM receiver gives the CDMA receiver a sequence at chip rate after OFDM modulation. Thereafter, CDMA signal processing is carried out in that there is a digital correlator that ensures channel isolation based on PN sequences and Walsh coding. The output of the correlator is then given to a Viterbi decoder () for convolution decoding. The output from this decoder is the required data sequence. RAKE receivers are not required in this case, unlike in DS-CDMA systems, because the OFDM system has no deleterious effects due to multipath.

Synchronization: Stringency of synchronization is, however, still required as the PN sequences need to be synchronized. However, in such a hybrid system, the burden of synchronization is transferred to the OFDM system. The OFDM synchronization system is more sophisticated than CDMA synchronization systems as the OFDM system utilizes the cyclic prefixes for synchronization. Hence, the PN sequences

emerging from the OFDM system and going to the CDMA system are already better synchronized than in a pure CDMA system. The reader will recall that synchronization is one of the limiting factors in CDMA systems for high data rates. It is expected that in our system, such problems will be considerably reduced, especially in the uplink because the mobile receivers, thanks to OFDM, will be better synchronized to the transmitter. This will reduce MAI as compared to a pure DS-CDMA system.

Bit-error probabilities: the proposed system is essentially a CDMA/OFDM/FH system because the transmission and reception are carried out by the OFDM-FH system. The CDMA aspect generates the data stream, but in a more complicated way. In section 7.5, we compare the simulation results in AWGN between OFDM, OFDM/CDMA (MC-CDMA) and the hybrid system (OFDM/CDMA/SFH).

Trade-off between OFDM and CDMA: The OFDM-FH system by itself does not solve the multimedia requirement because multimedia requires high bit rates, typically 155 Mbps. This requires large bandwidths of typically 100 MHz. By using FH among users to reduce the near-far effect suffered by CDMA systems, our number of users comes down drastically, as it is limited by the bandwidth available. By adding CDMA, we have rectified this problem by enhancing the number of users because CDMA supports additional users (being limited only by MAI) working at the same frequency. Hence, there is a trade-off, which we clarify using an example. Suppose in a hybrid system the CDMA and cannot handle more than 20 users due to MAI. These 20 users share a one hop set. Therefore, among these users there will be adverse performance due to near-far effect. If we find that this near-far effect is intolerable, we reduce the number of users

to, say, 10 and make the remaining 10 share another hop set. Due to bandwidth constraints, suppose we can use only two hop sets. Then, we once again we have a total of 20 users for this hybrid system. But on the other hand, if the near-far effect is not too serious for 20 users, we can assign the other hop set to another 20 users for 40 users in all. This trade-off between the control of near-far effect and the number of users depend on channel conditions. The hybrid system gives us this flexibility. Hence, there is eventually a trade-off between our desire to control the near-far effect and the number of users we desire.

CDMA signal processing: It will be argued that the present data rate of 1.2288 Mbps in IS-95 systems is woefully inadequate for multimedia applications. This is acknowledged. However, bear in mind that if we want a large number of users, we need to use CDMA techniques. Hence, efforts must be made to increase data rates using better phase locked loops (PLLs) for synchronization and high-speed digital electronics. In this proposed hybrid concept, the entire CDMA signal processing is carried out in the digital domain both for the transmitter as well as for the receiver.

9.4 The Hybrid System

We now examine the equations pertaining to the hybrid system without SFH. From now on, we shall call this OFDM-CDMA (hybrid)[1].

The transmitted signal of the *i*th user [1] is written as

$$s_{sp}^{i}(t)=\sum_{u=-\infty}^{+\infty}\sum_{n=0}^{p-1}\sum_{m=1}^{N_{PG}}\mathrm{Re}\left[b_n^i(u)c_m^i(u)\cdot p_c\left\{t-(m-1)T_c^{'}-uT_s^{'}\right\}\cdot\exp\left\{j2\pi(f_0+n\Delta f_{sp})t\right\}\right] \quad \text{Eq (9.1)}$$

Where $b^{i}_{n}(u)(=1\pm j,-1\pm j)$ is the uth input data at the nth carrier of the ith user after S/P conversion.

$c^{i}_{m}(u)$ is the mth chip of the spreading code for the ith user.

T'_s (= PT_s) is the symbol duration, and T'_c(= $T'_s/\mathrm{N_{PG}}$) is the chip duration after S/P conversion respectively.

f_0 is the lowest carrier frequency, and Δf_{sp}(= 1/ T'_c) is the carrier separation.

$p_c = 1$ ($0\le t\le T'_c$), $p_c = 0$ (otherwise).

In this system, the symbol period of T'_s becomes P times as long as T_s of the single-carrier case, and the influence of multipath fading is released. From (9.1), the transmitted signal of the ith user at $u = 0$ is represented as

$$s(t)=\sum_{n=1}^{P}\sum_{m=1}^{N_{PG}}\mathrm{Re}\left[b_n c_m p_c(t^{'})e^{j2\pi f_n t}\right] \quad \text{Eq (9.2)}$$

where

$$p_c(t^{'})=p_c\left\{t-(m-1)T_c^{'}\right\},\ f_n=f_0+n\Delta f_{sp} \quad \text{Eq (9.3)}$$

and i is not marked for simplicity. If the channel is considered unchanging for one symbol duration, the channel IR is expressed with the delta function $\delta(t)$ as

$$h(t) = \sum_{l=1}^{L} h_l \delta(t - \tau_l) \qquad \text{Eq (9.4)}$$

Where h_l and τ_l are the amplitude and delay of the lth path, respectively. The received signal is

given by

$$\begin{aligned} r(t) &= (s \otimes h)(t) + \mathrm{Re}[\, n(t) e^{j 2\pi f_{P/2} t} \,] \\ &= \sum_{l=1}^{L} \sum_{n=0}^{P-1} \sum_{m=1}^{N_{PG}} \mathrm{Re}\left[b_n c_m p_c(t) e^{j 2\pi f_n t} \right] + \mathrm{Re}\left[n(t) e^{j 2\pi f_{P/2} t} \right] \\ &= \sum_{n=0}^{P-1} \sum_{m=1}^{N_{PG}} \mathrm{Re}\left[H_k b_n c_m p_c(t) e^{j 2\pi f_n t} \right] + \mathrm{Re}\left[n(t) e^{j 2\pi f_{P/2} t} \right] \end{aligned} \qquad \text{Eq (9.5)}$$

Where $(s * h)(t)$ is the convolution of $s(t)$ and $h(t)$, and H_n is expressed by

$$H_n = \sum_{l=1}^{L} h_l e^{-j 2\pi f_n \tau_l} \qquad \text{Eq (9.6)}$$

In the receiver, r(t) is transferred by a local oscillator whose frequency is $f_{P/2}$. The resulting

complex signal becomes [1]

$$r'(t) = \sum_{n=0}^{P-1} \sum_{m=1}^{N_{PG}} H_n b_n c_m p_c(t) e^{j 2\pi \frac{n - P/2}{T_s'}} + n(t) \qquad \text{Eq (9.7)}$$

Therefore, the mth chip of the nth carrier after FFT is shown as

$$r_n = \frac{1}{T_c'} \int_0^{T_c'} r'(t) e^{-j2\pi \frac{n-P/2}{T_s'}} dt = H_n b_n c_m + n_n \qquad \text{Eq (9.8)}$$

9.5 Analytical performance in fading Channels

The output $S_K(t)$ of the OFDM modulator is given by

$$S_K(t) = \sum_m s_{km}(t - mT_B) \qquad \text{Eq (9.9)}$$

Where each waveform $s_{km}(t)$ is obtained by modulating a block of N consecutive bits $b^m{}_k[n]$, by n

SCs $f_n = n\Delta f$, $\Delta f = 1/T_0 \leq 1/NT$, $n = 0,\ldots..N-1$:

$$s_{km}(t) = \sum_{n=0}^{N-1} b_k^m[n] \exp(j2\pi f_n t) g_T(t) \qquad \text{Eq (9.10)}$$

Where $g_T(t)$is a rectangular pulse of duration $T_B = NT$. The samples of the OFDM signal $s_{km}(t)$ are generated using IFFT as discussed earlier.

We now frequency-hop the OFDM signal Eq (9.10) according to the kth hopping pattern $f_k(t)$ derived from a hop set of q possibilities. Hence, the transmitted signal can be expressed as

$$S_m(t) = V_m S_k(t) \cos(2\pi f_c t + 2\pi f_k t + \theta_m + \theta_k) \qquad \text{Eq (9.11)}$$

Where

$$V_m = \sqrt{A_{mc}^2 + A_{ms}^2} \; and \; \Theta = \tan^{-1}\left(\frac{A_{ms}}{A_{mc}}\right) \qquad \text{Eq (9.12)}$$

A_{mc} and A_{ms} are the information-bearing signals amplitudes of the quadrature carriers and $S_k(t)$ is the signal pulse. The hop frequency $f_k(t)$ and the phase θ_k are constant over one hop. The phase θ_k represents the phase shift introduced by the frequency hopper when it switches from one frequency to another. We correct the SNR for the number of parallel paths L, number of users K, and the sequence period N. Due to the GI, an SNR loss is taken into account as SNR * η_g. Normally we assume $\eta_g = 0.8$.

We can now express the de-hopper output as $r_i(t)$ as the jth hop of the ith receiver:

$$r_i(t) = V_m \sum_{k=1}^{K} \sum_{l=1}^{L} h_{kl} S_K(t - t_{KL}) \delta\left[f_k(t - \tau_{ij}), f_i(t - \tau_{ij})\right] \exp(A_{klj}) + N(t) \qquad \text{Eq (9.13)}$$

Where δ is the Dirac delta function and A_{klj} includes the phases introduced by the QAM modulator, hopper, radio channel, and de-hopper. The noise contribution $N(t)$ is white complex Gaussian noise. After sampling at frequency f_s, we have $r_i[m,n] = r_i\,(m\,T_B + n/f_s)$. The cyclic prefix is removed, and the resulting block of N_T samples enter the FFT

$$d[m,n] = \sum_{k=1}^{N_T - 1} r_i[m.k] \exp(-j 2\pi n k / N_T) \qquad \text{Eq (9.14)}$$

Results of Hybrid – OFDM systems are shown in next section,

To simulate these results multi-user PN- codes were used.

PN-code1=1101001100

PN-code2=0101111010

PN-code3=1110101100

PN-code4=0100010011

These results help us to understand that, using SPIHT coding technique or any other progressive coding techniques; we can increase the quality of service. Here we are transmitting at the same rate and bandwidth is not shared between any users. Thus we can say that hybrid systems are the next generation multi-media research area. The signal to noise ratio comparison is given in the Diversity combining chapter.

This test set-up also proves the theory of OFDM-based diversity combination techniques of this thesis works in hybrid environment, with proper error correction codes and new progressive coding techniques this can readily implemented for video and other high speed services

9.6 Results of hybrid OFDM system

image transmitted with CDMA PN code 1101001100 with diversity with QOS of 1/2 of total (bits) No Hops

image transmitted with CDMA PN code 0101111010 with diversity with QOS of 1/4 of total (bits) one Hops

Figure 9.4 Hybrid OFDM system (a) 1/2 of complete bits, (b) ¼ of total bits.

image transmitted with CDMA PN code 1110101100 with diversity with QOS of 3/4 of total (bits) No Hops

image transmitted with CDMA PN code 0100010011 with diversity with QOS of full of total (bits) 2 Hops

Figure 9.5 Hybrid OFDM system (c) 3/4 of complete bits, (b) complete bits.

CHAPTER 10

REAL TIME DSP IMPLEMENTATION USING TMS320C6713 BOARD

10.1 Introduction

Embedded Target for the TI TMS320C6000 DSP Platform integrates MATLAB® with Texas Instruments eXpressDSP™ tools [21]. The software collection lets us develop and validate digital signal processing designs from concept through code. The Embedded Target for TI C6000 DSP consists of the TI C6000 target that automates rapid prototyping on C6000 hardware targets. The target uses C code generated by Real-Time Workshop® and TI development tools to build an executable file for targeted processor. The Real-Time Workshop build process loads the targeted machine code to the board and runs the executable file on the digital signal processor.

The chip set used here is spectrum digital TI board. The MATLAB to DSP communication is made through RTDX channels. Real-Time Data Exchange (RTDX) provides real-time, continuous visibility into the way target applications operate in the real world. RTDX allows system developers to transfer data between target devices and a host without interfering with the target application. It is assumed that the reader has some exposure to DSP/BIOS.

DSP/BIOS is a scalable real-time kernel that supports real-time scheduling, synchronization, and real-time instrumentation. DSP/BIOS provide preemptive multi-threading, hardware abstraction, and real-time analysis. DSP/BIOS make use of RTDX

to transfer data for its real-time analysis tools and allow the user to insert and configure RTDX by providing an RTDX interface in its configuration tool. It also provides two other interfaces called the host channel (HST) and the host link driver (DHL) for communication between the host and target. These interfaces internally use RTDX to communicate with the host.

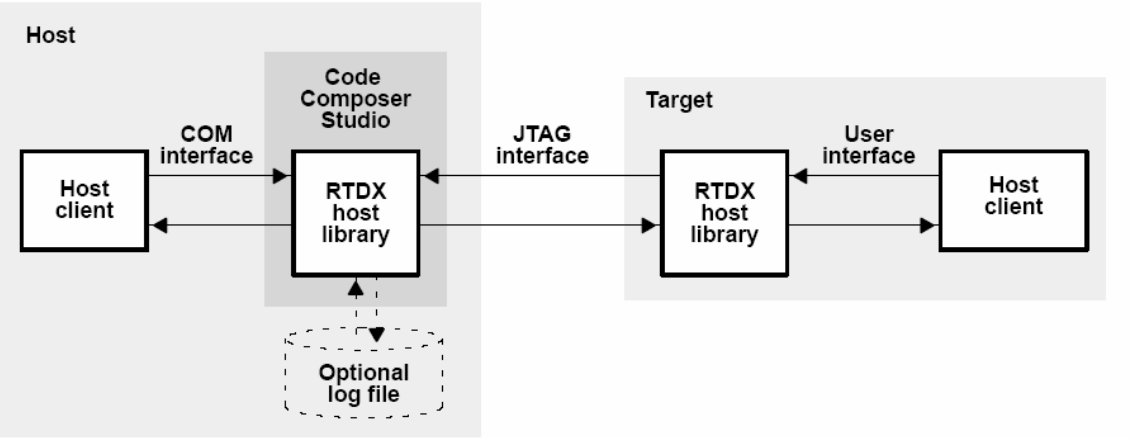

Figure 10.1 RTDX to Host Connection diagram.

In target-to-host communication, an output channel should be configured. Data is written to the output channel using the routines defined in the RTDX user interface. This data is immediately recorded into a target buffer defined in the RTDX target library. The data from this buffer is then sent to the host through the JTAG interface. The RTDX host library receives this data from the JTAG interface and records it into either a memory buffer or an RTDX log file. The transfer of data through JTAG from target to host is done without halting the target's processor. This data recorded by the host can then be collected by the host application and displayed in a meaningful way.

10.2 connection diagram

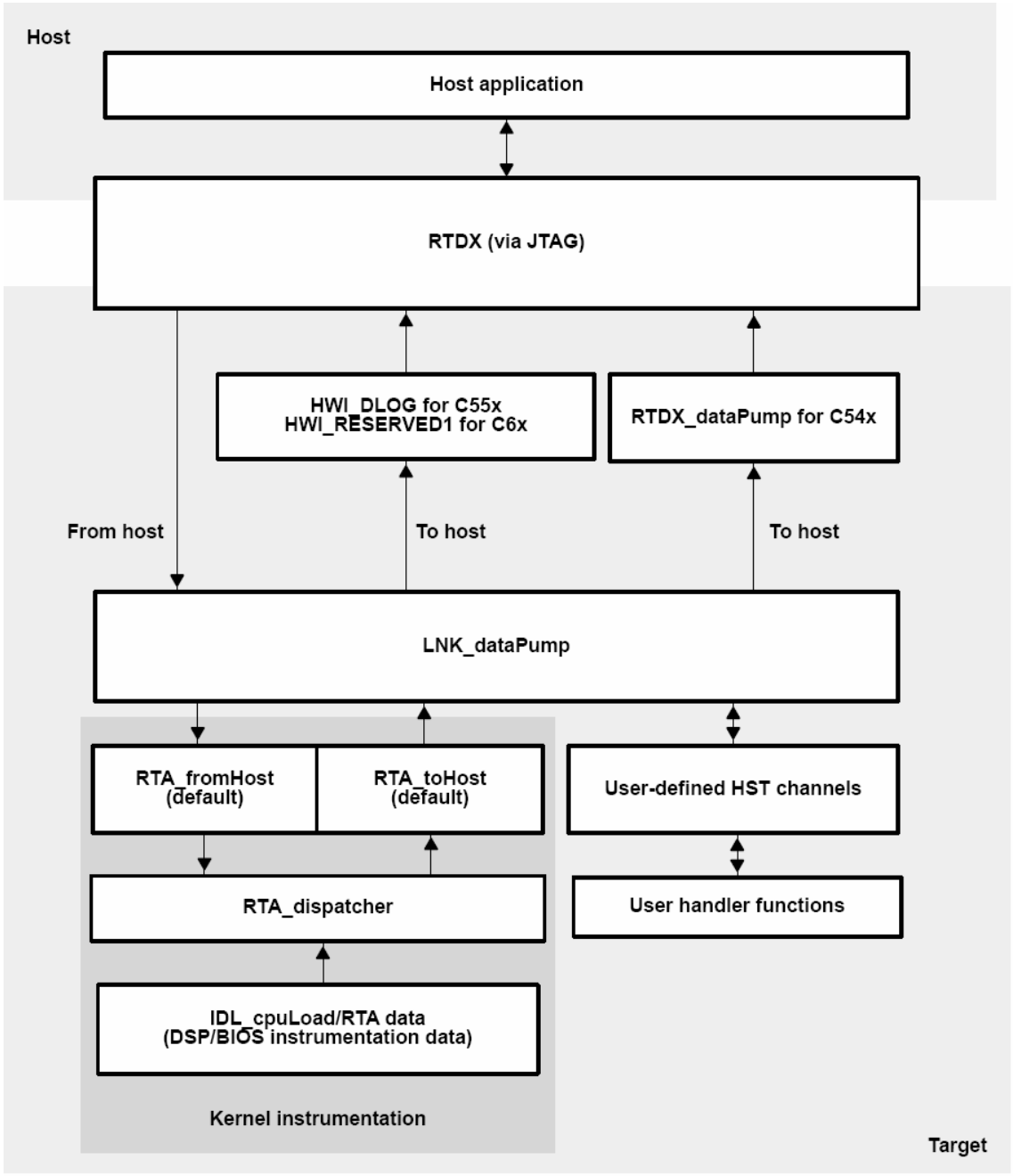

Figure 10.2 Flow diagram between the host and the Target and the RTDX initiation.

10.3 Reading a data from the target

1. Declare the function.
```
function void = h_readmsg()
```
2. Get a handle to Code Composer Studio.
```
cc = ccsdsp;
```
3. Get a handle to RTDX channel “ochan”.
```
rtdx_ochan = cc.rtdx;
```
4. Enable RTDX.
```
rtdx_ochan.enable;
```
5. Open the RTDX channel for reading.
```
open( rtdx_ochan, 'ochan', 'r' );
```
6. Read data within a loop until no more data is available.
```
timeout_msg = 'Timeout';
NOMOREDATAMSG = 'No more data is available!';
errmsg = NaN;

while ( isempty( findstr( timeout_msg , errmsg ) ) )
        try
                % read data
                data = readmsg( rtdx_ochan, 'ochan', 'int32' );
                % display data
                disp( data );
        catch
                errmsg = lasterr;
                disp( NOMOREDATAMSG );
                break;
        end
end
```
7. Close the RTDX channel.
```
close( rtdx_ochan, 'ochan' );
```
8. End function.
```
return;
```

Using the MATLAB command functions, the data from the output of QAM modulator is passed as I/0 streams through RTDX channels and using the DSP LIB functions, the processing of OFDM signals are done. 1024 point double precision FFT functions are used.

10.4 Clock cycle calculation

Number of clock cycles calculation is done through the formula

Cycles = (14*n/4 + 23)*log4(n) + 20

e.g., if n = 256, cycles = 3696.

n=1024, cycles= 8452

With the help of modern DSP processors the generation of OFDM symbol and its processing complexity is reduced twice fold.

CHAPTER 11

SUMMARY AND CONCLUSION

OFDM -Wavelet domain based diversity is discussed in this thesis. With the emerging demand for multimedia communications and with increase in research in millimeter wave channels, hybrid –OFDM system based wavelet diversity can be a tool for wireless transmission of images where quality desired heavily. The main goal of the thesis is fulfilled by showing that diversity can be carried out by arranging the data in suitable sub-carriers that separate themselves with considerable frequency spacing.

11.1 Summary of the thesis

1. *Orthogonal signals and its properties were discussed.*
2. *Relationship between orthogonality and diversity is derived.*
3. *Multiple access techniques are revisited.*
4. *OFDM and its properties are discussed in detail as per the requirement.*
5. *Channel properties of OFDM are simulated.*
6. *Wavelets and its relation to the thesis is discussed and explained in detail.*
7. *OFDM based - Diversity algorithms are designed and explained.*
8. *New approach is tested in hybrid-OFDM system.*
9. *Results are tabulated for reader's reference.*
10. *Real Time DSP implementation is discussed.*

REFERENCES

[1] OFDM for Wireless communication systems/ Ramjee Prasad.-(Artech house universal Personal communication series).

[2] Theory and Applications of OFDM and CDMA wideband wireless communications by Henrik Schulze and Christian Luders. Hohn wiley & sons,ltd

[3] Multi-carrier Digital communications Theory and Applications of OFDM by Ahmad R.S Bahai, Burton R. Saltzberg , Mustafa Ergen

[4] Microwave Mobile communications W C. Jakes IEEE classic reissue

[5] T. Rappaport, "Wireless Communications, Principle & Practice", IEEE Press, Prentice Hall, pp. 3, 1996.

[6] *G.* G. Raleigh and V. K. Jones, "Multivariate modulation and coding for wireless communication," IEEE *Journal* of *Selecred Areas in Communications.* vol. 17. No. 5. pp. 851-866, May 1999

[7] Channel Modeling and Characterization at 17 GHz for Indoor Broadband WLANManuel Lobeira Rubio, Ana García-Armada*, Member, IEEE*, Rafael P. Torres*, Member, IEEE*, and José Luis García*, Member, IEEE IEEE JOURNAL ON SELECTED AREAS IN COMMUNICATIONS, VOL. 20, NO. 3, APRIL 2002*

[8] H. Hashemi, "The indoor radio propagation channel," *Proc. IEEE*, vol. 81, no. 7, pp. 943–968, July 1993.

[9] C. Kikkert, “Digital Communication Systems and their Modulation Techniques”, James Cook University, October 1995.

[10] Chui C. K. (1992), *An introduction to wavelets*, Boston, Academic Press, ISBN 0121745848.

[11] Sayood K. (2000), *Introduction to data compression*, Morgan Kaufmann Publrs, US, 2 revised edition, ISBN 1558605584.

[12] Daubechies I., Barlaud M., Antonini M., Mathieu P. (1992), “Image coding using wavelet transform” in *IEEE Transactions on image processing*, Vol. 1, No. 2, pp. 205-220.

[13] Brislawn C. M.. (1996), “Classification of nonexapnsive symmetric extension transforms for multi rate filter banks” in *Applied and computational harmonic analysis*, Vol. 3, pp. 337-357.

[14] Boulgouris N. V., Athanasios L., Strintzis M. G. (2000), “Wavelet compression of 3d medical images using conditional arithmetic coding” in *IEEE International symposium on circuits and system*, Geneva, pp. 557-560.

[15] Said A., Pearlman W. A.(1996), “A new, fast, and efficient image codec based on set portioning in hierarchical trees” in *IEEE Transactions on circuits and systems for video technology*, Vol. 6, No. 3, pp. 243-250.

[16] Shapiro J. M. (1993), “Embedded image coding using zerotrees of wavelet coefficients” in IEEE Transactions on signal processing, Vol. 41, No. 12, pp. 3445-3462.

[17] V. Weerackody and W. Zeng, “ARQ schemes with switched antenna diversity and their applications in JPEG image transmission,” in *Proc. IEEE GLOBECOM*, vol. 3, 1995, pp. 1915–1919.

[18] L. C. Ramac and P. K. Varshney, “A Wavelet Domain Diversity Method for Transmission for Images over Wireless Channels ”, *IEEE Journal on Selected Areas in Communications,* Vol. 18, pp. 891-898, June 2000.

[19] P. Burlina and F. Alajaji, “An error resilient scheme for image transmission over noisy channels with memory,” *IEEE Trans. Image Processing*, vol. 7, pp. 593–600, Apr. 1998.

[20] P. G. Sherwood and K. Zeger, “Error protection for progressive image transmission over memoryless and fading channels,” *IEEE Trans. Commun.*, vol. 46, pp. 1555–1559, Dec. 1998.

[21] Texas Instruments RTDX communication with Matlab

BIOGRAPHICAL INFORMATION

Madhu Rangappagowda is working as a research associate in University of Texas at Arlington in RF DSP Labs. Prior to this, he was working as a research assistant in RF DSP labs. He did his summer internship in Orthofix Inc, McKinney, TX. Mainly was responsible for developing biomedical application embedded systems. He has 2.5 years of experience as a senior design engineer and has worked in British physical labs India from 2000 Dec to 2003 Jan. He was responsible for developing DSP algorithms and embedded software for telecom products during his tenure in British physical labs. He has also worked for Indian Space Research Organization as a project intern and was responsible for developing local user terminals with DSP plug in cards for processing search and rescue satellite data. He has completed his Bachelors degree in electronics and communication from Bangalore University, India and Masters of Science in electrical engineering from, University of Texas at Arlington.